University of Southern Queensland

Faculty of Health, Engineering and Sciences

The Effect of Resurfacing on the Lateral Resistance of Narrow Gauge Low Profile Concrete Sleepers

A dissertation submitted by

Ashley Poulton

in fulfilment of the requirements of

ENG4111 and 4112 Research Project

towards the degree of

Bachelor of Engineering (Honours) (Civil)

Submitted October, 2016

Abstract

Modern railway track construction employs the process of continuously welded rail (CWR), which increases the ride quality and operational speed of the track, while reducing maintenance requirements compared to traditional jointed track. However, CWR prevents the rails from freely elongating under elevated temperatures, which consequentially "locks" thermal stresses within the rails. This results in CWR track being susceptible to buckling when a combination of elevated rail temperatures, track misalignments, and weakened lateral sleeper resistance occurs.

Queensland Rail (QR) is currently installing low profile concrete sleepers on their narrow gauge CWR network, to replace aging timber sleepers in the Brisbane Suburban Area. A knowledge gap exists regarding the effect of track resurfacing on the lateral resistance of low profile concrete sleepers, and the consequent effect on the track's resistance to buckling. While many investigations of this topic have been completed on foreign rail networks; the results are usually network specific due to the local sleeper geometry and ballast conditions. Additionally, the majority of these investigations were conducted on networks with track gauges wider than 1067mm, and thus their results are not directly relevant to QR. Hence due to the negative implications of track buckling, it was pertinent an investigation relevant to QR's local track conditions was completed.

This investigation used mathematical and field testing methods to determine the lateral resistance of narrow gauge low profile concrete sleepers, before and after resurfacing. For the field testing component, a Single Sleeper Push Test (SSPT) device was developed to suit QR's narrow gauge low profile concrete sleeper.

The lateral sleeper resistance results were applied to a classical equation to model the track's critical buckling load, before and after resurfacing. The length and amplitude of the initial misalignment were modelled as variables to assess their sensitivity on the track's critical buckling load. The track's factor of safety against buckling after resurfacing was also determined.

The investigation concluded that resurfacing reduced the lateral resistance of narrow gauge low profile concrete sleepers by 24% and 14%, based on peak and limiting resistance respectively. Resurfacing was found to reduce the critical buckling load of track, constructed using 50kg/m rail, by 7.5% to 23%, and provide a factor of safety against buckling ranging from 0.9 to 14.6, depending on the span and amplitude of the initial misalignment encountered.

University of Southern Queensland

Faculty of Health, Engineering and Sciences

ENG4111 & ENG4112 Research Project

Limitations of Use

The Council of the University of Southern Queensland, its Faculty of Health, Engineering and Sciences, and the staff of the University of Southern Queensland, do not accept any responsibility for the truth, accuracy or completeness of material contained within or associated with this dissertation.

Persons using all or any part of this material do so at their own risk, and not at the risk of the Council of the University of Southern Queensland, its Faculty of Health, Engineering and Sciences or the staff of the University of Southern Queensland.

This dissertation reports an educational exercise and has no purpose or validity beyond this exercise. The sole purpose of the course pair entitles "Research Project" is to contribute to the overall education within the student's chosen degree program. This document, the associated hardware, software, drawings, and any other material set out in the associated appendices should not be used for any other purpose: if they are so used, it is entirely at the risk of the user.

Certification

I certify that the ideas, designs and experimental work, results, analyses and conclusions set out in this dissertation are entirely my own effort, except where otherwise indicated and acknowledged.

I further certify that the work is original and has not been previously submitted for assessment in any other course or institution, except where specifically stated.

Ashley Poulton

Student Number: 0061043080

Acknowledgements

First and foremost, thank you to my colleagues at Queensland Rail for the opportunity to conduct this investigation and perform field testing on the QR Network. I trust the information within this dissertation will be of some use to the organisation.

To Doctor Habib Alehossein, thank you for your guidance as Project Supervisor.

To the University of Southern Queensland, thank you for providing me an opportunity to undertake a dissertation in an area of my interests, which has enabled me to make a positive contribution to the research community.

Finally, to my family, thank you so much for your support and encouragement during this project. I now look forward to spending a lot more time with you all.

Table of Contents

List of Figures

List of Tables

Glossary of Terms

Buckle	A sudden track misalignment caused by temperature and/or rail creep induced stress, which requires the placement of a speed restriction and/or immediate attention by the Infrastructure Maintainer to allow trains to proceed safely
CWR	Continuously welded rail
Lateral Sleeper Resistance	The sleeper's resistance to lateral movement in the ballast bed
Limiting Resistance	The plateaued sleeper resistance measured by a SSPT
Low Profile Concrete (LPC) Sleeper	A low depth concrete sleeper designed to replace timber sleepers
LVDT	Linear variable differential transformer
Peak Resistance	The maximum lateral sleeper resistance measured by an SSPT
QR CETS	Queensland Rail Civil Engineering Track Standards
Resurfacing	Track maintenance process used to lift, align the track, compact ballast underneath the sleeper, and shaping of the ballast profile
ROA	Railways of Australia
Single Sleeper Push Test (SSPT)	A type of field test to measure lateral sleeper Resistance
Track Structure	Rails, rail fastenings, sleepers and the ballast, supported by the formation

1. Introduction

Queensland Rail (QR) is undergoing a program to replace aging timber sleepers on their narrow gauge network with low profile concrete sleepers within the Brisbane Suburban Area. Low profile refers to the reduced height of the sleeper compared to "full profile" concrete sleepers. Due to their comparable cross sectional shape with timber sleepers, low profile concrete sleepers can easily replace timber sleepers using existing track refurbishment processes. Additionally, benefits compared to timber sleepers include their increased durability and design life, an integrated resilient rail fastening system, and their resistance to termite attack and wood rot.

QR employs continuously welded rail (CWR) throughout the Brisbane Suburban Area. CWR results in many 110m lengths of rail being welded end-on-end to form a continuous length. While this provides enhanced ride quality due to the elimination of mechanical joints, it reduces the ability of the rails to elongate due to heat. Consequently, compressive thermal forces are "locked" in the rails, resulting in CWR track being susceptible to bucking if not managed suitably.

The consequences and costs of track buckling are significant. Between 1993 and 2005, there were 115 buckles on QR's then state-wide network. Up to 10% of the track buckles were found to result in derailments (Howie 2005). Other less catastrophic outcomes of track buckling include increased track repair and maintenance costs, train speed restrictions, reduced network throughput, reduced safety margins, and reduced customer confidence in the network's safety.

QR performs routine a track maintenance process across its network called track resurfacing. This process rectifies track geometry defects by using specialist equipment to lift and align the track, pack ballast underneath the sleepers, and re-shape the ballast profile. Before resurfacing, the individual stones of the track's ballast bed are packed together tightly due to the cumulative weight of rail traffic carried since the last track disturbance. During resurfacing, the individual stones of the ballast bed are unavoidably disturbed, which reduces the ballast bed bulk density, and consequentially weakens the lateral resistance of the sleepers. This situation, coupled with elevated rail temperatures and an initial track misalignment, creates an ideal condition for track buckling to occur.

Many studies have been completed by foreign rail networks to investigate the effect of resurfacing on the lateral resistance of sleepers. However, these studies have generally been carried out on standard gauge track with sleepers and ballast different to that used by QR.

As lateral sleeper resistance is known to be highly dependent on sleeper geometry and ballast properties, the results of these past studies have been generally network specific and incomparable to the results for QR's narrow gauge track.

QR's application of narrow gauge low profile concrete sleepers highlights a knowledge gap regarding the current unknown reduction in lateral sleeper resistance caused by resurfacing, and the consequent effect on the critical buckling load of the track.

Hence it is pertinent to investigate this knowledge gap to gain a deeper understanding of the relationship between track resurfacing, lateral sleeper resistance, and track buckling. This knowledge would be valuable not only to QR, and also other narrow gauge rail networks that have, or are planning to use, a low profile concrete sleeper design on their network.

1.1 Project Aim

To investigate the effect of railway track resurfacing on the lateral resistance of narrow gauge low profile concrete sleepers and the consequent effect on the critical buckling load of the track.

1.2 Project Objectives

The objectives of this project and their brief explanation are as follows:

1. Research Background Information

Initiating this project, a review of background information is required. This involves a review of the fundamentals of the track structure, track defects, resurfacing techniques, track buckling, lateral sleeper resistance, and methods to determine critical buckling load of the track. An appreciation of the relationship between resurfacing and lateral sleeper resistance will be gained. Methods for theoretical calculation and field measurement of lateral sleeper resistance will be investigated.

2. Calculate the Effect of Resurfacing on Lateral Sleeper Resistance

Previously developed theoretical approaches to calculate lateral sleeper resistance will be applied to estimate the resistance offered by low profile concrete sleepers. In the application of this method, measurement of the sleeper geometry will be completed and any assumptions made about the ballast conditions justified.

3. Develop a Single Sleeper Push Test (SSPT)

As an alternative approach, the lateral sleeper resistance of low profile concrete sleepers will be physically measured in the field, before and after resurfacing. To perform field measurements, a single sleeper push test device will be developed. Prior to use on track, the device will be "bench tested" to prove effectiveness and reliability.

4. Measure the Effect of Resurfacing on Lateral Sleeper Resistance

Physical measurement of the lateral sleeper resistance, before and after resurfacing, will be completed on the QR Network. Field testing will consist of two test zones - one not resurfaced, and other will be resurfaced. A sample of sleepers from both zones will have their lateral resistances measured by application of the developed SSPT device. A comparison of the results from before and after resurfacing will enable the effect of resurfacing on the lateral sleeper resistance to be assessed.

5. Comparison of Theoretical and Field Testing Results

The theoretical and field testing results will be compared to assess the level of agreement between the two approaches. Trends with regard to the effect of resurfacing on lateral sleeper resistance will be identified and reasons for variation between the methods discussed.

6. Calculation of the Effect of Resurfacing on Track Critical Buckling Load

Lateral sleeper resistance results will be used as inputs to calculate the critical buckling load of the track. Due to the unpredictable nature of initial misalignments, the span and amplitude of the initial misalignment required to initiate the buckling will be modelled as variables to assess their sensitivity. A model for prediction of track buckling will be developed by comparison of the critical buckling load against the maximum compressive force generated in the rails due to heat.

7. Draw Conclusions and Recommendations for Further Study

The relationship between resurfacing, the lateral resistance of low profile concrete sleepers, and the consequent effect on the critical buckling load of the track will be discussed. Additionally, further areas of study are outlined and briefly discussed.

1.3 Dissertation Overview

1.3.1 Background and Literature Review

This section details the background literature relating to the track structure, track geometry and resurfacing. Once this base information is presented, the analysis is then focused on literature relating to the causes of track buckling, lateral sleeper resistance, theoretical and physical measurement methods for lateral sleeper resistance, thermal forces generated in the rails due to heat, and methods to determine of the critical buckling load of track.

1.3.2 Methodology

This section outlines the process undertaken to obtain results to address the project aims and objectives. An explanation of the theoretical and field testing approaches used to measure lateral sleeper resistance before and after resurfacing is given. A detailed account of how the results of this testing was then applied to model the impact of resurfacing on the on the critical buckling load of track is given.

1.3.3 Results

This section displays the results of the theoretical calculation and field testing to determine the effect of resurfacing on lateral sleeper resistance, and the consequent effect on the critical buckling load of the track. Results are presented in the form of figures, charts and tables.

1.3.4 Discussion

The discussion comprises of three main sections. The first section discusses the theoretical calculation and field testing approaches employed to determine the effect of resurfacing on lateral sleeper resistance. The second section discusses the modelling performed to predict the effect of resurfacing on the critical buckling load of the track. The third section discusses the suitability of the test device developed in this project and areas for improvement of the equipment.

1.3.5 Conclusion

This section summarises the major findings of the study. Opportunities for further study are also outlined and briefly discussed.

2. Background and Literature Review

A literature review was conducted to understand the fundamental background material relating to resurfacing and its impact on lateral sleeper resistance and the critical buckling load of the track. The following topics were covered:

- Track structure and constituent components
- Track geometry and defects
- Track resurfacing and its effect on lateral sleeper resistance
- Methods to measure lateral sleeper resistance
- Track buckling and methods to calculate the critical buckling load of track.

Completion of this review enabled a thorough understanding of the implications which resurfacing has on the track. The review also enabled knowledge gaps in the literature, relating to the relationship between resurfacing and the lateral resistance of narrow gauge low profile sleepers, to be identified.

2.1 Track Components

Railway track is a system of components which comprises of a steel rail, rail fastenings, sleepers, ballast, capping layer and formation material. Together, these components form a track structure which serves two main functions:

- To safely guide the wheels of the rolling stock
- To distribute loads of the rolling stock to the natural ground
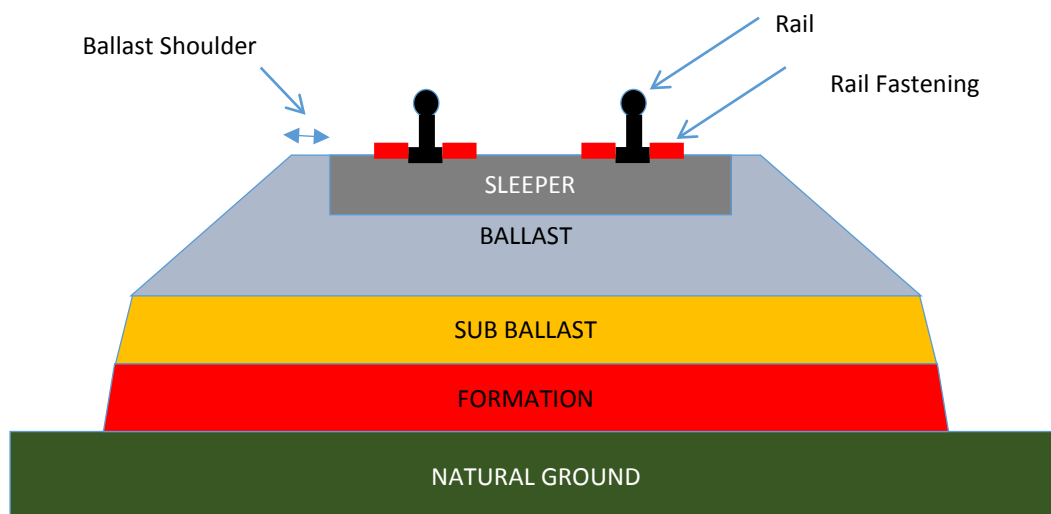
Figure 2-1: Track Structure

2.1.1 Formation

Formation is the specially prepared surface of compacted soil on which the track is constructed (QR 2012). Historically, the formation was simply the local surrounding earth dragged up into a loose mound, on which the track would then be constructed.

Modern track construction uses a compacted road base material for the formation layer, similar to that used in highway construction. It is essential that the track is constructed on a solid base to maintain correct track geometry during operation. Key functions of the formation layer are:

- To distribute the load of rail traffic evenly over the natural ground (QR 2012)
- Provide bearing, stability and settlement requirements similar to roadways (Gill 2007)
- Have a slight grade from the centre line to the edges to help with drainage (Esveld 1989)

To ensure adequate drainage for the track structure, Queensland Rail Civil Engineering Track Standards (QR CETS 2005) specifies a nominal 2.5% lateral cross fall on the foundation.

2.1.2 The Capping Layer

Above the formation is the "capping layer". This layer defines the shape of the ballast layer above, and together with the ballast layer, forms the "track bed". The capping layer improves water removal away from the foundation. Esveld (1989) identifies that the capping layer acts as a transitional layer between the firm, compacted formation layer below and the coarse particles of the ballast layer above. Heeler (1979) describes that the capping layer may consist of a range of various sub-layers, including geotextiles to provide enhanced filtration, reinforcement and drainage performance of the track. Where poorer formation exists, a capping layer (alternatively called "bottom ballast") is used to provide better distribution of the rail traffic loads to the foundation (QR 2012).

2.1.3 Ballast

Ballast is the loose, course grained material used for track bedding. It is the "rock" layer typically seen beneath the railway sleepers. A key requirement of ballast is to withstand the compressive and shock loading applied from the sleepers above, and spread this loading to the layers below.

QR (2012) identifies the following functions of the ballast layer:

- Distributes the load imposed by rail traffic evenly to the foundation
- Absorbs the shock loading of rail traffic by giving a resilient cushion
- Provides a firm, even bearing surface on which sleepers are laid
- Prevents longitudinal track creep
- Provides drainage and a material which can be worked to reinstate track geometry

Queensland Rail currently uses the following materials for ballast (QR 2012):

- Crushed basalt (predominantly used)
- Gravel
- Sand
- Screening
- Ashes

Generally the particle size for ballast ranges between 50mm to 100mm. QR (2012) describes a system for ballast classification, with four types of ballast (Type 1 to Type 4), with the lower number being the higher quality. Additionally, there are two grades of ballast per type. "A" grade has a maximum 63mm nominal size, which is the type mainly used in the Brisbane Suburban Area. QR's grade "B" ballast has a 53mm maximum nominal size, and is mostly used in railway sidings and yards where low speed operation of trains occurs.

2.1.4 Sleepers

Sleepers are structural members bedded into the ballast layer. They evenly distribute the weight of the rail and rolling stock to the ballast layer below. QR (2012) advises that together with the rail fastenings, the primary functions of sleepers are to:

- Provide support to the rail under the loading of the rail traffic
- Maintain the gauge of both rails
- Prevent longitudinal creep

Heeler (1979) provides further detail regarding the functions of sleepers to:

- Distribute loads through the ballast to eliminate the overstressing of the layers below
- Hold rail to the correct position, including inclination and gauge
- Prevent rails from rolling when undergoing traffic loading
- Provide lateral and vertical resistance to movement due to traffic and thermal expansion
- Electrically insulate the rails from one another for track circuit operation

Here Heeler has identified that sleepers play a chief role in track buckling prevention.

Historically sleepers were made from timber, however in modern times sleepers have been manufactured from steel, concrete and more recently, composite materials. Generally for heavy axle-load freight and passenger applications, concrete is the preferred material due to its strength and resilience. The geometry of the sleeper depends on the application, such as whether the sleeper is being used for plain track, turnouts or crossings.

2.1.5 Rail Fastenings

Rail fastenings provide restraint to the rail in three directions: laterally, vertically and longitudinally (QR 2012). Together with sleepers, they hold the rail to the correct gauge and prevent longitudinal rail creep.

Gill (2007) lists the main functions of rail fastenings are to:

- Provide the correct location of the rail in the sleeper's rail seat
- Prevent rail rock
- Absorb the rail forces elastically, and transfer these forces to the sleeper
- Maintain rail inclination and gauge
- Dampen vibration from traffic loading
- Provide electrical resistance between the sleeper and rail (particularly for steel sleepers)
- Prevent longitudinal rail creep

Typically there are two classes of rail fastenings:

- Non resilient fastening, which rely on mechanical engagement of the fastener with the sleeper – for example a dog spike. Although historically proven, they do not provide sufficient rail restraint for modern high speed, high axle-load railways.
- Resilient fastenings. These provide a clamping force usually due to elastic deformation of the fastener, and consequentially are retained by an elastic force. Such fasteners include Pandrol E-clip and Fastclip systems. These are a superior type of fastening and are generally used on all modern high axle-load track construction projects.

2.1.6 Rail

The main purpose of the rail is to carry and guide the flanged wheels of rolling stock. Heeler (1979) describes the main purpose of the rail to be a "hard and unyielding medium to carry a rigid wheel with limited damage caused to it and the wheel". The rail guides and carries traffic by acting as a beam to distribute the weight of the rolling stock over the track structure (QR 2012). Functions of the rail have also been outlined by Esveld (1989) as to:

- Provide a smooth running surface and guide way for the flanged wheels of rolling stock
- Accommodate wheel loads and act as a beam, distributing loads over the sleeper
- Provide lateral guidance of the flanged rolling stock wheels
- Distribute the longitudinal traction and braking forces of the rolling stock
- Serve as an electrical conductor for an electrified permanent way
- Conduct current for traffic signals

Typical Rail used in Australia is "flat bottomed rail" (Heeler 1979), and comprises of the following three main sections, head, web and foot, as shown below:
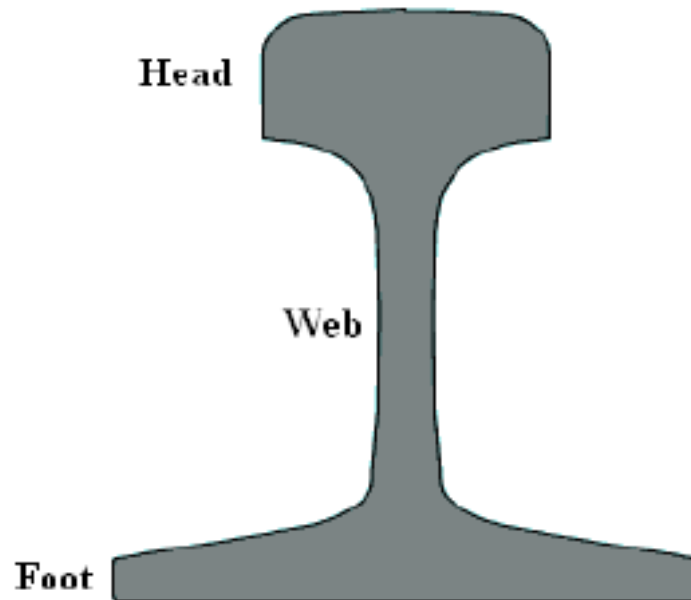
Figure 2-2: Flat Bottomed Rail (Gill 2007)

Rail is typically manufactured from low carbon steel and comes in varying sizes, categorised by its mass per unit length, generally in kg/m units. Drawings for common rail sizes are given in Appendix H. QR (2012) indicates that rail size is selected based on the application of the track, which considers the following factors:

- Magnitude of axle loading
- Speed of the rolling stock

Rail is generally manufactured in 27m lengths in Australia. Hence there is a need to join rails to form continuous lengths. There are two methods in which rails are joined, as detailed below:

- Mechanical Joints: Comprises of individual lengths of rail which are bolted together with splice plates called "fishplates". Small gaps between the rails at each fishplate joint provided space for controlled thermal elongation of the rails due to heat.
- Continuous Welded Rail (CWR): Modern railway track construction tends to use this method of rail joining. Many individual lengths are welded together, forming a single continuous length of rail. While this method eliminates mechanical joints and provides a superior ride quality, fewer thermal expansion gaps are provided between the rails. This "locks in" thermal stresses within the rail. Hence CWR track, when at elevated temperatures, is susceptible to track buckling and requires rail stress management.

2.2 Track Geometry

The key geometric parameters of track geometry are as follows:

2.2.1 Gauge

Gauge is the perpendicular distance between the inside faces of the running rails, measured 16mm below the top running surface. Correct gauge width is imperative to ensure the rolling stock is properly guided along the rails. Excessive gauge widening above allowable tolerances should be rectified. Typical causes of gauge widening include:

- Defective sleepers and rail fasteners
- Excessive rail wear to the inside running surfaces of the rail

2.2.2 Horizontal Alignment

Horizontal alignment, often referred to as "line", is the position of the gauge face of both rails viewed in the horizontal plane. Line dictates the horizontal profile of the running edge of the rail which the rolling stock follows, thus it is imperative that line is maintained so that:

- A good ride is given to the rolling stock
- The risk of derailment is reduced
- Wear on rails, other track components and rail wheels is minimised

Line defects are typically categorised as (QR 2012):

- Kink: a short and sharp loss of line
- Swing: a line defect over a distance
- Kicked joint: a misalignment at a joint
- Badly aligned welds due to poor workmanship

The cause of line defects are generally attributed to running surface defects, rail expansion, or gauge irregularities due to skewed sleepers or incorrect gauge (QR 2012).

2.2.3 Vertical Alignment

Vertical alignment, also referred to as "top" is the position of the top running surface of both rails, viewed in the vertical plane. As top dictates the vertical profile of the running surface of the rail, it is important to maintain good top to ensure a smooth ride of the rolling stock and to reduce the risk of derailment.

The types of vertical alignment defects are generally categorised as (QR 2012):

- Hole: a short sharp loss of top
- Dipped joint: a short sharp loss of top at a welded or mechanical joint
- Slack: a top defect over a distance
- Pumping sleepers: a top defect due to unsupported sleepers

The cause of top defects generally occurs due to poor formation and drainage, rail expansion, insufficient or sub-standard ballast, defective, incorrectly spaced, or insufficiently packed sleepers (QR 2012).

2.2.4 Cant

Cant, or "superelevation", is the difference in elevation or height of the running surface of the two rails. It is used to assist the rolling stock when negotiating curves. Generally the greater curve radius, the greater the cant required.

The purpose of implementing cant includes:

- Improved distribution of load across both rails
- Reduction of wear at the rail/wheel interface
- Reduction of lateral forces when curve transitioning, thus reducing risk of derailment
- Increased ride quality

Cant and top defects are closely related, with poor formation and drainage chiefly responsible.

2.2.5 Twist

Twist is the rate of change in cant along a section of track. It is required when transitioning from straight to curved track, where a "cant ramp" is applied at the beginning and end of a curve. Queensland Rail has two rates of twist for cant ramps, 1:500 or 1:1000 (QR 2012). Excessive twist is a serious track defect which increases the risk of derailment due to wheel unloading and wheel flange climb. Generally excessive twist is caused by top defects, such as dips, at the end of cant ramps located at the beginning or ends of curves.

2.2.6 Versine

All curves on railway track have a design radius. Versine is a measurement which is a function of the curvature radius. It is determined by measuring the lateral distance from the midpoint of a chord, which spans the arc of the curve, to the running face of the rail. It is important to maintain the correct curve versine to ensure that the curvature of the track is accurate and can be negotiated safety by rolling stock at the intended line speed.

2.3 Track Maintenance

Geometric deterioration of a track structure is inevitable. When the track geometry is measured to be outside of set tolerances, a speed restriction is typically placed on the section of track. This is a reactive administrative control which reduces the allowable speed which rail traffic can travel over the non-compliant section of track, until the track geometry is restored to within acceptable tolerances. To restore the required track geometry, so that the speed restriction may be lifted the track returned to normal operating speed, the track requires maintenance process called "resurfacing" to be completed. The following machines are typically used to perform track resurfacing works:

2.3.1 Tamper Liner

Tamper Liners are a type of track machine used to rectify track deterioration and defects by:

- Lifting the track to restore the correct vertical alignment
- Levelling the track to reinstate the correct cant
- Lining of the track to reinstate the correct horizontal alignment and curve versine
- Tamping of the ballast underneath the sleepers to prevent premature track settlement

Figure 2-3: Tamper Liner

The lifting, levelling and lining is achieved by a "clamp frame" that has flanged rail clamps which connects the machine to the track. The actual track geometry is recorded by the machine as it travels over the track, which and is compared with the design track geometry inputted into the machine's computer. The differences between measured and design track geometry is computed and the resultant corrective movements of the track are carried out by lifting, lining and levelling movements of the clamp frame.

Figure 2-4: Clamp Frame of a Tamper Liner

Additionally, the machine has "tamping workheads" which are fitted with paddle-like steel tamping tools. The tamping workheads plunge the tamping tool into the ballast bed between sleepers, which squeeze the ballast underneath the sleeper to increase the level of compaction of ballast in this area. Variation of the squeeze pressure, squeeze time and tamping tool plunge depth are configurable to suit the prevailing ballast bed conditions.
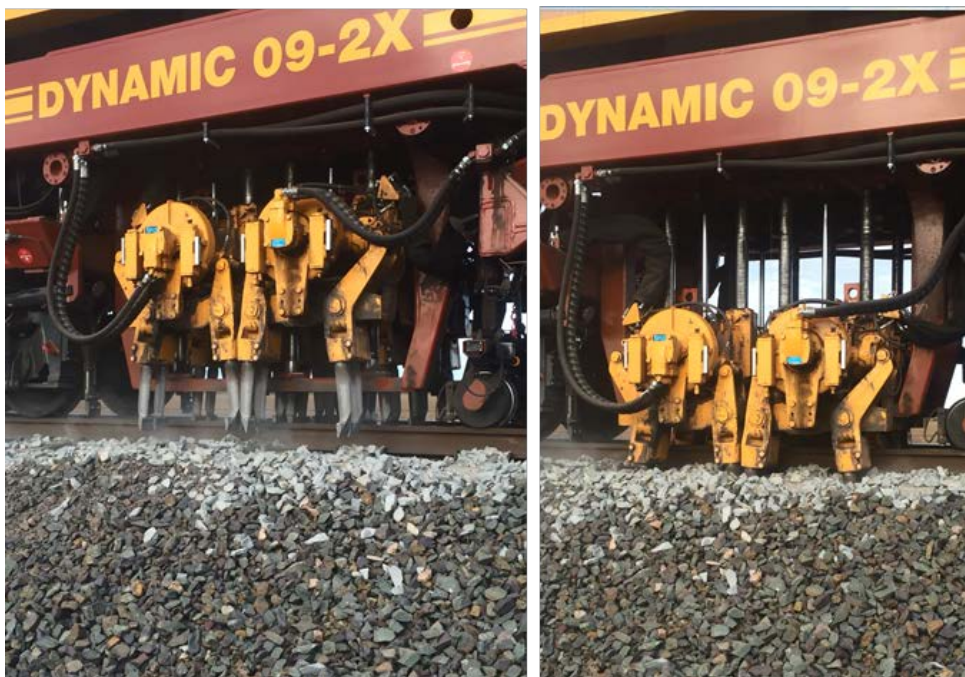
Figure 2-5: Tamping Workheads raised (right) and mid-tamping (right)

2.3.2 Ballast Regulator

Ballast Regulators are another type of track machine which generally follow behind the Tamper Liner, working as a pair. Their purpose is to shape the ballast bed profile to ensure adequate ballast is located in the cribs (the space between sleepers) and on the ballast shoulder. Generally as the track deteriorates, the ballast bed profile loses its correct shape, and ballast finds its way further away from the sleeper shoulder. This reduces the available confining pressure of ballast on the sleeper ends, which reduces the resistance provided by the sleeper against lateral movement in the ballast bed. Typically ballast regulators carry out the following operations in sequence:

- Ballast is recovered from the edges to the centre of the track via "shoulder ploughs"
- "Centre ploughs" distribute the recovered ballast across the track to the correct profile
- A rotating "sweeper broom" gathers excess ballast sitting on top of the sleeper and rail, and discharges it to the side of the track
- Steel "rail fastening sweeps" brush any remaining ballast away from around the rail fastenings

Figure 2-6: Ballast Regulator working its Shoulder Ploughs

2.3.3 Track Disturbing Work

Prior to track resurfacing, the ballast bed prior is generally well consolidated due to the cumulative weight of rail traffic loading carried over some period of time. The individual ballast stones are well interlocked, and this provides good resistance to lateral movement of the sleeper. While resurfacing is necessary to restore the defective track geometry back to acceptable tolerances, the nature of the work causes the interlocking ballast particles to become disturbed. This unavoidable "track disturbing work" results in an immediate loss of lateral sleeper resistance, until the ballast particles are once again reconsolidated or "packed".

Historically this reconsolidation was achieved by running rail traffic over the disturbed section of track at a reduced speed until a certain number of tonnes had passed over the track. While generally effective, this reduced the throughput of the network and consequentially reduced the number of people who could be transported, or the number of tonnes of coal which could be delivered to the port per day. Additionally, this method was found to cause uneven settlements of the track (Plasser & Theurer), and thus generated sites for initiation of new track defects.

2.3.4 Ballast Deterioration

Ballast degradation occurs when the corners and edges of ballast particles are worn away, caused by high local loading or alternating stresses on the ballast (Plasser & Theurer).

The wear of ballast occurs mainly from two sources:

- Traffic loading by rolling stock, which applies a compressive load on the ballast
- Track maintenance work by tamping and ballast regulator machines, which have tools which penetrate into the ballast bed, squeezing and pushing on the ballast

The loss of the unique facets, corners and edges of the individual ballast particles means that the ballast does not lie in a stable position in the ballast bed (Plasser & Theurer), and contributes towards large, non-uniform settlements of the track. As the settlements are not uniform, the track geometry subsequently deteriorates over time to outside allowable tolerances. When this occurs, the track requires resurfacing. This causes the ballast to deteriorate further and thus the cycle of ballast and track deterioration repeats. Hence the literature indicates that it is prudent to limit the frequency of track resurfacing to preserve the quality of ballast.

2.3.5 Stabilisation of the Ballast Bed

The preceding two sections outlined that:

- The ballast bed is unavoidably disturbed during track resurfacing
- Resurfacing causes ballast degradation due to the loss of unique ballast edges and corners
- Speed restrictions are required after resurfacing until the ballast bed is sufficiently reconsolidated

Consequentially, the operational hindrances of speed restrictions and cost of ballast renewal were motives for an alternative method of ballast bed consolidation to be developed, called Dynamic Track Stabilisation. This method provides immediate consolidation of the ballast bed post resurfacing, so that:

- Ballast particles are returned to their most stable positions
- The resistance of the track to lateral movement is improved
- The settlement of the ballast bed is achieved in a controlled manner
- Enhanced safety is provided against track bucking
- The track may immediately carry rolling stock at the normal line speed

Furthermore, this method provides a homogenous consolidation throughout the ballast bed, to prevent uneven settlement and later track irregularities (Plasser & Theurer).

2.3.6 Dynamic Track Stabilisation

In 1975 Plasser & Theurer introduced the first Dynamic Track Stabiliser, DTS 62N. This machine homogenises the density of the ballast bed and stabilises the track geometry (Plasser & Theurer). The machine carries out this function by making a combined application of a vertical downforce and a horizontal vibration of the track through the four flanged rollers of the machine's stabilising units.

Figure 2-7: Dynamic Track Stabiliser (Kish 2011)

Figure 2-8: Stabilising units of a Dynamic Track Stabiliser

The degree of consolidation achieved in one pass of the DTS 62N amounts to approximately 50% of the equivalent settlement of 1 million gross tonnes (1GMT) of traffic (Plasser & Theurer). The controlled settlement by the uniform dynamic action is only around 30% of the maximum forces occurring due to traffic loading, therefore the ballast is not unduly stressed (Plasser & Theurer).

The vertical force and horizontal oscillation applied to the rails is transmitted through the sleepers and rail fastenings to the ballast bed. This allows the ballast to settle in a stable manner, providing virtually force-free spatial consolidation of the ballast bed (Plasser & Theurer). The dynamic track stabiliser can be used on timber, concrete and steel sleepers. The parameter range for the DTS 62N is advised to be a maximum down force of 320kN, a horizontal vibrational frequency of 0 to 45Hz, and a work speed of 0 to 3km/h (Plasser & Theurer).

Van den Bosch (2006) found that the vibration range of 30 – 37 Hz is ideal regardless of the type of sleepers used. Frequencies below 30 Hz may lead to higher vibration amplitudes, and consequently settlements which are difficult to control. Similarly, for frequencies above 37 Hz, the liquefying properties of the ballast increase and lead to settlements which are difficult to control.

The DTS 62N is designed to be used in the course of scheduled track maintenance following track geometry correction by resurfacing. However, the forces and vibrations generated during dynamic stabilisation are significant and Plasser & Theurer advise limitations of its use. These limitations include prohibiting machine use in or near tunnels; near stone or brick arched bridges, or fixed masonry constructions such as culverts and ballast deck bridges, as these objects may have natural frequencies lower than the frequencies developed by the Dynamic Track Stabiliser.

2.4 Track Buckling

Buckling is defined by Queensland Rail's Civil Engineering Track Standards (QR CETS 2005) as:

"A sudden track misalignment caused by temperature and/or rail creep induced stress, which requires the placement of a speed restriction and/or immediate attention by the Infrastructure Maintainer to allow trains to proceed safely".

Figure 2-9: Derailment due to Track Buckling (Kish 2011)

Continuously welded rail (CWR) is widely used throughout Queensland Rail's Network. CWR is defined by welding a series of short lengths of rail together to form a single, continuous length of rail. For CWR track, there are very few mechanical joints in the rail, and hence there are very few opportunities for the rail to freely elongate due to thermal expansion caused by heat. Forces generated during the thermal expansion and contraction of the rail is therefore "locked" within the rail. Consequentially, CWR is inherently susceptible to buckling. The amplitude of the resulting track misalignment caused by a track buckle can be large, including up to 30 inches, and the associated buckling lengths be in the order of 40 to 60 feet (US Department of Transportation 2013). Misalignments due to track buckles can cause rolling stock derailments, as they often occur suddenly without warning and the defect cannot be negotiated by the rolling stock at the normal line speed. Hence there is an importance for railroad operators such as Queensland Rail to understanding the factors which contribute to the occurrence of track buckling.

2.4.1 Theory of Track Buckling

The track structure, consisting of rails attached to sleepers via rail fasteners, can be idealised as a long slender member. Such members subject to an axial compressive force act as columns. Slender columns are inherently vulnerable to buckling. At a critical compressive load, columns buckle, which results in a sudden and large lateral deflection. Leonard Euler developed a classical equation which predicts the critical buckling load of an ideal column. This equation is presented in Hibbeler (2005) is the form below:

$$Pcr = \frac{n^2\pi^2 EI}{(kL)^2} \qquad Equation\ 2.1$$

Where:

Pcr = Critical Buckling Load (kN)

E = Modulus of Elasticity of Column material (Pa)

I = Least moment of inertia for the Column's cross sectional area (m^4)

L = Column length (m)

K = Effective length factor, dependant on end conditions of column

N = Buckling mode

Euler's formula is based on an ideal column, which makes the following assumptions:

- It is initially straight and of a finite length
- The axial load acts perfectly through its centroid
- It is made from a material which has a homogenous Modulus of Elasticity
- It has constant cross section
- It does not yield prior to buckling
- It has perfect end conditions (fully pinned, fully fixed, etc.)

However in reality, no column is perfect. The application of Euler's formula to track buckling is not completely accurate due to the following real-world complexities:

- The track is never perfectly straight due to curvatures and alignment imperfections
- The track's effective length is essentially infinite for CWR track
- Axial loading through the centroid of the track structure would seldom occur
- The track's cross section and moment of inertia often changes along its length
- The end conditions of the track cannot be perfectly modelled as either pinned or fixed
- The lateral resistance provided by the sleeper in the ballast bed is non-linearly proportional to the lateral displacement of the track

Considering this, Ole (2008) advises "the modelling and determination of the critical buckling load for a particular section of track is a complex process which is best left to finite element analysis packages". Despite this, there have been mathematical techniques developed, by a range of contributors over the past 40 years, to investigate the critical buckling load of the track.

2.4.2 Causes of Track Buckling

Kish (2013) outlines the five main causes of track buckling:

- High longitudinal compressive forces
- Reduced rail neutral temperature
- Misalignments created by track shift
- Weakened lateral track resistance
- Train loads and dynamics

These will now be discussed in greater detail.

2.4.2.1 Longitudinal Compressive Forces

Longitudinal compressive forces generated by the restrained thermal expansion of continuously welded rails are the primary cause of track buckles. In a survey of track buckles throughout the late 1980s, Railways of Australia (ROA) found that buckles occurs markedly more in the warmer summer months compared to the cooler winter months (ROA 1988).

Continuously welded rails are longitudinally restrained at their ends due to a lack of expansion gaps, and also prevented from freely expanding and contracting with temperature variations due to friction between the rail/sleeper, and sleeper/ballast interfaces. This restriction results the in generation of internal longitudinal forces, which are locked within the rails.

Determination of longitudinal force caused by thermal expansion of rail is dependent on several factors, including the:

- Cross sectional area and ambient temperature of the rails
- Coefficient of thermal expansion for the steel rail material
- The rail neutral temperature, RNT (or stress free temperature)

The RNT is the ambient temperature of the rail at the time of rail installation, when the rail is neither in tension or compression and is essentially stress free. Compressive forces are generated when the rail temperature rises above the RNT, where the rail wants to elongate while at the same time being restrained longitudinally. Thus ROA's observation that track buckling is more prevalent in summer months is supported by the physics relating to the retrained thermal expansion of the rail under heat.

31

For a length of free rail, the change in length due to thermal expansion or contraction is:

$$\Delta l = \alpha \Delta T L_o \quad Equation\ 2.2$$

Where:

$\Delta l =$ Change in length

$\alpha =$ Coefficient of Thermal Expansion for Steel Rail

$\Delta T =$ Change in Temperature

$L_o =$ Initial Length

However due to the longitudinally restrained nature of the rails, the change in length caused by the thermal expansion is prevented. Instead, the rails are placed in compressive strain, equal and opposite to the thermal strain. Rearranging Equation 2.2 enables determination of the strain (ε) within the rail as follows:

$$\frac{\Delta l}{l_0} = \varepsilon = \alpha \Delta T \quad Equation\ 2.3$$

Strain is also related to stress (σ) and the Modulus of Elasticity (E) by the following equation:

$$\sigma = E\varepsilon \quad Equation\ 2.4$$

Rearranging Equation 2.4 gives:

$$\varepsilon = \frac{\sigma}{E} \quad Equation\ 2.5$$

Additionally, stress (σ) is related to axial force (P) and cross sectional area (A):

$$\sigma = \frac{P}{A} \quad Equation\ 2.6$$

Substitution of Equation 2.5 and 2.6 into Equation 2.3 gives:

$$P = AE\alpha \Delta T \quad Equation\ 2.7$$

Considering there are two rails, the total compressive force for the track is:

$$P_{MAX\ COMPRESSIVE} = 2AE\alpha\Delta T \qquad Equation\ 2.8$$

2.4.2.2 Reduced Rail Neutral Temperature

When the rail is laid and welded in track, it is under neither tensile nor compressive forces, an in a "neutral" stress state. The temperature at which the rail is installed is deemed the rail neutral temperature (RNT). An acceptable RNT is required to be achieved at the time of installation. The desired RNT is generally advised by the track management authority and is determined by consideration of the local temperature conditions expected where the rail is laid, specifically the expected maximum and minimum temperatures which the rail will experience in track. Typically for QR's Brisbane Suburban Area, the RNT is approximately 37°C. If the RNT is set too low at the time of rail installation, then in hot weather the rails will experience a greater temperature differential from the RNT, resulting in increased compressive forces generated in the rail and increased likelihood of track buckling. Conversely, if the RNT is set too high, track buckling will generally be avoided , however during cold weather the rails will be subject to high tensile forces, and thus susceptible to rail breakage.

2.4.2.3 Lateral Imperfections in Track

No rail is perfectly straight. Many opportunities for lateral imperfections exist, such as mechanical joints, defective welds, track curvatures and residual alignment defects post resurfacing.

Mechanical joints and defective welds are initiation sites for track buckles due to the reduction in rail stiffness about the vertical axis compared to the adjacent rail (Ole 2008). If the mechanical joint is seized, this prevents the freedom of the rail to expand and contract, providing a weak point in the track and an opportunity for a buckle to initiate. For CWR track, misaligned welds and residual horizontal misalignments left behind by track resurfacing works provide the necessary eccentricity for a compressive rail forces to form a buckle. As started by ROA, a rail misalignment is a prerequisite, along with a compressive rail force, to generate a track buckle.

"If a rail were completely straight, then it would be impossible for an axial force of any magnitude to cause it to buckle." ROA (1988)

2.4.2.4 Weakened Lateral Track Resistance

The passive resistance of the track structure to resist lateral shift and track buckling is an important, yet highly variable quality of the track. Lateral track resistance is the ability of the track structure to resist lateral movement. Thompson (1991) advises the lateral resistance of track is dependent many factors including the following:

- Sleeper condition

- Ballast condition

- Rail condition

- Fastener type

- Loading type

Hence, lateral resistance is a site specific quality of the track which is difficult to compare between rail networks of varying gauge and track structure components.

2.4.3 Buckling Behaviour

The shape of buckled track is dependent on the type of misalignment. US DOT (2013) comments that the resultant shape of the buckle is represented generally by three shapes as shown below:
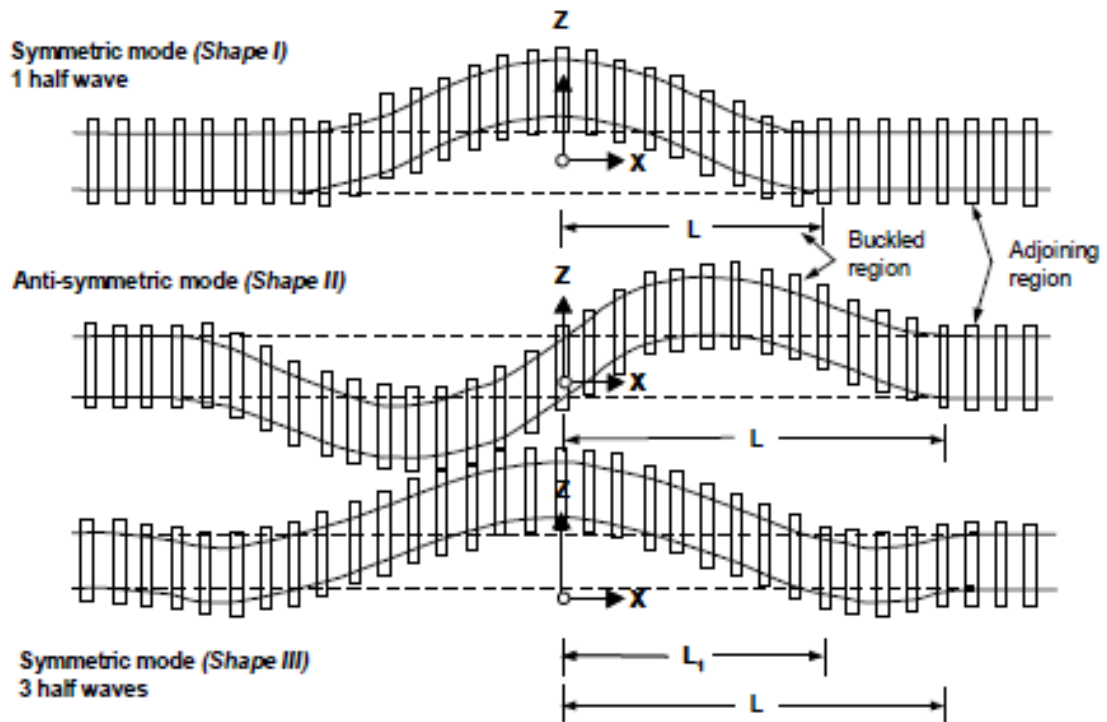
Figure 2-10: Track Buckling Modes (US DOT 2013)

Buckles on tangent (straight) sections of track tend to exhibit Shape III type buckling, with explosive lateral deflection in either direction, generally depending on the side of track which has a weaker lateral resistance or has the misalignment. Typically, the largest deflection is in the central half wave of the buckle, with smaller opposite deflections on the outer half waves.

Buckling of curved track in contrast tends to display the single half wave buckled shape as per Shape I type buckling. As the initial curvature exists, it would require significant energy to deflect the rail against the existing curvature, as per buckling Shapes II and III. Curved track buckling tends to be a progressive, non-explosive failure, particularly where low lateral sleeper resistance or high radius curvatures exist.

Furthermore, curved track is susceptible other radial displacement due to rail "breathing". Temperatures above the RNT can cause a radially outward movement of the track; similarly temperatures below the RNT can cause an inward "sucking" movement of the track. Rail "breathing" can cause longitudinal rail stress, a reduction of RNT, further misalignments and decrease of lateral resistance which fosters conditions prone to rail buckling.

2.4.4 Track Buckling Models

Currently accepted models for track buckling resistance simplify both rails of the track to be modelled as a single beam. An equal and opposite compressive axial force is applied at the ends of the beam. The beam is elastically supported laterally which represents the lateral resistance provided by the sleepers within the ballast bed. The lateral resistance is proportional to the track's lateral deflection.

Kish (2011) presents this track resistance model as a series of springs, where the

- Sleeper against the ballast provides lateral resistance, modelled as a lateral spring
- Rail secured by fastenings and sleeper against the ballast provides longitudinal resistance, modelled as longitudinal spring
- Rail secured by the fastenings provides torsional resistance, modelled as a torsional spring
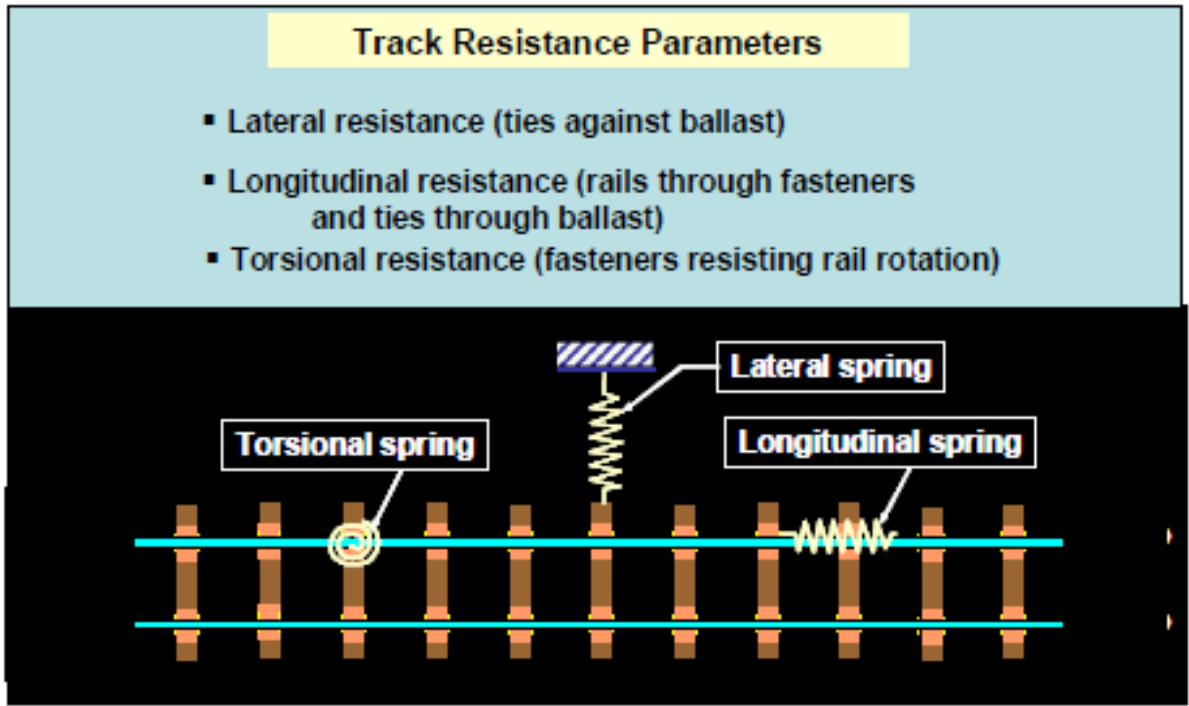
Figure 2-11: Track Buckling Resistance (Kish 2011)

Bartlett (1960) identified that the structural elements of the track collectively provide resistance of the track against lateral movement. Bartlett developed a formula which determines the critical load required to cause track buckling, as per the equation below.

$$Pcr = \frac{\pi^2 EI_s}{L_b{}^2 10^3} + \frac{\pi^2 C_t}{16S}\left[\frac{\pi L_b}{q_b}\right]^{0.5} + \frac{w_l L_b{}^2}{\pi^2 q_b} \quad Equation\ 2.9$$

Bartlett's equation consists of three resistance components relating to the resistance provided by the rail, rail fasteners, and sleeper respectively as per the equations below:

$$\frac{\pi^2 EI_s}{L_b{}^2 10^3} = Rail\ Resistance \quad Equation\ 2.10$$

$$\frac{\pi^2 C_t}{16S}\left[\frac{\pi L_b}{q_b}\right]^{0.5} = Rail\ Fastener\ Resistance \quad Equation\ 2.11$$

$$\frac{w_l L_b{}^2}{\pi^2 q_b} = Sleeper\ Resistance \quad Equation\ 2.12$$

Where:

E = Modulus of Elasticity of the two rails (Pa)

I_s = *Moment of Inertia of two rails about their vertical axis (m^4)*

L_b = *Length over which buckling is likely to occur (m)*

S = Sleeper spacing (m)

w_l = *Maximum sleeper lateral resistance per meter (kN/m)*

q_b = *Maximum misalignment acting over the buckling length (m)*

C_t = *Torsional resistance of rail fastener ($kNm/rad^{-0.5}$)*

Bartlett's equations were validated by experimental testing, where the track was compressively loaded until buckling failure of the track occurred. The theoretical results were compared with the experimental data, and were found to have good agreement. Bartlett's study found that the percentage contribution of the track's components to the critical buckling load was as follows:

- Rail resistance, 11-16%
- Rail fastener resistance, 13-37%
- Sleeper/ballast bed resistance, 50-70%

However, Bartlett's investigation did not identify which rail fastening systems was tested in his investigation. Later testing by Vink (1978) recreated Bartlett's investigation and found that Bartlett's results for the torsional resistance offered by the rail fasteners matched those for dog spikes in new timber sleepers. While Sinha (1967) assumed the rotational resistance of dog spikes to be effectively zero, the results of Bartlett and Vink indicate that torsional resistance of dog spikes in timber sleepers is significant but depends on the age and condition of the sleeper. Additionally, Vink performed work to determine that the torsional resistance of resilient Pandrol fasteners to be 10 $kNm/rad^{-0.5}$. This value will be subsequently used throughout this study for the calculation of the critical buckling load for low profile concrete sleepers, as these sleepers use the Pandrol Fastclip system.

2.4.5 Key Controlling Parameters of Buckling

The US DOT (2013) discusses the following three key actions to manage track buckling:

2.4.5.1 Reduction of misalignments

As per ROA (1988), if the rail was perfectly straight, then it would be impossible for any axial compressive force to buckle the track. In the real world, perfectly straight rail is not possible or feasible, simply because curved track is required to negate the terrain between two places. Misalignments inevitably exist, which provides the imperfections in straightness required for axially loaded columns to buckle. Prevention of initial track misalignments reduces the likelihood of track bucking. Regular track geometry recording (monitoring), and routinely correction will result in the track being more capable of resisting compressive forces due to heat, and thus better at resisting buckling.

2.4.5.2 Management of Rain Neutral Temperature

Routine monitoring of rail stress and management of the track's design rail neutral temperature (RNT) enables greatest band of temperatures which the track can safely operate within. Track maintenance work can often result in an unintended lowering of the rail neutral temperature due to rail creep. Timely rail stressing works is required to reinstate the design RNT and the consequent improve the buckling resistance of the track. Typically railway operators strive for the greatest possible RNT, however caution must be taken to ensure the RNT is not too high, as this may result in high tensile forces and rail breakages in cold weather conditions.

2.4.5.3 Improving the Lateral Resistance

Increasing the lateral resistance of the sleepers in the ballast bed can be achieved by:

- Increasing the consolidation level of the ballast bed through:
    - Cumulative traffic loading (traditional method)
    - Dynamic track stabilisation, or other means to compact the ballast
- Providing a deeper amount of ballast at the shoulders of the sleeper
- Filling the cribs in between sleepers with ballast
- Improved sleeper design, such as:
    - Larger cross sectional area
    - Heavier mass
    - Frictional surfaces or shear tabs on the bottom and sides of the sleeper.

From the literature, particularly Bartlett (1960), it is clear that the main influencing factor in for the critical buckling load of the track is the lateral resistance of the sleeper in the ballast bed. This is called the "lateral sleeper resistance". Without adequate lateral sleeper resistance, the track is most vulnerable to buckling failure.

2.5 Lateral Sleeper Resistance

This section discusses the fundamental background to lateral sleeper resistance.

2.5.1 Contributory Factors

Bartlett (1960) identified that track's buckling resistance is heavily weighted by the sleeper's lateral resistance– that is the resistance provided by the ballast bed to prevent lateral movement of the sleeper. Factors affecting lateral sleeper resistance include (Kish 2011):

- Sleeper shape and weight
- Ballast type and condition
- Ballast bed geometry (shoulder width and crib content)
- Degree of ballast consolidation
- Degree of disturbance due to track geometry
- Rail traffic loads

Doyle's (1980) review of Shenton and Powell (1973) indicated that from the range of aforementioned factors, it was the weight of the sleeper and the packing condition of the ballast that were the greatest influencing factors for lateral sleeper resistance.

The primary method which sleepers resist movement in response to an applied force is through friction between the sleeper and the ballast bed. Doyle (1980) separated the total lateral resistance of a sleeper into three frictional components:

- Base of the sleeper, with the ballast underneath the sleeper
- Sides of the sleeper, with the ballast in the cribs between sleepers
- Ends of the sleeper, with the ballast at the shoulders of the sleeper

Doyle (1980) summarised from the study that aforementioned components contributed 50%, 30% & and 20% respectively to the total lateral resistance of the sleeper.

Further conclusions drawn were by Doyle (1980) were:

- Concrete had greater lateral resistance than timber for the same ballast conditions
- Sleepers in ballast with a higher level of consolidation had a greater lateral resistance
- Increased ballast shoulder depth increased lateral sleeper resistance, until a depth of 460mm where no benefit was gained for increased shoulders depth

Similar to Doyle (1980), Kish (2011) also modelled the lateral resistance of a sleeper as the sum of the following three components:

- Side friction
- Bottom friction
- End resistance

The approximate contributions each component had on the total lateral sleeper resistance were estimated to be 30-35%, 35-40% and 20-25% respectively. The literature indicates that the component contributions are wide ranging, not definite and fixed contribution values for these components can't reliably be assigned. Hence a contribution range value was a suitable way to represent the components in this mathematical model.
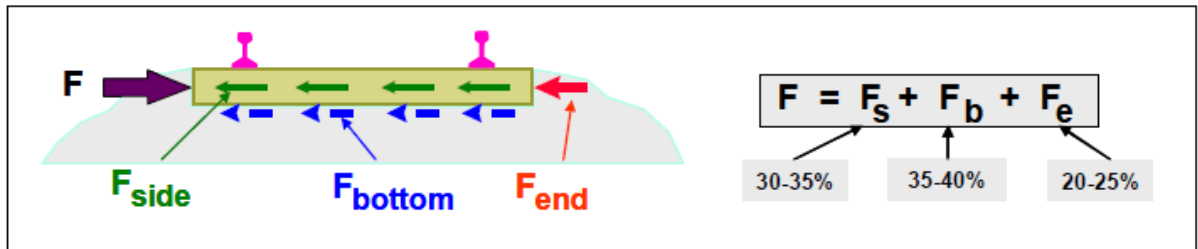
Figure 2-12: Lateral Sleeper Resistance Components (Kish 2011)

Hence from the literature, the sleeper lateral resistance could be defined as:

$$F = F_{side} + F_{base} + F_{end} \quad Equation\ 2.13$$

Where:

F = Lateral sleeper resistance

F_{side} *= Lateral resistance due to the side of the sleeper*

F_{base} *= Lateral resistance due to the base of the sleeper*

F_{base} *= Lateral resistance due to the end of the sleeper*

2.5.2 Measurement Techniques

This section details the theoretical and physical methods used to determine the lateral resistance of sleepers.

2.5.2.1 Theoretical Calculation

Miura (1991) and the Japanese Railway Technical Research Institute (RTRI 2012) provide a theoretical method for calculating lateral resistance of sleepers in the ballast bed, which is based on the bearing capacity of shallow foundations. The lateral resistance per sleeper in a track panel is estimated as per the equation:

$$F = aW + brG_e + crG_s \qquad Equation\ 2.14$$

Where:

- *F = Lateral sleeper resistance (kg)*
- *W = Mass of sleeper (kg)*
- *r = Bulk density of ballast (kg/ m^3)*
- *G_e = first moment of the end area about top edge of sleeper (m^3)*
- *G_s = first moment of side area about the top edge of sleeper (m^3)*
- *a, b & c = coefficients depending on the sleeper and ballast material*

2.5.2.2 Qualitative Experimental Methods

QR (1998) investigated the link between lateral sleeper resistance and the quantity of ballast packed under the hollow "pods" of steel sleepers. Their investigation discussed a number of methods to determine quantity of ballast within the sleeper pods in order to evaluate the effectiveness of Dynamic Track Stabilisation (DTS) on lateral sleeper resistance. Their qualitative assessment was to assess of the amount of settlement achieved from DTS by experienced personnel. While no measurable data could be achieved by this method, a rating system was used to qualitatively asses the lateral sleeper resistance achieved.

2.5.2.3 Basic Quantitative Experimental Methods

QR (1998) also discussed the British Rail method of lateral sleeper resistance assessment which involves drilling holes at various locations in the steel sleepers. The level of ballast under the sleeper would be measured, the distance from the bottom of the sleeper to the ballast level, for various stages of the resurfacing and DTS process. A cone penetrometer was to be used through the drilled inspection holes; however this method did not proceed due to the high degree of variables regarding the approach.

41

Another proposal by QR (1998) involved determining the average density of ballast within the steel sleeper pod by removing surrounding ballast from the steel sleeper in question, and cutting the sleeper in half. Each half sleeper would be removed and quantity of ballast inside the pod (from the edges of the sleeper walls up into the pod of the sleeper) could be measured and the average density recorded. However due to practical and logistical reasons, QR (1998) abandoned employing this method.

2.5.2.4 Quantitative Experimental Methods

Zakeri (2012), QR (1998) and Kish (2011) discuss the following quantitative methods to determine lateral sleeper resistance:

1. Single Tie Push Test (SSPT), which involves laterally pushing a single sleeper in the ballast bed approximately 25mm, with the resistance measured by the load-displacement response of the sleeper. Generally a hydraulic cylinder applies the force to mobilise the sleeper, with a load cell measuring the applied force. A string potentiometer or linear variable differential transformer (LVDT) is used to measure the displacement of the sleeper with respect to the rail. A key conclusion from QR (1998) was the suggested purchase of a STPT apparatus and performing tests on various track types in various conditions, such as 60kg/m rail on concrete sleepers.

Figure 2-13: Single Sleeper Push Test Device (left) and Testing (right) (Kish 2011)

2. Discrete Panel Cut Pull Test, where a finite length of track is cut at the rails, and then pulled laterally, with the displacement recorded (Kish 2011).

3. Continuous Track Panel Pull Test

4. Continuous Dynamic Measurement (Plasser & Theurer DTS)

Van den Bosch (2006) elaborates on this method where the energy required to drive the dynamic track stabilisation units of a DTS are measured and equated to a frictional force of "rubbing" the track grid (rail, fastenings and sleepers) into the ballast bed. This enabled an equation for lateral resistance of the sleepers to be developed. Validation of this method was conducted against the SSPT method. Nine sections of track were selected, and over the nine sections, one dynamic track stabilisation parameter was changed (speed, down pressure and vibration frequency). SSPT tests were performed on sleepers in each of the nine test sections, and compared to the Continuous Dynamic Measurement results from the DTS. A linear regression line established and the equation of this line was determined. The equation was found to give good approximation of the relationship between the lateral sleeper resistance of determined by SSPT and the Continuous Dynamic Measurement.

5. Empirical Model

6. Derailment wagon method, however not recommended by QR (1998) as it requires a purpose built test vehicle fitted with measurement devices.

7. Mechanical shift method which employs the use of a tamping machine. This method uses the clamp frame of the tamping machine to provide the lateral track shifting forces, and the lining transducer to measure resultant lateral displacement of the track. The method was used with moderate success by Queensland Rail (QR 1998) to measure lateral stability during trials of the Tilt Train.

Kish (2011) and QR (1998) indicate the SSPT is the most suitable way to measure lateral sleeper resistance because the results are in a more fundamental characteristic of ballast resistance, it is an easier test to perform, and the test is portable and requires minimal training. QR (1998) advises that the main disadvantages of the SSPT being that the test results vary between sleepers, however this could be overcome with the random selection and measurement of at least 3 sleepers or more to give a statistical basis for the analysis.

It was found that while many lateral sleeper resistance tests have been performed in Europe and the United Stated using the SSPT, very little testing has been performed by Australian rail authorities on the track materials and conditions available in Australia (ROA 1988). Generally SSPT devices were found to be developed by the rail networks themselves and suited to the design of their track structure, considering the gauge of the track and the type of the sleeper to be tested.

2.5.3 SSPT Testing on the Queensland Rail Network

Gill (2007) investigated the development of a Single Sleeper Push Test (SSPT) device on the Queensland Rail Network for the testing of "full profile" concrete sleepers. The device involved installation of a frame which attached laterally across both rails of the track. The rails were lifted off the test sleeper using rail jacks. In order to apply a force to the test sleeper, one shoulder of the sleeper had the ballast removed down to the base of the sleeper, so that a hydraulic cylinder reacting against the frame could push off the end area of the sleeper.

Figure 2-14: Queensland Rail SSPT Device

Figure 2-15: Hydraulic Cylinder Pushing End Area of Test Sleeper

A key factor in the use of the device was the requirement for excavation of ballast way from the sleeper shoulder. The depth of the excavation was to the bottom of the sleeper and the width of the excavation approximately one metre so that the frame can be fitted to the track without interference with the ballast. This required a significant amount of material removed away from the track. Due to the accessibility of the track, machinery could not be relied on to perform this task, so track workers were required to manually shift the material.

Figure 2-16: Excavation Required to Perform Test

Gill comments about this excavation: "only enough ballast should be removed so that the frame can be positioned correctly, all other ballast must not be disturbed as this will affect the results by altering the effect of the ballast".

When reinstating the track to operating condition after testing, ballast was required to be replaced at the sleeper end where it was previously removed. During this replacement task, the ballast would be highly disturbed, increasing the likelihood that the lateral sleeper resistance, and critical buckling load of the track, would be reduced post testing. This is not desirable as it renders the track more prone to buckling as a by-product of the testing.

It was apparent from the literature that there is a lack of SSPT devices which are suited to Queensland Rail's track conditions and are minimally destructive on the track.

2.5.4 Typical Lateral Sleeper Resistance Values

Shenton and Powell (1973) conducted an extensive investigation into the lateral resistance of standard gauge timber and concrete sleepers under varying track conditions on the British Rail Network. Their laboratory testing found that typical total lateral resistance for timber and concrete sleepers, in consolidated 75mm nominal sized ballast, was 4.44kN and 8.50kN respectively. In loose conditions, the total lateral resistance was 2.21kN and 3.25kN respectively. Hence, there is a clear relationship between the compaction level of the ballast and the lateral resistance of the sleeper.

Furthermore, Shenton and Powell (1973) replicated the laboratory testing of the lateral resistance of timber and concrete sleepers in 38mm nominal sized ballast, and found that the lateral resistance values of the sleeper were consistently smaller than when the sleeper was situated in 75mm nominal sized ballast. Hence there is also a relationship between the nominal size of the ballast and the lateral resistance of the sleeper.

Field testing by Shenton and Powell (1973) found that the lateral resistance of sleepers varied by 22% for identical ballast conditions. Standard gauge concrete sleepers were found to have a nominal lateral resistance of 10.5kN, with a 3.5kN range between the upper and lower values.

 Kish (2011) also investigated lateral resistance of standard gauge sleepers on the US Rail Network and found that typically the concrete sleepers in a consolidated ballast bed has an average lateral resistance of 9-11kN. "Average" lateral resistance values were considered to between 11-14kN, and "strong" values above 14kN. Values for timber sleepers were measured to be 2.2kN less than those for concrete on average.

The lateral resistance values determined by Kish (2011) were measured through Single Sleeper Push Testing (SSPT), and represent the "peak" resistance values. The US Department of Transport (2013) suggest that the peak resistance values are achieved within the first 12mm of sleeper displacement during a SSPT.

For consolidated track, as the displacement of the sleeper increases, there is a reduction of lateral resistance from the peak value, which converges to a constant value where the sleeper achieves its "limiting" resistance. Kish represents presents the characteristic SSPT curves for strong, average and weak track as shown below:
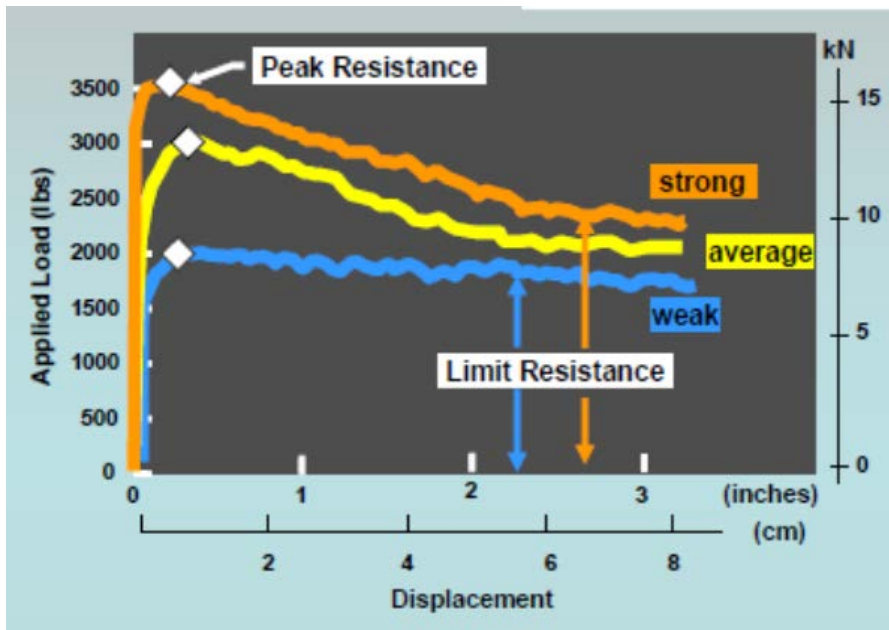
Figure 2-17: Typical SSPT Curve for Standard Gauge Concrete Sleepers (Kish 2011)

It can be seen that for sleepers with weak lateral resistance, there is no reduction between the peak and limiting values, but rather a plateauing, which is also characteristic of STPT results for freshly resurfaced track. The US Department of Transportation (2013) presents the characteristic SSPT curves for consolidated and resurfaced track as per the figure below.
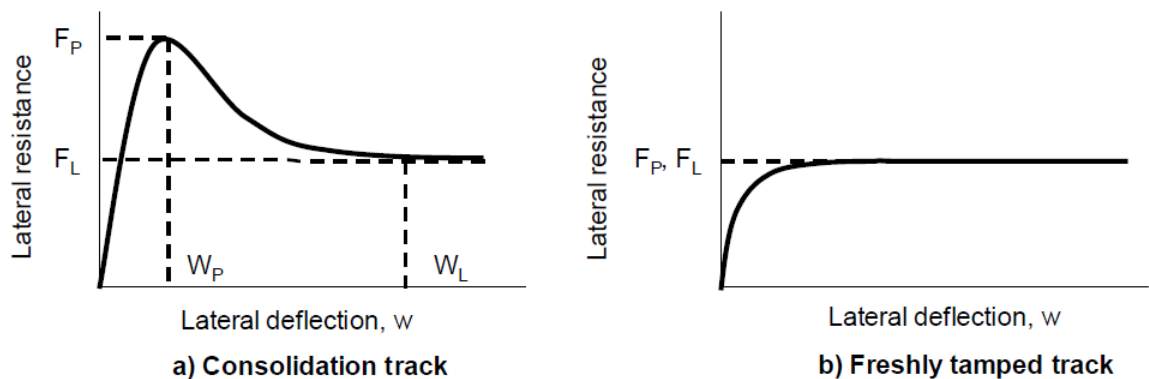
Figure 2-18: Characteristic SSPT Curves (US DOT 2013)

Throughout the literature, lateral sleeper resistance results were generally based on standard gauge timber or full profile concrete sleepers, which are heavier than narrow gauge sleepers for the same material type. Hence from the literature it could be hypothesised that low profile concrete narrow gauge sleepers will return a lower lateral sleeper resistance value compared to the standard gauge concrete sleeper for the same track conditions, due to reduced sleeper geometry size and mass. It is apparent that there is a knowledge gap relating to the lateral resistance of narrow gauge low profile concrete sleepers, before and after resurfacing.

2.5.5 Effect of Track Maintenance of Lateral Sleeper Resistance

Lateral sleeper resistance is temporarily reduced immediately after track maintenance due to the disturbance of the ballast and loss in consolidation of the ballast bed. This is gradually restored through traffic loading. Shenton & Powell (1973) investigated loss and restoration of lateral sleeper resistance by measuring the lateral sleeper resistance before resurfacing, immediately after resurfacing, and then over time to assess the effect of cumulative traffic loading. It was found that the lateral sleeper resistance recovery followed the figure below, and was 93% recovered after 1.3MGT traffic, which equated to 34 days rail traffic for the test conditions.
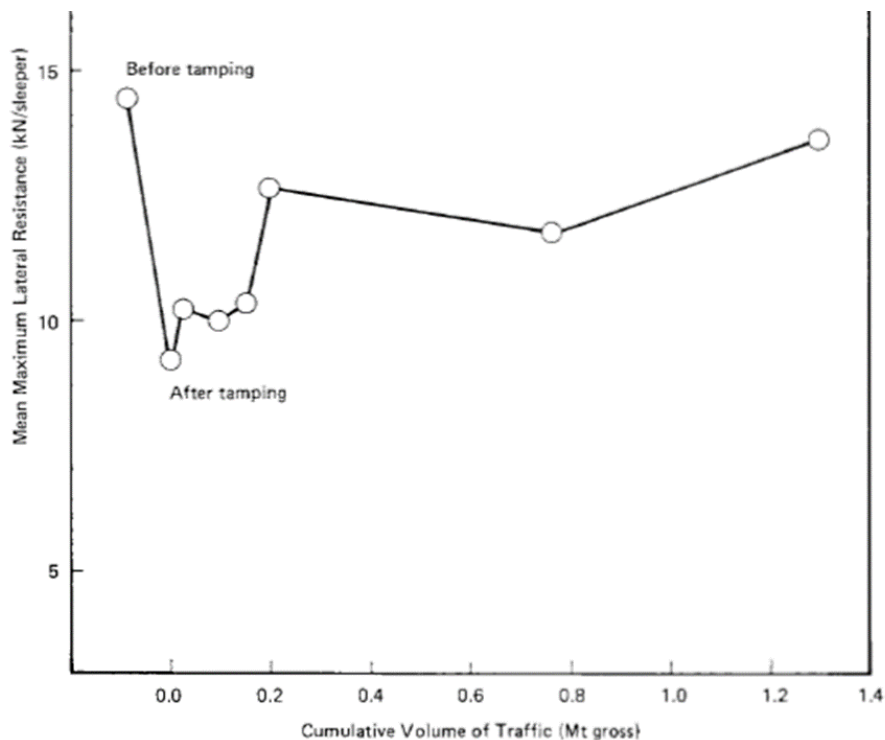
Figure 2-19: Relationship between Lateral Sleeper Resistance and Rail Traffic (Sheldon & Powell 1973)

Shenton & Powell's work (1973) also provided the following values for the immediate lateral sleeper resistance loss after various track maintenance operations:

- Resurfacing only – 16 - 37% reduction
a. Resurfacing and crib consolidation – 15% reduction
b. Resurfacing and crib and shoulder consolidation – 12% reduction

Kish (2011) also investigated loss of lateral resistance post resurfacing and found that the loss of lateral sleeper resistance caused by maintenance operations ranged from 40 – 70%.

The Japanese Railway Technical Research Institute (RTRI) performed lateral pull testing of sleepers to understand the lateral resistance of sleepers under varying ballast conditions, the result of their testing shown in the figure below:
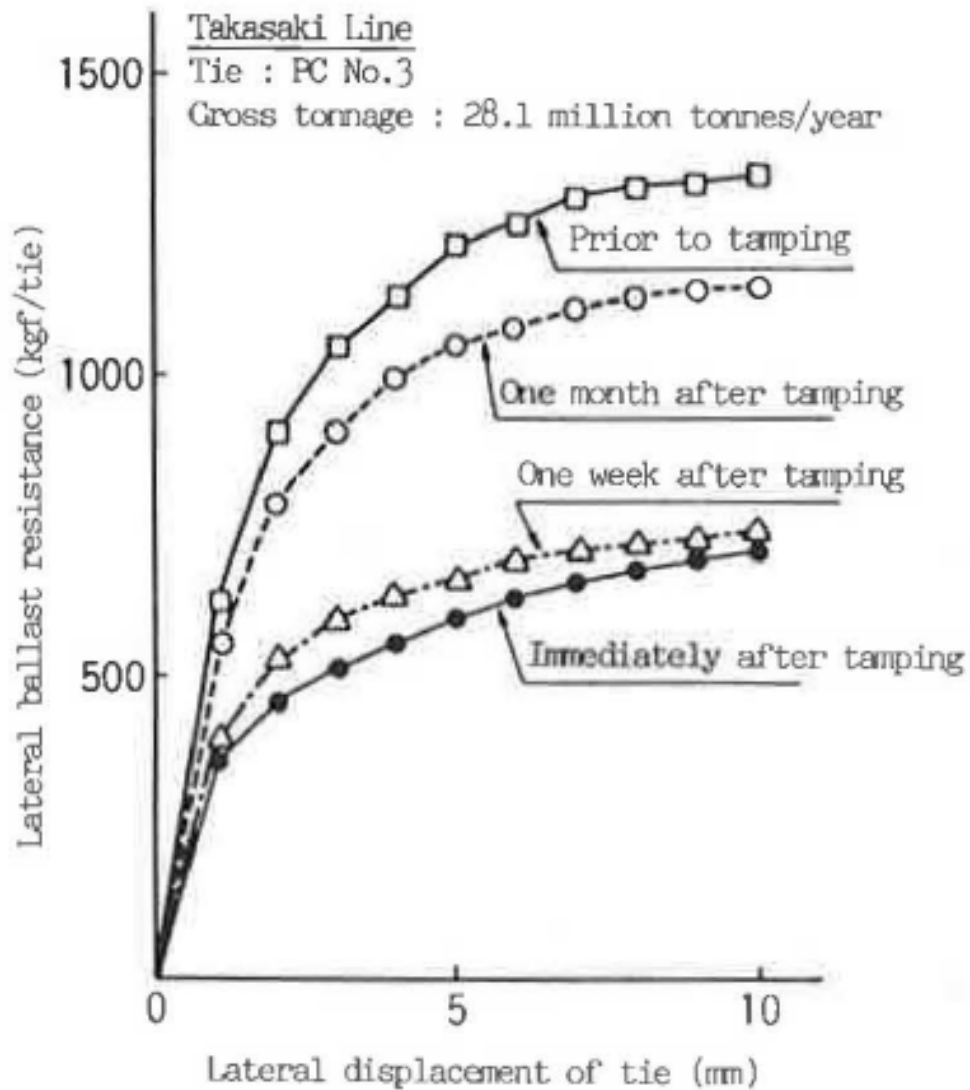
Figure 2-20: Effect of Resurfacing on Lateral Sleeper Resistance (RTRI 2012)

Gill (2007) advises that the characteristics of SSPT results for before and after resurfacing should be fairly constant regardless of the type of ballast or sleepers involved, however the specific values for the resistance would, however, vary greatly. Thus it can be drawn from the literature that there is a significant reduction in lateral sleeper resistance after track disturbing work such as resurfacing, however the magnitude of the reduction is site or network specific due to the local sleeper and ballast conditions.

Therefore the impact of resurfacing on the lateral resistance of low profile concrete sleepers is a knowledge gap which is unique to QR. Due to a lack of understanding in this area, and the negative implications of track buckling, there is a need to quantitatively understand the lateral sleeper resistance loss incurred immediately after resurfacing, based on QR's local conditions.

2.5.6 Lateral Resistance Restoration Techniques

Two approaches are chiefly used to restore lateral sleeper resistance, firstly the traditional traffic loading method, and secondly the method of dynamic track stabilisation. The outcomes of some relevant studies are summarised below.

Plasser & Theurer investigated the comparison of lateral sleeper resistance before resurfacing, after resurfacing, and after passing by a Dynamic Track Stabiliser (DTS). After use of the DTS, their investigation found lateral resistance after resurfacing increased between 32-42%.

Sari (1981) dissects the study performed by the Hungarian State Railways in 1977, who conducted the first comprehensive study of the effect of a DTS on track lateral sleeper resistance recovery. Two 200m test sections were resurfaced. One section was then compacted by a crib compactor, the other section passed over by a DTS. The lateral sleeper resistance of the test sections were measured before and after treatment with the crib compactor and DTS, and also repeated after 2 and 142 days of rail traffic. Testing was done by Single Sleeper Push Tests (SSPTs). Test sleepers were placed sufficiently far apart so that disturbance of the surrounding ballast would not affect the lateral resistance of other test sleepers. Average values were gathered across 5 measurements. It was found that the DTS increased lateral sleeper resistance by 44% compared to the crib compactor, which increased lateral sleeper resistance by 25% after resurfacing.

Zakeri (2012) measured lateral sleeper resistance during various stages of track maintenance processes on the Iranian railway network. His work measured the lateral sleeper resistance prior to resurfacing, after resurfacing, and immediate after application of the DTS prior to revenue traffic. The results of his study found that resurfacing reduced the lateral sleeper resistance by 43%, while stabilising increased the lateral sleeper resistance by 31% after resurfacing. The comparison of the after resurfacing only versus resurfaced and stabilisation results found that the stabilised track had a showed a characteristic curve associated with stronger, stiffer, more densely packed ballast bed.

Over the past 30 years the US Department of Transportation's Volpe Centre and the American Association of Railroads have performed a number of studies on the effect of track maintenance, dynamic track stabilisation and train tonnages on lateral sleeper resistance. In each study lateral sleeper resistance was measured using a SSPT. The outcomes of some of these studies are summarised below:

Sluz (1985) investigated lateral sleeper resistance recovery after resurfacing via rail traffic loading, with 11% lateral sleeper resistance recovery achieved on one test section after 0.073MGT of traffic has passed, while the other test section had 9% recovery after 0.076MGT traffic.

Sluz (2000) investigated testing on the Union Pacific network. After resurfacing, 17% lateral sleeper resistance recovery was achieved after 0.35MGT traffic, while 33% lateral sleeper resistance recovery was achieved immediately after use of the DTS.

Sussmann et al. (2003) found that a 43% reduction in lateral sleeper resistance occurred when a 12mm lift was applied when resurfacing. The DTS was found to provide 32% lateral sleeper resistance recovery after this lift.

Samavedam (2001) found that resurfacing reduced lateral sleeper resistance by 39-70%. The DTS was found to increase lateral sleeper resistance by 22% after resurfacing. An unexpected result of this investigation was that after the DTS, the lateral sleeper resistance was found to initially decrease slightly, and then increase over time.

2.6 Summary

From the literature it was found that the resurfacing is a critical track maintenance process necessary to rectify track defects and restore correct track alignment. The process involves physical shifting the track by using equipment which causes an unavoidable disturbance of the ballast bed.

Modern railways are built using continuously welded rail (CWR), which reduces opportunities for the rail to elongate due to heat. Without correct rail stress management, CWR track is to the susceptible to the undesirable consequence of track buckling. Lateral sleeper resistance is the key factor in the prevention of track buckling, and is highly dependent on the sleeper geometry and the bulk density of the ballast bed. The ballast disturbance caused by resurfacing results in reduced lateral sleeper resistance, and consequently lowers the critical buckling load of the track.

While many studies have been performed to assess the reduction in lateral sleeper resistance caused by resurfacing, these studies have generally been performed on standard gauge track, on sleepers of varying geometry, and in ballast of uncertain properties. Hence, the results of these studies are generally site or network specific and are not directly able to predict the performance of the narrow gauge low profile concrete sleepers which QR has installed on their network.

Hence it is pertinent for QR to understand the magnitude of lateral sleeper resistance offered by the narrow gauge low profile sleeper, before and after resurfacing, and the consequent impact this has on the buckling resistance of the track.

While lateral sleeper resistance is calculable using previously developed theoretical approaches, the review has indicated the best way is the measurement of lateral sleeper resistance in the field using a Single Sleeper Push Test (SSPT). As no suitable "off the shelf" SSPT device suited to Queensland Rail's narrow gauge track exists, a suitable device is required to be developed for this purpose.

Buckling of track cannot occur without an initial misalignment, and the critical buckling load of the track was found to be dependent on the amplitude and span of the initial track misalignment. Bartlett's equation was found to be an effective way to determine the critical buckling load of the track once the lateral sleeper resistance vales, and size of misalignment are known.

3. Design and Methodology

This chapter presents the methodology undertaken to determine the effect of resurfacing on the lateral resistance of low profile concrete sleepers, and the consequent effect on the critical buckling load of the track.

3.1 Theoretical Calculation of Sleeper Lateral Resistance

This section discusses the methodology undertaken to theoretically calculate the lateral resistance of narrow gauge low profile sleepers, before and after resurfacing.

3.1.1 Measurement of Sleeper Geometry

To theoretically calculate the lateral sleeper resistance, the sleeper geometry and mass required to be known. To obtain this information, a site visit was made to a Queensland Rail materials depot to inspect and measure the narrow gauge low profile sleeper at the focus of this study.

Figure 3-1: Narrow Gauge Low Profile Concrete Sleeper

The actual geometry of the low profile concrete sleeper types was observed to be a relatively complex shape. As the base, side and end areas of the sleepers would need to be determined; the sleeper geometry was simplified to a trapezoidal prism with the dimensions as shown below.
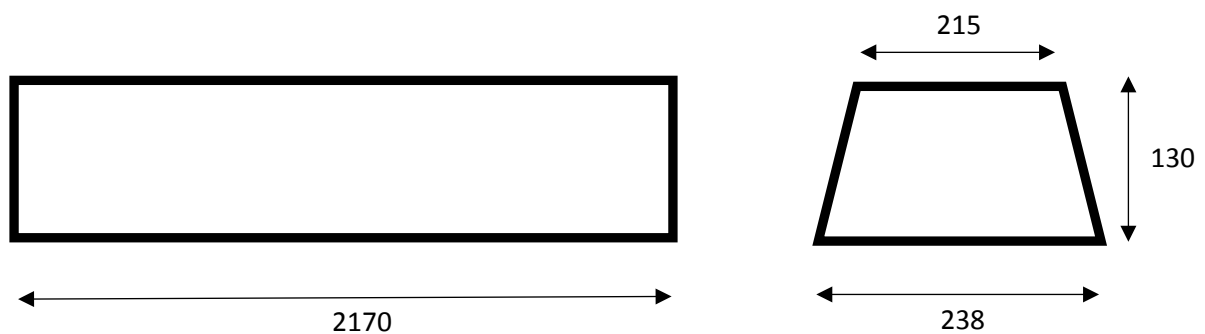
Sleeper mass = 165kg.

Figure 3-2: Low Profile Sleeper Simplified Geometry

3.1.2 Comparative Mass Method

Previous studies by Gill (2007) indicated that the peak lateral resistance of a full profile concrete sleeper in a consolidated ballast bed was approximately 20kN. Based on the literature, resurfacing could be roughly assumed to reduce the peak resistance by 25%, to 15kN. Assuming lateral sleeper resistance is a function of sleeper mass, an estimate for the lateral resistance of the low profile sleeper could be calculated by the ratio of the sleeper masses.

$$F_{FPeak} = \mu \times m_F \quad Equation\ 3.1$$

Where:

F_{FPeak} = Peak lateral resistance of a full profile concrete sleeper

   = 20kN before resurfacing, 15kN after resurfacing

μ = Coefficient of friction between sleeper and ballast

m_F = Mass of full profile concrete sleeper = 275kg

Assuming the coefficient of friction between the sleeper and ballast is constant for the same sleeper material (concrete), the lateral resistance for a low profile concrete sleeper could be estimated as per the following equation:

$$F_{LPeak} = \left[\frac{m_L}{m_F}\right] \times F_{FPeak} \quad Equation\ 3.2$$

Where:

F_{LPeak} = Peak lateral resistance of low profile concrete sleeper (kg)

m_L = Mass of low profile concrete sleeper = 165kg

Hence, the estimated peak lateral resistance for the low profile concrete sleeper was:

$$F_{LPeak} = \frac{165}{275} \times 20 = 12kN\ [Before\ Resurfacing]$$

$$F_{LPeak} = \frac{165}{275} \times 15 = 9kN\ [After\ Resurfacing]$$

3.1.3 RTRI Calculation Method

The method developed by RTRI (2012) was also employed as an alternative means to calculate lateral sleeper resistance, before and after resurfacing, as per the equation below:

$$F_{Peak} = aW + brG_e + crG_s \qquad Equation\ 3.3$$

Where:

F = Sleeper lateral resistance (kg)

W = Bulk mass of sleeper (kg)

r = Bulk density of ballast (kg/ m^3)

G$_e$ = First moment of the end area about top edge of sleeper (m^3)

G$_s$ = First moment of side area about the top edge of sleeper (m^3)

a, b & c = coefficients depending on the sleeper and ballast material as per the table below:

Coefficient for Sleeper/Ballast Material Combination	a	b	c
Concrete Sleeper with crushed stone ballast	0.75	29	1.8
Wooden Sleeper with crushed stone ballast	0.75	29	1.3
Wooden Sleeper with gravel ballast	0.60	29	1.4

Table 3-1: Sleeper / Ballast Material Coefficients

For this method, an assumption of the ballast's bulk density before and after resurfacing was required to be made. From the literature, Dingqing et al. (2002) indicated that the bulk density for ballast before, and after resurfacing, was estimated to be 1760g/m^3 and 1600kg/m^3 respectively. However, bulk density reductions of up to 30% had been measured post resurfacing.

Hence for this approach, the bulk density before resurfacing was estimate to be 1760kg/m^3, while post resurfacing was assumed to be 1496kg/m^3. This was equivalent to a 15% bulk density reduction due to resurfacing.

3.2 Single Sleeper Push Test Development

The literature indicated the most accurate way to determine lateral sleeper resistance was to physically measure it by performing the Single Sleeper Push Test (SSPT). This method has several advantages over other measurement techniques, such as:

- The results provide a more fundamental characteristic of ballast resistance
- The test procedure is relatively easy to set up and execute with minimal training
- The hardware is lightweight and portable
- The mobilisation of a single sleeper is least destructive compared to other tests

Hence, the SSPT was chosen as the experimental method to measure lateral resistance of low profile concrete sleepers, before and after resurfacing. This section details how the SSPT device was developed, from concept to manufacture.

3.2.1 SSPT Device Development

Research of SSPT devices employed in the literature review revealed that they were not an "off the shelf" product, but rather a bespoke design suited to the track gauge and type of sleeper being tested. No commercially available SSPT device was found to be available which suited the low profile narrow gauge concrete sleepers used on the Queensland Rail Network. Hence there was a need design a SSPT device suited for these conditions.

The design intent of the SSPT device was to apply a force to the test sleeper in order to cause a lateral movement of the sleeper relative to the rail, with the force-displacement behaviour of the sleeper measured. Examples of SSPT devices from the literature showed the force is usually applied by a hydraulic cylinder, and is measured by either a pressure transducer, or load cell. The sleeper's displacement relative to the rail was usually measured by a string potentiometer or an LVDT.

The literature indicated that were two alternative ways to apply the force to produce the sleeper's displacement relative to the rail:

a. Attach the SSPT device to the test sleeper, and apply the force to the rail
b. Attach the SSPT device to the rail(s), and apply the force to the test sleeper

Due to the geometry of the low profile sleeper and the shape of the integrated rail fastener shoulders, it was decided that the best way to provide the lateral force was to attach the device to the sleeper and react the cylinder against a single "reaction" rail, as shown below.
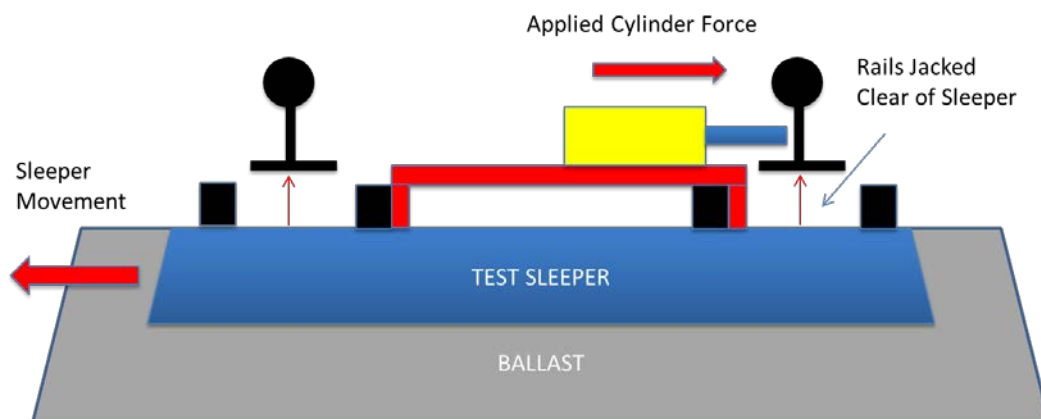
Figure 3-3: SSPT Device Concept

Several concept designs were developed, which were progressed based simplicity of operation, weight, ease of installation and removal on track, and ease of manufacture. The design chosen to progress consisted of a rectangular hollow section strut which attached to the rail fastener shoulders between both rails. A 5t hydraulic cylinder was mounted in an adjustable housing at one end of the device, beneath which gripper plates latched around the fastener shoulder. At the opposite end of the device, a lateral plate was fitted which beared against the backside of the fastener shoulder. When the device was installed on a test sleeper, the line of action of the hydraulic cylinder was in the same horizontal plane as the centre of the rail head, and the force was transferred to the test sleeper via the gripper plates. The adjustable housing enabled the height of the cylinder to be adjusted to suit different sized rails which could be encountered during testing on the Network, which include 41kg/m, 50kg/m and 60kg/m rail sizes.
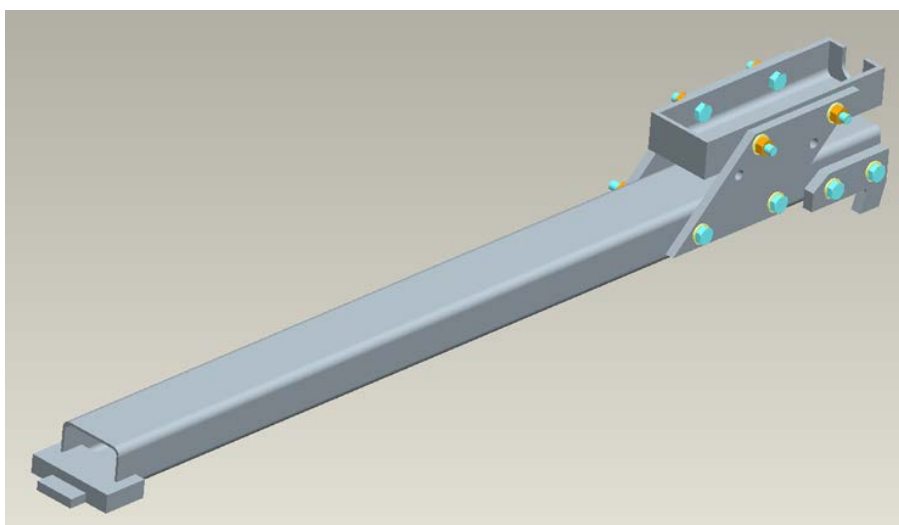
Figure 3-4: SSPT Device Model

To use this device, both rails were required to be unfastened on the test sleeper and at least seven sleepers either side of the test sleeper. Both rails would then be lifted clear of the test sleeper using rail jacks. This was required so the measured resistance was completely due to the sleeper resistance in the ballast bed, and not due to any contribution from rails resting on the test sleeper.

Due to the rail being unfastened approximately four meters either side of the test sleeper; the rails would have a lateral span of 8m which was unsupported. Under the applied cylinder load, this centrally loaded span would deflect unless it was held laterally in position. Rail deflection is undesirable as the LVDT results would show rail displacement rather than sleeper displacement, thus affecting the accuracy of the SSPT results obtained.

Therefore, a pair of rail fixtures was designed which were to hold the reaction rail in place during the testing. The fixtures were fitted both side of the test sleeper, and prevented the rail from deflecting laterally under the applied load. This ensured the measured LVDT results were of the sleeper displacement, and not that of the reaction rail deflection.

Classical hand calculations, along with calculations from AS4100-1998 – Steel Structures, were used to appropriately size the members, and the bolted and welded connections of the SSPT device and rail fixtures. The design was then modelled using Computer Aided Design (CAD) software, where production drawings were then developed to enable manufacture of the design.

3.2.2 SSPT Device Prototyping and Manufacture

The SSPT device and rail fixtures were then manufactured from commonly available steel sections. The main strut of the SSPT device was constructed from 75mm x 50mm x 3mm grade 350 rectangular hollow tube, while the plate components were manufactured from 10mm and 25mm thick grade 250 steel plate.

Bolted connections, using grade 8 bolts, were used where this was practicable as this provided a non-permanent connection which allowed adjustment of the design if modifications became evident during prototyping and testing phases.

Figure 3-5: Manufacture of SSPT Device

The gripper plates which latched over the rail fastener shoulder at the cylinder end of the device were an important aspect of the design. The load was required to be transferred to the test sleeper through the gripper plates, without the device working itself off the sleeper during testing. Hence the profile of the gripper plates was initially prototyped from plastic, where its shape could be refined. The final gripper plates were laser cut from steel plate to ensure the dimensional accuracy required was provided.

Figure 3-6: Gripper Plate Prototype (left) and Final Design (Right)

3.2.3 Proof of Concept Testing

After manufacture, the SSPT device was subject to testing to validate the equipment could successfully:

- Attach itself to a low profile concrete sleeper

- Transfer a load to the sleeper without working itself off the sleeper

- Withstand the expected loads incurred in service

- Withstand a proof load twice the expected load to be incurred in service

To validate the device meets these requirements; the device was attached to a dummy test sleeper as shown below. A large pack of sleepers was used to simulate the immovable reaction rail, and the smaller pack of sleepers to simulate the lateral resistance of the sleeper in the ballast bed. A hydraulic hand pump was used to extend the hydraulic cylinder and apply a load through the device to the test sleeper.

Figure 3-7: Proof Load Testing of SSPT Device

Given that the lateral resistance loads calculated by the theoretical method were estimated to be approximately 3kN, the expected load in service for the purpose of the testing was conservatively assumed to be 10kN. As the size of the hydraulic cylinder was known, the load applied to the sleeper could be determined by monitoring the pressure shown in the gauge. The force from applied through the device could be determined as per the calculation:

$$P = \frac{F}{A}$$

Where:

$P =$ Pressure generated in the hydraulic circuit (Pa)

$F =$ Force applied by the hydraulic cylinder (N)

$A =$ The effective area of the hydraulic cylinder (m^2)

Figure 3-8: Pressure Gauge used to Measure Test Loads

The device was tested to 75%, 150% and 200% of the 10kN expected load, and for each test the load was held for one minute. Upon release of the 200% load, the SSPT device was disassembled and inspected for deformation or cracks. No damage was identified. Therefore, the test provided sufficient confidence that the device was ready for field trial.

3.2.4 Data Acquisition System

The key function of a SSPT device was to measure how far the test sleeper displaces under an applied load, so that the characteristic resistance vs displacement relationship for the sleeper could be determined.

Hence a data acquisition system was required to be developed which measure these two measured parameters simultaneously. A data acquisition system used on an existing test rig belonging to Queensland Rail was employed, which consisted of:

- 5 tonne load cell
- Linear voltage differential transformer (LVDT)
- 12V data logger
- Notebook computer

Figure 3-9: Data Acquisition Setup

The load cell was used to measure the force applied by the hydraulic cylinder to the test sleeper. It was inserted between the base of the hydraulic cylinder and the cylinder holder. During testing, as the cylinder pushes against the reaction rail, the force is reacted though the load cell, providing a voltage signal that is sent to a data acquisition unit.

The LVDT was used to measure the test sleeper displacement. It was mounted off the side of the SSPT device, with the spring loaded plunger end of the LVDT touching the side of the reaction rail. During testing, the plunger of the LVDT extends as the sleeper displaces further away from the reaction rail, which provided a voltage signal which is sent to a data acquisition unit.

The data acquisition unit collected both the load cell and LVDT voltage signals simultaneously at a frequency of 10Hz. Software on the notebook computer enabled the measured voltages from both sensors to be converted into meaningful units of force and displacement. The Graphical User Interface of the software displayed the lateral sleeper resistance versus displacement plot in real time. Once the test has ended, the test data was saved in .csv format which could be opened in notepad, and exported to Microsoft Excel. Once in a spreadsheet, the data was able to be manipulated and the test sleeper's lateral resistance versus displacement characteristic curve plotted.

Figure 3-10: Load Cell and LVDT Setup

3.3 Field Testing

Once the SSPT device was developed and bench tested to be satisfactory, it was then applied for use in field trials to measure the lateral resistance of sleepers before and after resurfacing. This section details the methodology use to conduct this field testing.

3.3.1 Test Site Selection

The field testing was conducted on the Queensland Rail Network, on the Balloon Loop Departure Road at the Port of Brisbane.

Figure 3-11: Test Site at Port of Brisbane

The site was chosen due to the following factors:

- The track at the test site was constructed from low profile concrete sleepers
- The opportunity for testing existed due to a planned track closure for maintenance works
- Resurfacing machines were already scheduled to operate at the site during the closure
- Track workers were available to support the execution of testing
- The track had carried rail traffic of over several months since the last disturbance; so the ballast would be fairly consolidated and provides adequate "before resurfacing" results

3.3.2 Track and Sleeper Conditions

The test track was a relatively uniform section of straight track, consisting of low profile concrete sleepers and 41kg/m rail which was fastened by the Pandrol Fastclip system. The sleeper spacing was nominally 685mm centres as per Queensland Rail CETS. The track cant (superelevation) was nominally 0mm. The ballast bed profile was generally trapezoidal shaped, with a ballast shoulder width of nominally 0.35m. The size of the ballast was noted as the smaller, Grade B type material with a nominal size of 53mm. The level of consolidation of the ballast bed was visually assessed to be average.

Figure 3-12: Test Site Conditions

3.3.3 Identification of Test Zones

Two separate test zones were established. Each zone was approximately 30m long and contained approximately 50 sleepers.

- Zone 1 was not resurfaced, and would be the location of the "before resurfacing" tests
- Zone 2 was resurfaced, and was the location for the "after resurfacing"' tests

Within both zones, a selected number of sleepers were identified to be tested. The US DOT (2013) advised that at least three sleepers in a 50ft section of track are required to adequately determine the lateral sleeper resistance characteristics. Consequentially, at least three sleepers were marked for testing in each zone. This provided a range of results that could be averaged for improved accuracy of the overall result. Marking of sleeper involved applying a small paint dot to the top of the test sleeper for ease of identification amongst the other sleepers. A spacing of at least one sleeper was used between any two test sleepers. This prevented the loosened ballast caused by one test affecting the results of a subsequent test.
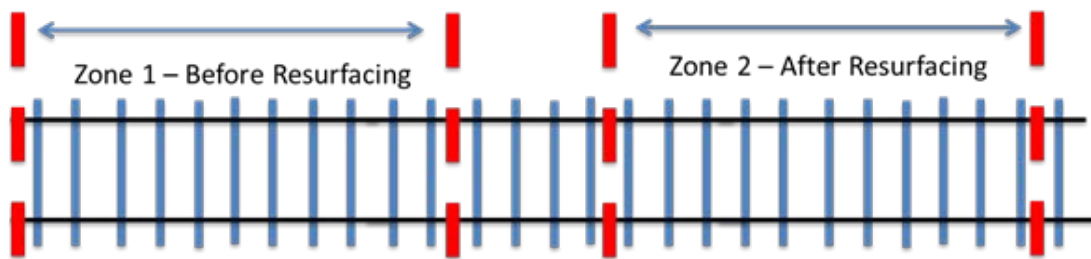
Figure 3-13: Test Zone Setup

3.3.4 Test Equipment

The equipment used to perform the Single Sleeper Push Testing consisted of:

- The Single Sleeper Push Test (SSPT) device developed earlier in the project

- An Enerpac RC55 hydraulic cylinder

- An Enerpac manual hand pump to power the hydraulic cylinder

- Load cell to record the force delivered to the test sleeper

- Linear Voltage Differential Transformer (LVDT) to measure test sleeper displacement

- Data acquisition unit and notebook computer to view and record the test results

- Two rail fixtures, to prevented the deflection of the reaction rail

- Hand tools including socket wrenches, shifters and hammers

- Crow bars to unfasten the rail fasteners

- Two rail jacks to lift both rails clear of the test sleeper
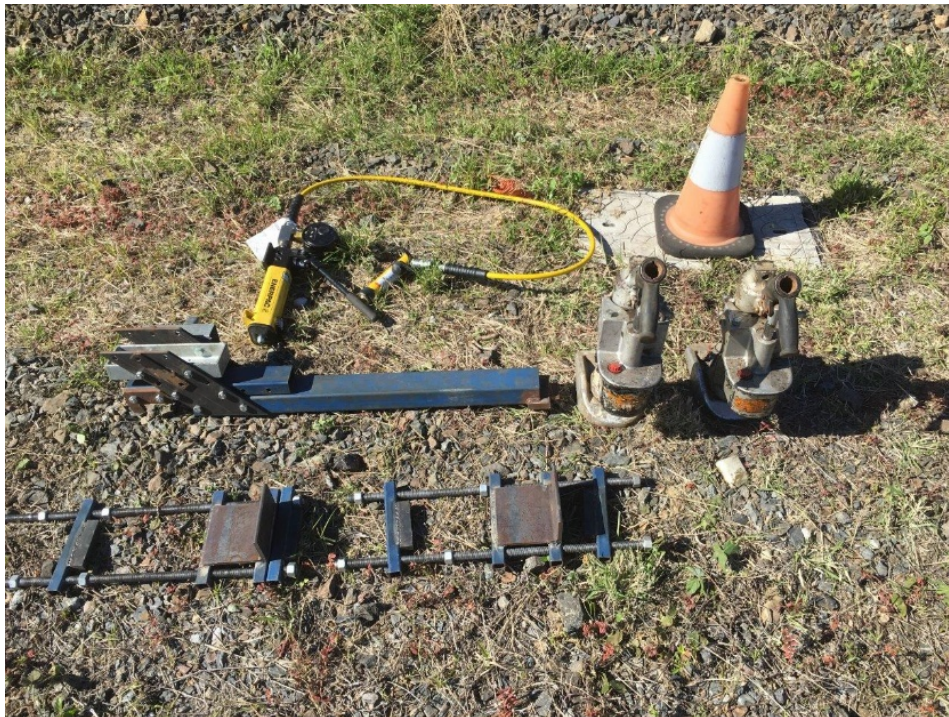
Figure 3-14: SSPT Equipment

3.3.5 Test Procedure

The rail fasteners of seven sleepers both sides of, and including the test sleeper, were removed using crow bars. Rail jacks were inserted underneath both rails and used to lift the rails approximately 50mm off the sleeper, so that the rail just clears the fastener shoulders – which were the highest point of the test sleeper. This clearance was required to enable the test sleeper to move freely beneath the rail. Care was taken not to jack the rail excessively clear of the test sleeper, as sleepers further away from the test sleeper, still fastened to the rail, would be lifted from the ballast bed. This would disturb the ballast around these sleepers and thus voided any results for those sleepers.

The ballast shoulder width of the test sleeper was measured prior to the SSPT device being attached to the test sleeper. The load cell was fitted behind the base of the hydraulic cylinder and was secured by applying light initial load through the SSPT device, by bringing the hydraulic cylinder just into contact with the head of the reaction rail. The LVDT was also installed so that the spring loaded plunger end was parallel to the SSPT device and touching the head of the reaction rail.

Rail fixtures were then fitted at the reaction rail end of the sleepers either side of the test sleeper.

Figure 3-15: SSPT Equipment Attached to Test Sleeper

Figure 3-16: Rail Fixture attached to Reaction Rail

At this stage, the data recording could commence. The data acquisition system was activated through the notebook computer. The hydraulic hand pump was operated smoothly and slowly to gradually apply an increasing load to the sleeper. The resistance-displacement characteristic curve of the sleeper was viewed on the notebook computer in real time during the test, and was used a guide to determine how far the sleeper needed to be pushed. As per the literature, sleepers were pushed so that a clear peak resistance load identified and continued until the load was found to plateau to a limiting resistance. Generally all data was captured within 25mm displacement of the test sleeper.

The results were saved to a Notepad file on the computer, where they could be extracted to Microsoft Excel. Here the data could be used to produce charts of the test sleeper's characteristic resistance-displacement curve, and enable visual identification of peak and limiting resistances.

At the completion of the test, the hydraulic pressure to the cylinder was released, and the SSPT device removed from the test sleeper, along with the rail fixtures. The displaced test sleeper moved laterally back into its original position by use of a crow bar, and then the rail jacks were released, lowering the rail back down onto the sleeper.

For subsequent tests, the equipment was moved along to the next test sleeper location, with additional fasteners removed as required to achieve the adequate 8m span of unfastened rail. At the completion of all testing, all rail fasteners were re-applied to the rail to ensure the track was returned to the same state as before testing, and was able to resume carrying rail traffic.

3.3.6 Test Operations

The testing was conducted in two stages. The first stage comprised of tests on four sleepers within Zone 1, which had not been resurfaced. Tests of these sleepers measured the "baseline" lateral resistance prior to resurfacing.

The second stage comprised of tests on five sleepers within Zone 2, which had been resurfaced. These tests measured the lateral resistance of the sleeper within a ballast bed which had been disturbed due to the resurfacing work. The results of these tests would be compared to the results of Zone 1 tests, so that the effect of resurfacing on lateral sleeper resistance could be measured.

The resurfacing process on both zones was carried using a Plasser 08-475 4S Switch Tamper Liner machine, which lifted, lined and tamped the track. The following machine settings were used:

- Track Lift = 20mm

- Number of workhead insertions per sleeper = 1

- Number of workhead tamps per insertion = 1

- Frequency of workhead vibration = 35Hz

Figure 3-17: Preparing the Zone B – Resurfacing

Behind the Tamper Liner, a Plasser SSP302 Ballast Regulator was used to pull ballast from the edges into the centre of the track, filling the cribs between the sleepers. Excess ballast was then pushed to the outside edges of the track, and evenly distributed to provide the correct trapezoidal ballast bed profile. All of this work was performed in one pass of the machines.

3.3.7 Field Test Post Processing

At completion of the field testing, the data for each test was extracted into Notepad and inserted into a Microsoft Excel spreadsheet. Two charts, one for the "before resurfacing" tests, and the other for the "after resurfacing" test were created. On these charts, lateral displacement was plotted along the x axis in millimetre units, and lateral sleeper resistance was plotted along the y axis in kilonewton units. During the testing process, if a test was found to be invalid due to inaccurate test execution, then the invalid data was identified and removed from the test data.

On both charts, an average SSPT curve for "before resurfacing" and "after resurfacing" conditions was established by creating a 6th order polynomial trend line for each individual test curve, and then producing a curve which is the average of each trend line. Both average curves were shown superimposed on a third chart, which enabled identification and comparison of the average "peak" and "limiting" resistances "before resurfacing" and "after resurfacing".

Consequentially the theoretical and field test results for lateral sleeper resistance were able to be compared. The most effective way to present this data was by a column chart.

3.4 Calculation of Critical Buckling Load

Bartlett's Equation was then used to calculate the Critical Buckling Load of the track, as per the Equation 2.9. The maximum average lateral resistance values measured "before resurfacing" and "after resurfacing" were applied to determine the Critical Buckling Load in both ballast conditions.

To use Bartlett's Equation, it was necessary to provide the amplitude and span of the initial misalignment as inputs into the Critical Buckling Load calculation. As initial misalignments are unpredictable by their nature, the amplitude and span were modelled as variables so their sensitivity on the Critical Buckling Load could be assessed. Consequentially, the results of Bartlett's Equation were presented in the form of four charts, as discussed below.

3.4.1 Critical Buckling Load versus Initial Misalignment Amplitude

This chart, 50kg A1, showed the variation of Critical Buckling Load with increasing misalignment amplitude. The initial misalignment amplitude was modelled as a variable with a range of value between 20mm and 100mm on the x axis of the chart. Critical Buckling Load was shown in kN on the Y axis of the chart. Two initial misalignment spans were modelled, 10m and 20m.

3.4.2 % Critical Buckling Load Loss, and Buckling FOS versus Initial Misalignment Amplitude

This chart, 50kg A2, showed the percentage reduction in Critical Buckling Load, and reduction of Buckling Factor of Safety, due to resurfacing against increasing misalignment amplitude. The initial misalignment amplitude was modelled as a variable with a range of value between 20mm and 100mm on the x axis of the chart. Percentage reduction in Critical Buckling Load, and buckling factor of safety, were shown on the primary and secondary Y axis of the chart respectively. Two initial misalignment spans were modelled, 10m and 20m.

3.4.3 Critical Buckling Load versus Initial Misalignment Span

This chart, 50kg B1 showed the variation of Critical Buckling Load with increasing misalignment span. The initial misalignment span was modelled as a variable with a range of value between 5m and 25m on the x axis of the chart. Critical Buckling Load was shown in kN on the Y axis of the chart. Two initial misalignment amplitudes were modelled, 25mm and 50mm.

3.4.4 % Critical Buckling Load Loss, and Buckling FOS versus Initial Misalignment Span

This chart, 50kg B2, showed the percentage reduction in Critical Buckling Load, and reduction of Buckling Factor of Safety, due to resurfacing against increasing misalignment span. The initial misalignment span was modelled as a variable with a range of value between 5m and 25m on the x axis of the chart. Percentage reduction in Critical Buckling Load, and buckling factor of safety, were shown on the primary and secondary Y axis of the chart respectively. Two initial misalignment amplitudes were modelled, 25mm and 50mm.

3.4.5 Calculation of Maximum Compressive Force.

To predict whether buckling is likely to occur, the Critical Buckling Loads calculated needed to be compared the maximum compressive force generated in the rails. Equation 2.8 was used to calculate the maximum compressive force, with the following inputs used:

- Rail size: 50kg/m
- Rail Neutral Temperature: 37 degrees Celsius
- Maximum Rail Temperature: 65 degrees Celsius

This scenario represents an extreme scenario expected on Queensland Rail's Network. The calculated maximum compressive force could then be determined and used to prediction of whether track buckling would occur after resurfacing, considering an initial misalignment with a known span and amplitude.

Prediction of buckling was possible using charts 50kg A1 and 50kg B1, by observing whether the "after resurfacing" Critical Buckling Load curves were located below the maximum compressive force line. Similarly, for charts 50kg A2 and 50kg B2, buckling was expected if the buckling factor of safety was less than one.

4. Results

This chapter presents the results pertaining to the two main sections of this study:

- The effect of resurfacing on lateral sleeper resistance of low profile concrete sleepers
- The effect of resurfacing on the Critical Buckling Load of the track

4.1 The Effect of Resurfacing on Lateral Sleeper Resistance

Two methods were used to determine the effect of resurfacing on lateral sleeper resistance:

- Theoretical calculation
- Field testing

This section presents the results acquired from both of these methods.

4.1.1 Theoretical Calculation of Lateral Sleeper Resistance

The equation developed by RTRI (2012) was applied to calculate the approximate lateral resistance expected from low profile sleepers, before and after resurfacing. The information used as inputs to perform this calculation, and the calculation output, is shown in the tables below.

$$F_{Peak} = aW + brG_e + crG_s$$

Where:

Parameter	Description	Value
F_{Peak}	Peak Lateral Sleeper Resistance	Calculated
W	Bulk mass of sleeper	165kg
r	Density of ballast	1760 kg/m^3 (before resurfacing) 1496 kg/m^3 (after resurfacing)
G_e	First moment of end area about top edge of sleeper	Refer Appendix K - 18.93 x 10^-3 m^3
G_s	First moment of side area about top edge of sleeper	Refer Appendix K - 2.08 x 10^-3 m^3
a	RTRI Sleeper/Ballast coefficient for Base Resistance	0.75
b	RTRI Sleeper/Ballast coefficient for End Resistance	29
c	RTRI Sleeper/Ballast coefficient for Side Resistance	1.8

Table 4-1: RTRI Equation Inputs

Ballast Condition	Peak Lateral Sleeper Resistance - F_{Peak} (kN)
Before Resurfacing	2.84
After Resurfacing	2.59

Table 4-2: Theoretical Equation Results

4.1.2 Field Testing of Lateral Sleeper Resistance

Single Sleeper Push Tests (SSPTs) were then conducted on the Queensland Rail Network to physically measure the lateral sleeper resistance of low profile concrete sleepers, before and after resurfacing. The resultant resistance-displacement curves obtained from this testing is shown in the sections below.

4.1.2.1 Single Sleeper Push Test Results – Before Resurfacing

Four sleepers from Zone 1 - the "before resurfacing" condition - were subject to Single Sleeper Push Tests, with the following results obtained:
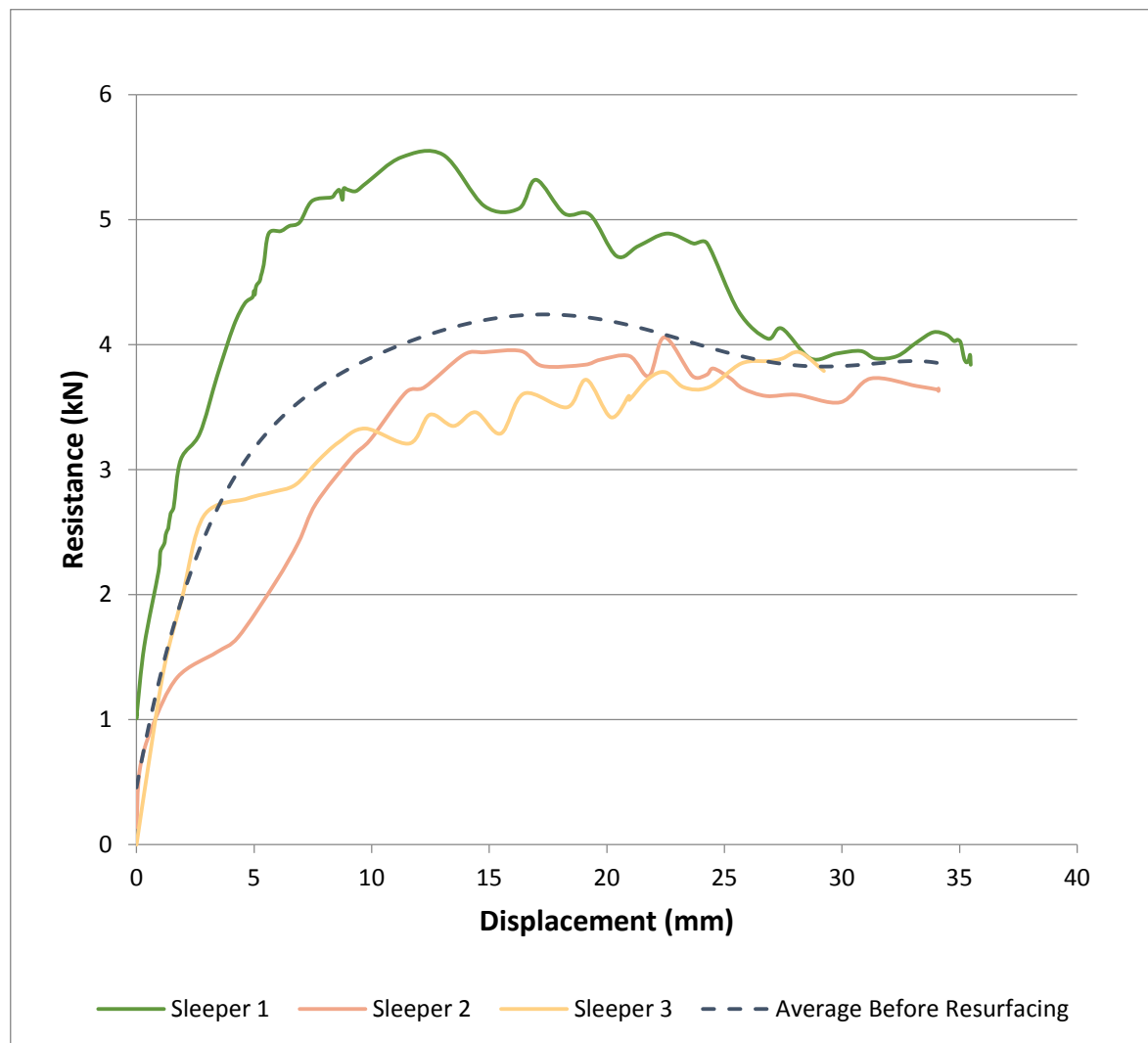
Figure 4-1: Before Resurfacing SSPT Results

Peak and limiting resistance was generally found within 15mm and 25mm lateral displacement respectively. Note that the results of Sleeper 4 were omitted from the final data set due to failed execution of its test. This will be further discussed. The raw data for these tests is found in Appendix B.

4.1.2.2 Single Sleeper Push Test Results – After Resurfacing

Five sleepers from Zone 2 - the "after resurfacing" condition - were subject to Single Sleeper Push Testing, with the following results obtained:
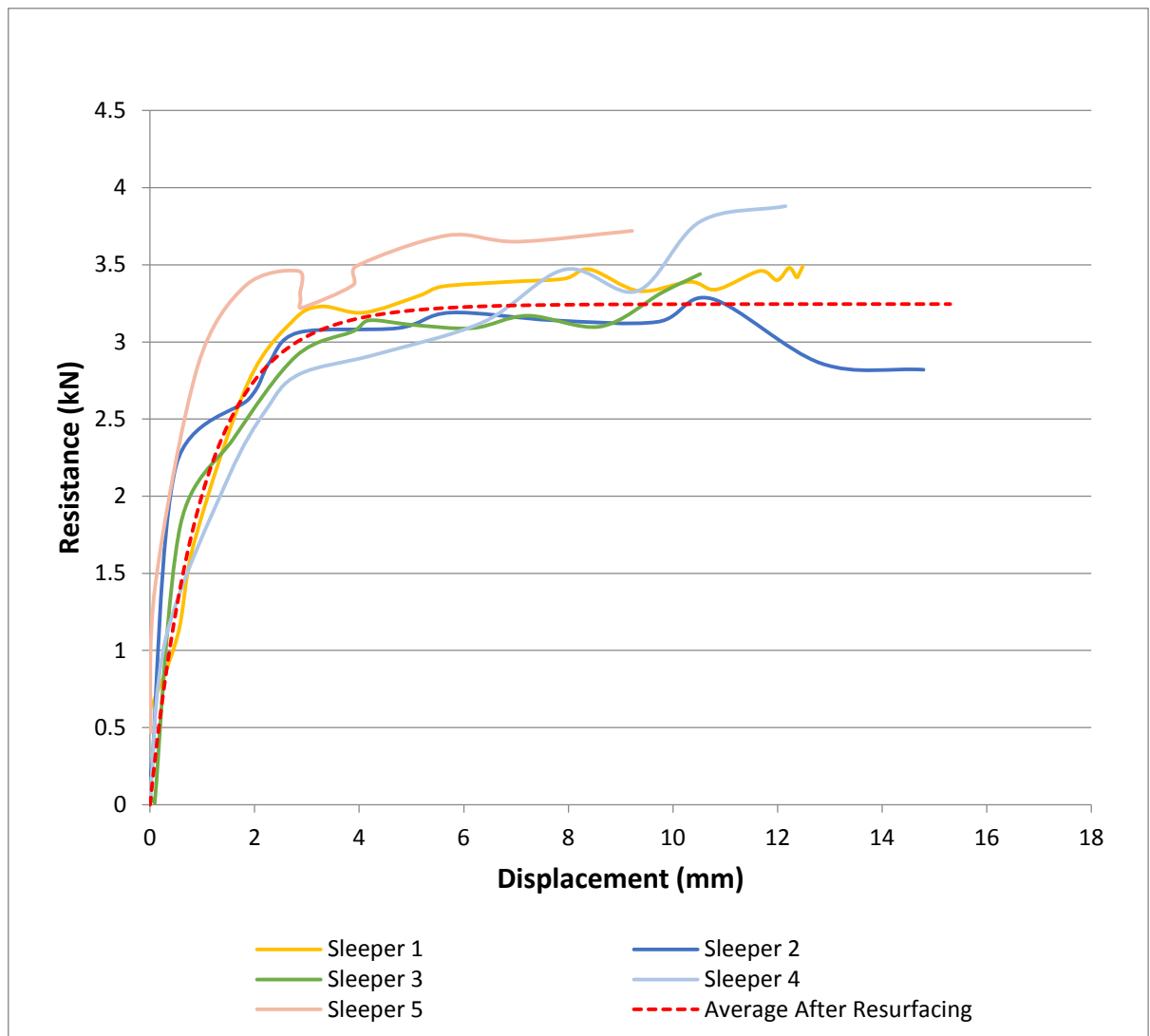
Figure 4-2: After Resurfacing SSPT Results

Limiting resistance was generally reached after 6mm of lateral displacement.

The "after resurfacing" tests were generally found to have a closer grouping of repatable results compared to the 'before resurfacing" tests. The raw data for these tests is found in Appendix C.

4.1.2.3 Single Sleeper Push Test Results – Average Before Versus After Resurfacing

The average "before resurfacing" and "after resurfacing" curves were then developed and overlaid on the same chart to assess the effect of resurfacing on lateral sleeper resistance, as shown below:
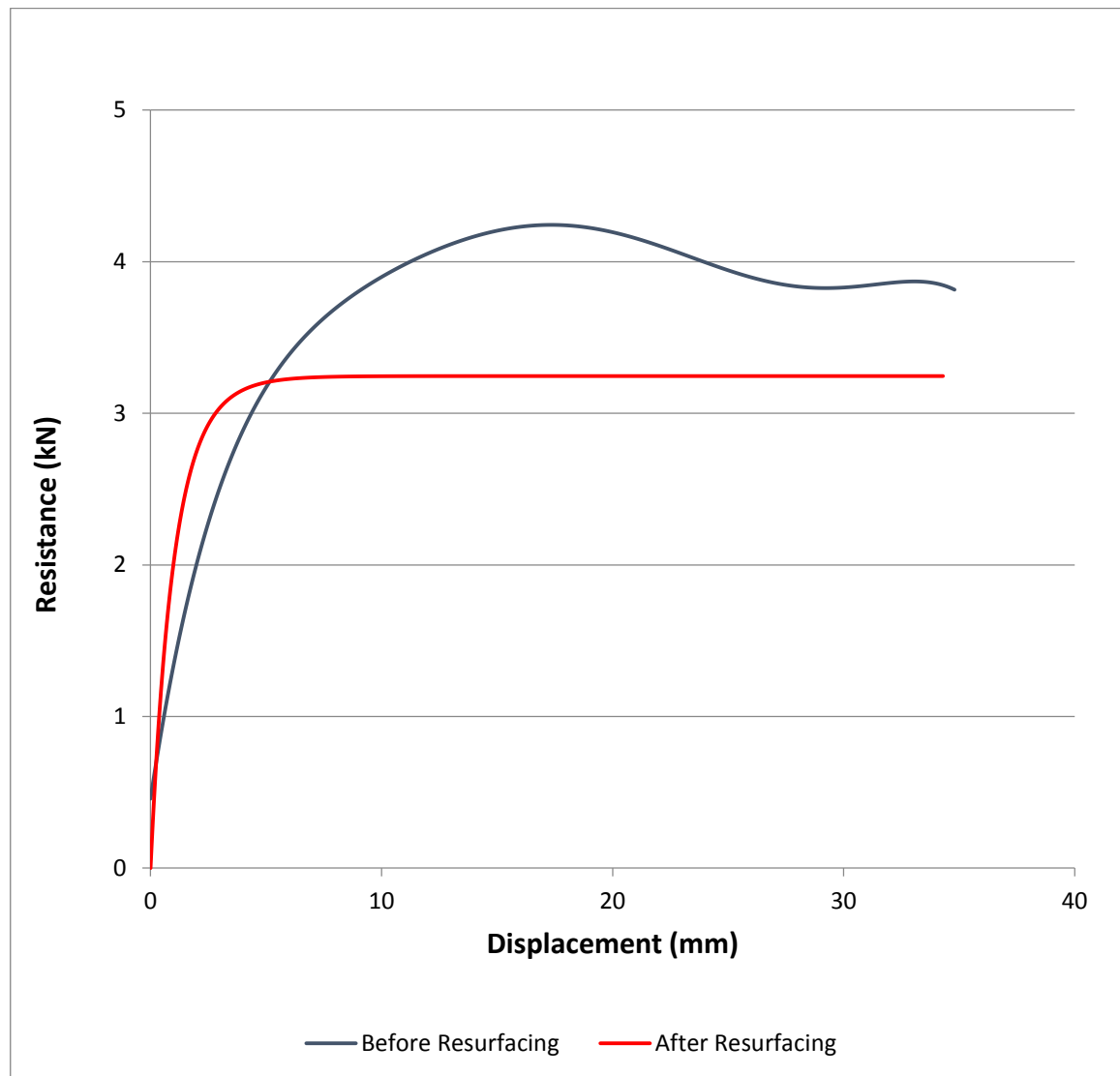
Figure 4-3: SSPT Result Comparison - Before vs After Resurfacing

4.1.3 Lateral Sleeper Resistance – Theoereitcal versus Experiemental Approaches

A comparison between the "before resurfacing" and "after resurfacing" lateral sleeper resistance results determined by theoretical and field testing was completed, as shown in the column chart below.
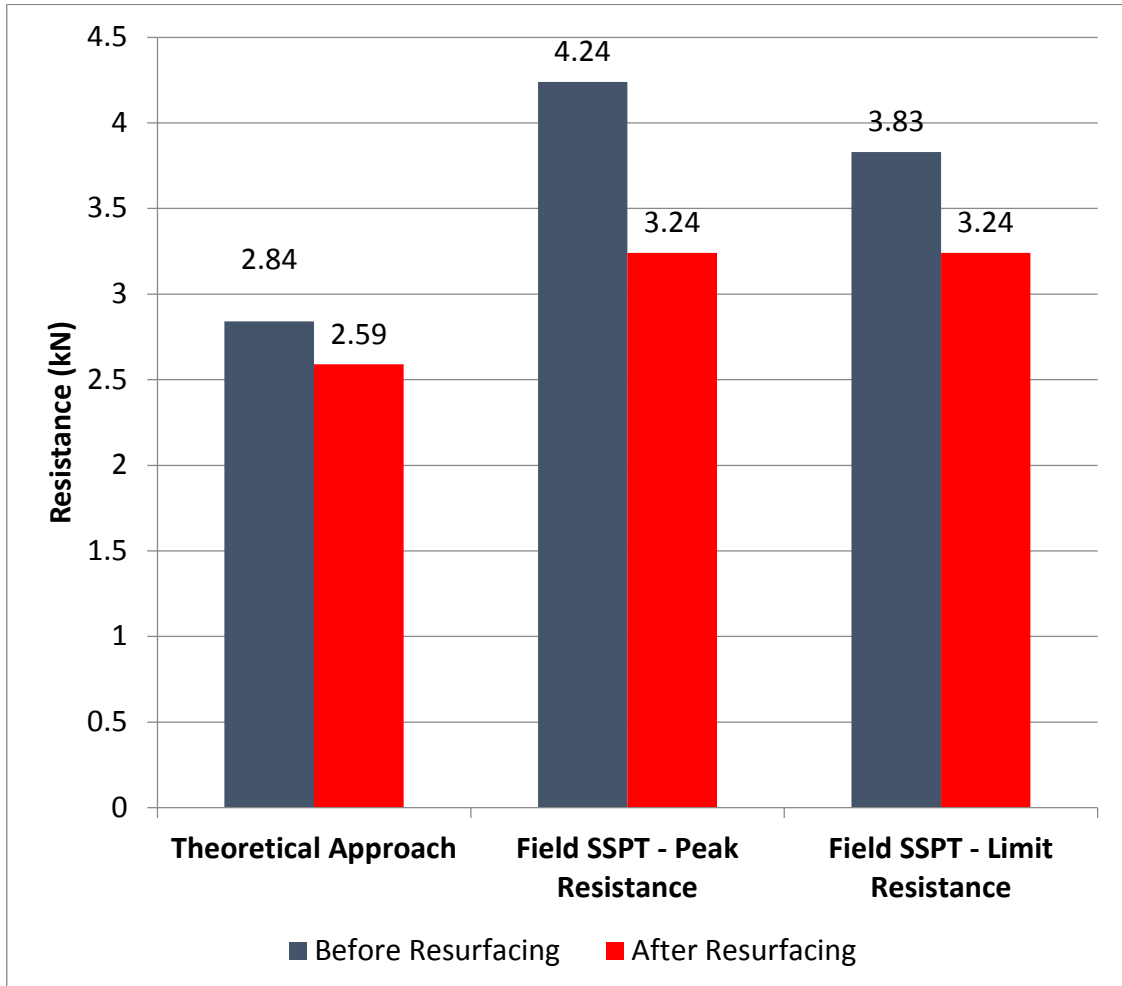
Figure 4-4: Theoretical vs SSPT Results

4.2 The Effect of Resurfacing on Critical Buckling Load

The average lateral sleeper resistance results provided by the field testing was then applied to determine the effect of resurfacing on the Critical Buckling Load of the track, according to Bartlett's Equation shown below.

$$Pcr = \frac{\pi^2 EI_s}{L_b{}^2 10^3} + \frac{\pi^2 C_t}{16S}\left[\frac{\pi L_b}{q_b}\right]^{0.5} + \frac{w_l L_b{}^2}{\pi^2 q_b} \quad Equation\ 2.9$$

Where:

Parameter	Description	Value
E	Modulus of Elasticity of Steel Rail	200 x 10^9 Pa
I_s	Moment of Inertia of two 50 kg/m rail about vertical axis	2 x 3.26 x 10^-6 m^4
L_b	Misalignment span	Variable (m)
C_t	Torsional stiffness of rail fastener	10 kNm/rad$^{0.5}$
S	Sleeper spacing	0.685m
w_l	**Maximum sleeper lateral resistance/meter (From Single Sleeper Push Tests)**	4.24/0.685 = 6.2kN/m (Before Resurfacing) 3.24/0.685 = 4.73kN/m (After Resurfacing)
q_b	Maximum misalignment amplitude	Variable (m)

Table 4-3: Bartlett's Equation Inputs

The initial misalignment span and amplitude were modelled as variables due to their unpredictable nature. Consequentially, four charts for the 50kg/m rail size were developed:

- Critical Buckling Load verses Initial Misalignment Amplitude (50kg A1)
- % Critical Buckling Load Loss & Buckling FOS versus Initial Misalignment Amplitude (50Kg A2)
- Critical Buckling Load verses Initial Misalignment Span (50kg B1)
- % Critical Buckling Load Loss, and Buckling FOS versus Initial Misalignment Span (50kg B2)

The charts were used as a model to predict whether buckling was likely to occur due to resurfacing. This was possible either by comparing the "after resurfacing" Critical Buckling Load against the maximum compressive force generated in the rail, or by simply identifying the buckling factor of safety after resurfacing, for a given initial misalignment with a known span and amplitude. Charts are provided in Appendices F and which are applicable for track constructed of 41kg/m and 60kg/m rail respectively.

This section presents the results of this modelling.

4.2.1 Calculation of Maximum Compressive Force

To predict whether buckling is likely to occur, the Critical Buckling Load needed to be compared the maximum compressive force generated in the rails due to heat.

Equation 2.8 was used as shown below.

$$P_{MAX\ COMPRESSIVE} = 2AE\alpha(T_{MAX} - T_0) \quad Equation\ 2.8$$

The input parameters used in the calculation of the maximum compressive force were as follows. Note that calculations for 41kg/m and 60kg/m rail sizes are given in Appendix E.

Parameter	Description	Value
A	Cross sectional area of 50kg/m rail	6451 mm^2
E	The Modulus of Elasticity for steel	200×10^9Pa
α	Coefficient of Thermal Expansion for steel rail	11.7×10^{-6} m/mk
T_{MAX}	The maximum expected rail temperature	65°C
T_0	The rail neutral temperature	37°C

Table 4-4: Maximum Compressive Force Inputs

Therefore, the maximum compressive load was calculated as follows:

$$P_{MAX\ COMPRESSIVE} = 2 \times 6451 \times 200 \times 10^9 \times 11.7 \times 10^{-6} \times (65 - 37)$$

$$P_{MAX\ COMPRESSIVE} = 845\text{kN}$$

4.2.2 Chart 50kg A1 - Critical Buckling Load versus Initial Misalignment Amplitude

The relationship between resurfacing and initial misalignment amplitude on the track's Critical Buckling Load was modelled using the chart below.
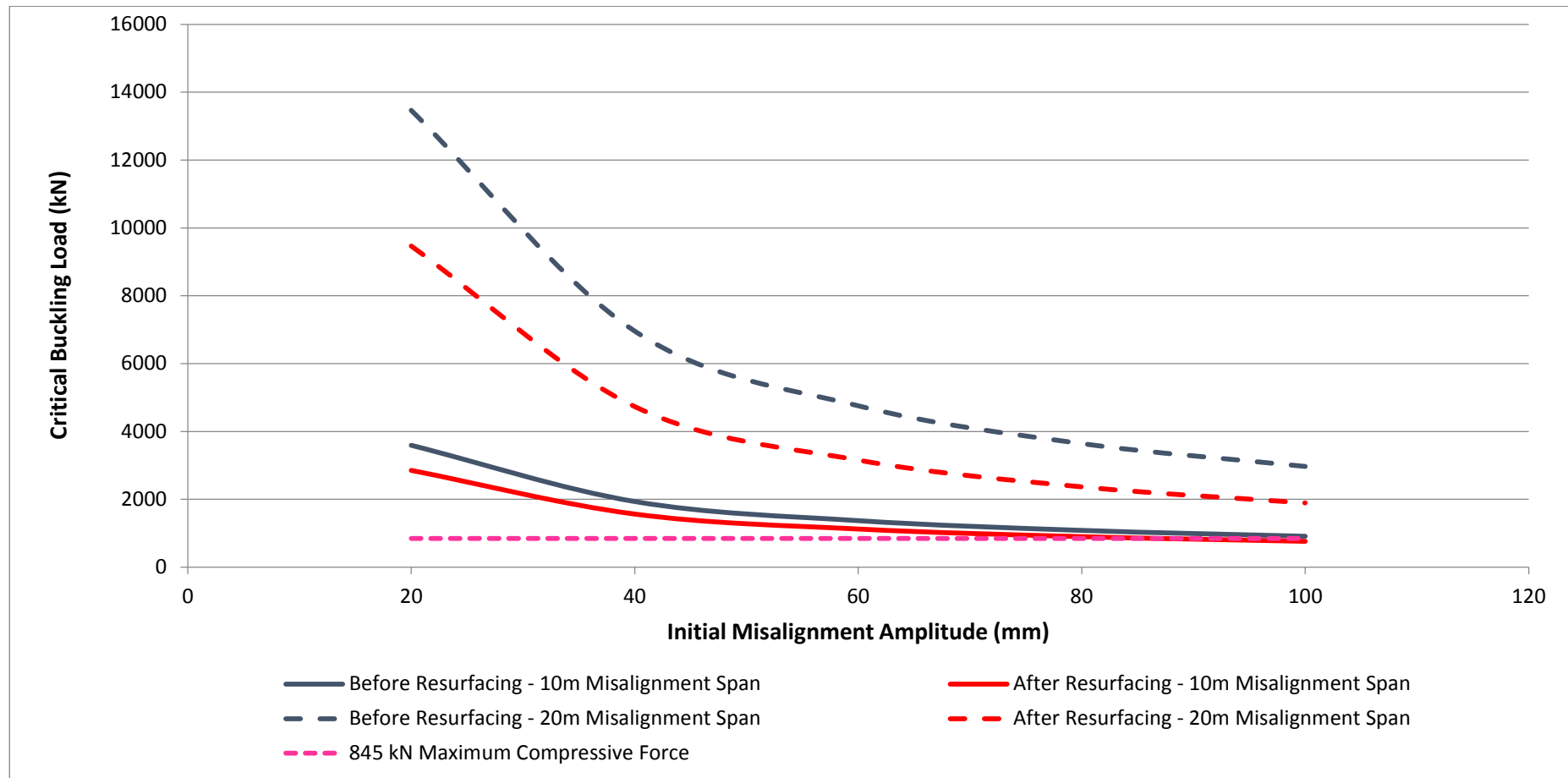
Figure 4-5: Chart 50kg A1 - Critical Buckling Load vs Initial Misalignment Amplitude

4.2.3 Chart 50kg A2 - % Critical Buckling Load Loss & Buckling FOS versus Initial Misalignment Amplitude

The relationship between the reduction in Critical Buckling Load, and the buckling factor of safety after resurfacing versus initial misalignment amplitude was modelled using the chart below.
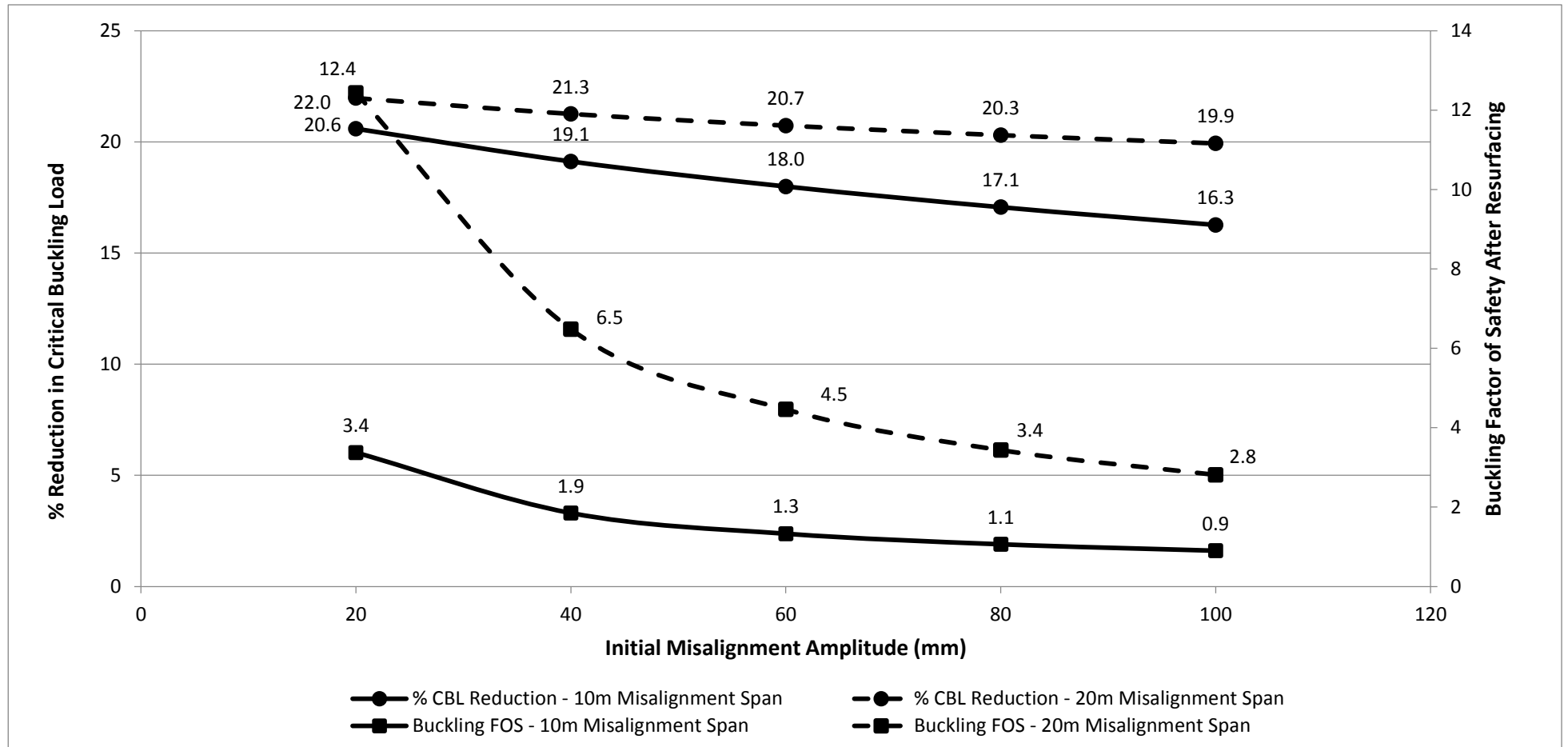
Figure 4-6: Chart 50kg A2 - % Reduction of Critical Buckling Load and Buckling FOS versus Initial Misalignment Amplitude

4.2.4 Chart 50kg B1 - Critical Buckling Load versus Initial Misalignment Span

The relationship between resurfacing and initial misalignment span on the Critical Buckling Load of the Track were modelled using the chart below.
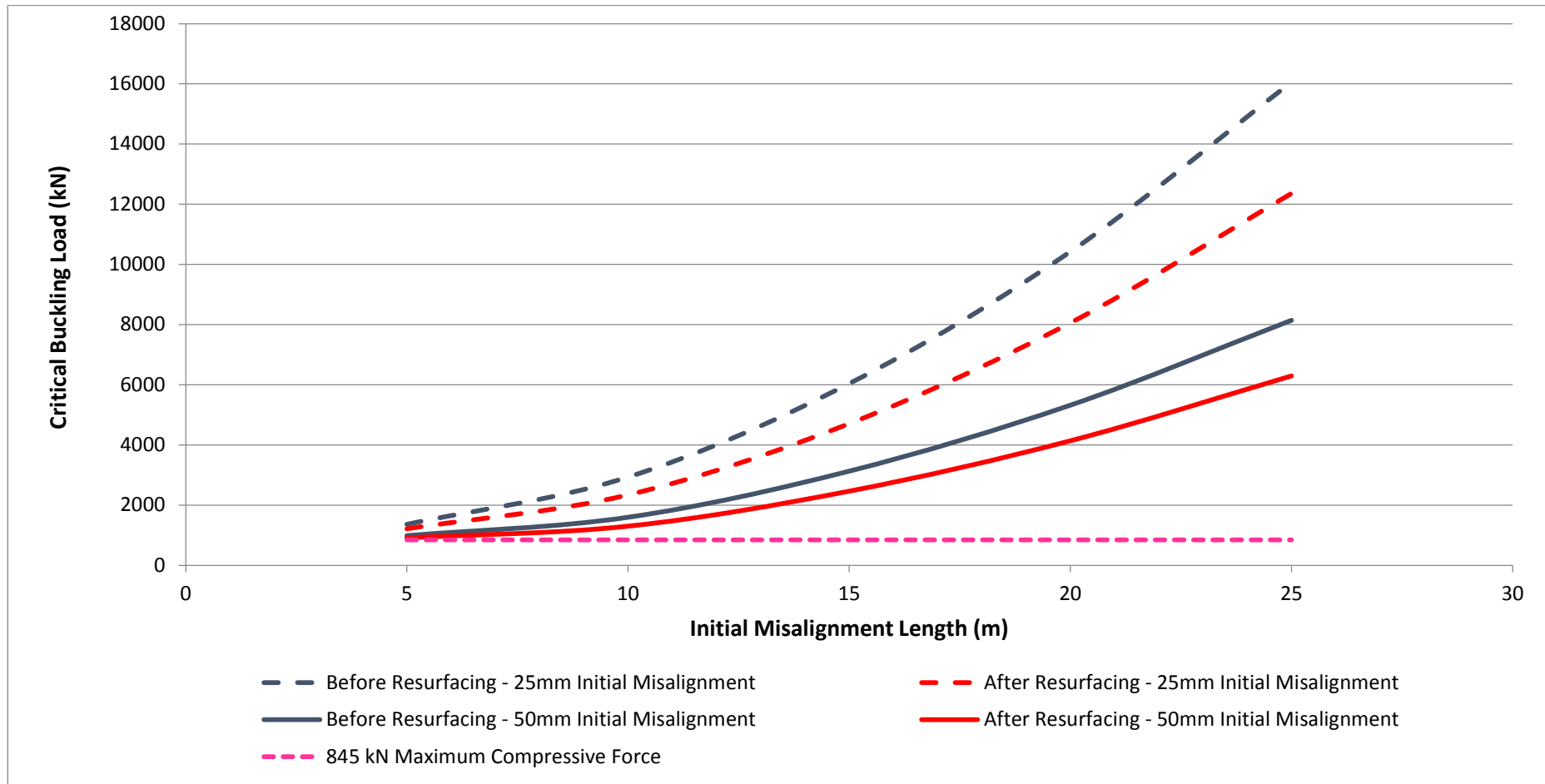
Figure 4-7: Chart 50kg B1 - Critical Buckling Load versus Initial Misalignment Span

4.2.5 Chart 50kg B2 - % Critical Buckling Load Loss & Buckling FOS versus Initial Misalignment Span

The relationship between the reduction in Critical Buckling Load, and the buckling factor of safety after resurfacing versus initial misalignment span was modelled using the chart below.
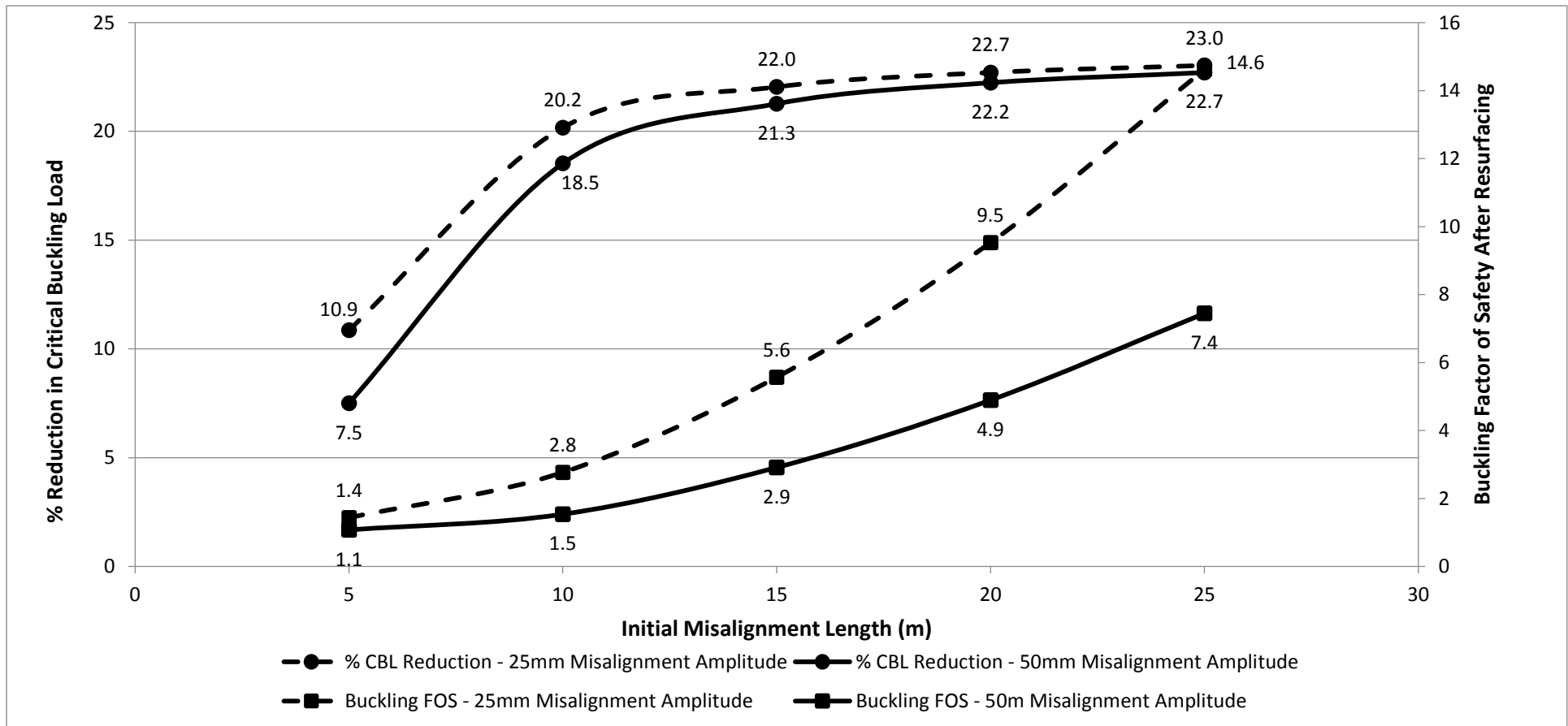
Figure 4-8: Chart 50kg B2 - % Reduction of Critical Buckling Load and Buckling FOS versus Initial Misalignment Span

4.3 Summary

The results indicate that resurfacing has an initial detrimental impact on the lateral resistance of low profile concrete sleepers.

The theoretical approach predicted an 8.8% reduction in lateral resistance after resurfacing, from 2.84kN to 2.59kN per sleeper.

The experimental approach involved performing Single Sleeper Push Tests on Queensland Rail's Network. Four SSPTs were performed on sleepers which had not been resurfacing, which resulted in an average peak and limiting lateral resistance of 4.24kN and 3.83kN respectively. Five SSPTs were performed on sleepers immediately after resurfacing, which found these sleepers had a limiting lateral resistance of 3.24kN. Hence resurfacing was found to reduce lateral resistance by 24% based on peak resistance, and 14% based on limiting resistance.

The lateral sleeper resistance data acquired through field testing was then used to determine the effect of resurfacing on the critical buckling load of the track. Modelling was used to predict whether buckling was likely to occur after resurfacing by comparing the Critical Buckling Load to the maximum compressive load generated in the rails due to heat.

It was found that resurfacing reduced the Critical Buckling Load of the track in a range between 7.5% and 23%, dependant on the span and amplitude of the initial misalignment. After resurfacing, the buckling factor of safety was observed to be in a range of 14.6 to 0.9, depending on the span and amplitude of the initial misalignment.

The worst case for buckling factor of safety was found to be a large amplitude misalignment acting over a short span. For example, a 50mm misalignment acting over 5m on resurfaced track was expected to reduce the Critical Buckling Load by 7.5%, and return a factor of safety against buckling of 1.1. For this situation, the buckling factor of safety is marginal and buckling would be imminent under these conditions.

5. Discussion

5.1 Theoretical Calculation of Lateral Sleeper Resistance

Theoretical calculation of lateral sleeper resistance, before and after resurfacing, was estimated to be 2.84kN and 2.59kN respectively using the calculation offered by RTRI (2012). Hence the reduction in lateral sleeper resistance due to resurfacing was 0.25Kn or 8.8%. The application of this theoretical approach required some assumptions and simplifications to be made, which have an influence on the results as discussed below.

5.1.1 Assumption of Bulk Ballast Density

An assumption was made regarding the bulk density of the ballast. Dingqing et al. (2012) advised that the ballast bulk density before and after resurfacing was approximately 1760 kg/m^3 and 1600kg/m^3 respectively; however density reductions of up to 30% have been noted. The ballast densities estimated in the use of this method were 1760kg/m^3 and 1496kg/m^3 respectively. As ballast density is dependent on a range of factors including ballast material, size and level of disturbance, the advice of Dingqing et al. (2012) may not be directly applicable considering the type of ballast used by Queensland Rail. Inaccuracies in this assumption would directly impact the accuracy of this theoretical calculation and agreement with the field test results.

5.1.2 Simplified Sleeper Geometry

The theoretical approach required the determination of the first moment of the side and end areas of the sleeper, about the top edge of the sleeper. To simplify this calculation, the geometry of the sleeper was idealised to be a trapezoidal prism. This simplification ignored some minor features and facets of the sleeper, such as the narrowing of width at the ends of the sleeper. While this did not fully represent the actual sleeper geometry, it did model the geometry sufficiently for practical calculation and application of the formula. The calculation of the first moment of area can be found in Appendix G. Some error between the theoretical and field measurement approaches could be attributed the geometry simplification used.

5.1.3 Assumed Ballast & Sleeper Material Coefficients

The coefficients used in the theoretical calculation were those offered by RTRI (2012). Due to the current gap of knowledge, it was assumed that the coefficients for "concrete sleeper in crushed rock ballast" offered were equivalent to Queensland Rail's sleeper and ballast conditions. However, this assumption may not be completely accurate do to basic differences in the ballast material, size and density of QR's locally sourced basalt ballast compared to those tested by RTRI.

5.2 Field Testing Results

This section discusses the SSPT results acquired on sleepers, before and after resurfacing.

5.2.1 Before Resurfacing SSPT Results

The "before resurfacing" SSPTs were conducted on four sleepers to measure the baseline lateral sleeper resistance available prior to resurfacing. The resultant SSPT curves as shown in figure 4-1 generally agreed with the literature by displaying following typical characteristics:

- a steep initial resistance gradient
- a distinctive "peak" resistance
- A softening of the resistance after the peak resistance
- A gradual plateauing to a constant limiting resistance value

Across the three valid SSPTs performed, the average peak lateral resistance was 4.24kN, while the average limiting lateral resistance was 3.83kN.

5.2.2 After Resurfacing SSPT Results

The "after resurfacing" tests were conducted to measure the effect of resurfacing on the lateral resistance of the sleeper. This testing was conducted immediately after resurfacing, when the ballast was significantly disturbed and loosened. The resultant SSPT curves shown in figure 4-2 matched the typical curve expected for resurfaced track, where the resistance increased proportionally to sleeper displacement up to a constant limiting resistance value. Any further lateral movement of the sleeper beyond this point did not increase the lateral resistance of the sleeper. The test data appeared to be more uniform than the "before resurfacing" test data.

For five SSPTs performed, the average limiting resistance was 3.24kN.

5.2.3 Comparison of Average Before and After Resurfacing Results

When the average "before resurfacing" and "after resurfacing" results were comparted, resurfacing was found to reduce the lateral sleeper resistance by 1 kN based on "peak resistance", or 0.59kN based on "limiting resistance".

The initial resistance of the "before resurfacing" result was found to be less stiff when compared to the after resurfacing result, as shown by the shallower gradient of the "before resurfacing" curve. The "before resurfacing" result achieved the peak resistance of 4.24kN at approximately 17mm displacement, while the "after resurfacing" result achieved it's the maximum resistance of 3.24Kn only after 4mm displacement.

While there is no clear reason why the post resurfacing result is stiffer than the pre resurfacing results, a possible explanation for this could be attributed to the packing of ballast around the

sleeper during resurfacing. Ballast is compacted underneath and between the sleepers during resurfacing, causing a high initial resistance "stiffness". However due to the global disturbance of the ballast around the sleeper, the high initial resistance is effective only through a small range of sleeper displacement. At a certain point, further sleeper displacement results in the ballast failing to provide any increase in resistance.

Conversely, before resurfacing the ballast bed has been compacted by cumulative train loadings. The unique edges of the ballast particles interlock with one another, and the bulk density of the ballast bed is increased. The robust interlocking of ballast particles throughout the ballast bed results in a lateral sleeper resistance which is effective through a larger range of sleeper displacement. Hence the sleeper has a greater lateral resistance to displacement before the ballast reaches a limiting resistance condition compared to the "after resurfacing" condition.

5.3 Comparison of Theoretical Calculation versus Field Testing Results

Comparison of theoretical and field testing results agreed that resurfacing results in a temporary loss in lateral resistance of the sleeper, which was consistent with the findings of the literature.

The theoretical results indicated that an 8.8% reduction was expected due to resurfacing, from 2.84kN to 2.59kN. The field testing results showed that a reduction of 24% in lateral sleeper resistance based on peak resistance – from 4.24kN to 3.24kN, or a 14% reduction based on "limiting" resistance – from 3.83kN to 3.24kN.

It can be seen that the theoretical results were considerably lower than the field testing results. Explanations for this difference are thought to be due to the range of assumptions and simplification made in the process of using the theoretical approach, as discussed in section 5.1. Recapping, these assumptions and simplifications were:

- Assumption of the ballast bulk density values before and after resurfacing
- Simplification of the sleeper geometry
- Assumption that the sleeper/ballast material coefficients offered by RTRI (2012) are accurate

5.4 Effect of Resurfacing on Critical Buckling Load of the Track

Using the lateral sleeper resistance data acquired through field testing, Bartlett's Equation was then used to calculate the Critical Buckling Load, before and after resurfacing. Two of the input parameters to this equation were the span and amplitude of the initial misalignment. As the shapes of initial misalignments are unpredictable, the span and amplitude were modelled as variables in the calculation of Critical Buckling Load. Consequentially, the effect of resurfacing on Critical Buckling Load was presented in the form of four charts discussed below. Across all charts, resurfacing was found to reduce the Critical Buckling Load of the track.

5.4.1 Chart 50kg A1: Critical Buckling Load versus Initial Misalignment Amplitude

The results of this chart indicated that as the initial misalignment amplitude increased; the Critical Buckling Load of the track was reduced. The relationship was not linear, but rather modelled by a second order polynomial. An initial misalignment with a small amplitude was relatively much more tolerable than a larger amplitude misalignment.

Two misalignment spans were modelled - 10m and 20m. It was found that the larger the misalignment span, the Critical Buckling Load increased. Thus, it could be deduced that severe initial misalignments acting over a short span is a far worse scenario for track buckling compared to a minor initial misalignment acting over a large span. For example, "kicks" are worse track defects for initiating track buckles compared to "swings".

This chart could be used to predict whether resurfacing would cause sufficient reduction in bucking resistance to cause a track buckling condition. This was achieved by comparing the critical buckling load curve to the 845kN compressive force expected when rail temperatures reach 65 degrees Celsius – the maximum rail temperature expected for Queensland Rail track.

5.4.2 Chart 50kg A2: % Critical Buckling Load Loss, and Buckling FOS versus Initial Misalignment Amplitude

This curve used the data from Chart 50kg A1 show to the following functions

- % loss in Critical Buckling Load after resurfacing versus misalignment amplitude
- Buckling Factor of Safety after resurfacing versus misalignment amplitude

The charts could be used to predict the likelihood of buckling as discussed below.

Considering an initial misalignment of 40mm acting over a 20m span, after resurfacing the Critical Buckling Load was expected to be reduced by 21.3% and return a factor of safety against buckling of 6.5.Hence a substantial buckling resistance exists in this situation, with the track at a low risk of buckling.

Alternatively, considering an initial misalignment of 80mm acting over a 10m span, after resurfacing the Critical Buckling Load was expected to be reduced by 17.1% and return a factor of safety against buckling of 1.1.Hence a marginal buckling resistance exists in this situation, with the track at a high risk of buckling.

5.4.3 Chart 50kg B1: Critical Buckling Load versus Initial Misalignment Span

This chart presented the relationship between Critical Buckling Load and Initial Misalignment span. The results indicated that as the span of the initial misalignment increased, so too did the Critical Buckling Load of the track. The relationship was found not to be linear, but rather best modelled by a second order polynomial. The results indicated that for the same initial misalignment amplitude, a large span was relatively much more tolerable than a small span.

Two initial misalignment amplitudes were modelled, 25mm and 50mm, with the greater amplitude found to reduced Critical Buckling Load, thus supporting results obtained from Chart 50kg A1.

Similar to Chart 50kg A1, this chart could be used to predict whether resurfacing would cause sufficient reduction in bucking resistance to cause a track buckling condition. This was achieved by comparing the critical buckling load curve to the 845kN compressive force expected when rail temperatures reach 65 degrees Celsius – the maximum rail temperature expected for Queensland Rail track.

5.4.4 Chart 50kg B2: % Critical Buckling Load Reduction, and Buckling Factor of Safety versus Initial Misalignment Span

This curve used the data from Chart 50kg B1 show to the following functions

- % loss in Critical Buckling Load after resurfacing versus initial misalignment span
- Buckling Factor of Safety after resurfacing versus initial misalignment span

The charts could be used to give an indication of the likelihood of buckling as discussed below.

Considering an initial misalignment of 25mm acting over a 20m span, after resurfacing the Critical Buckling Load was expected to be reduced by 22.7% and return a factor of safety against buckling of 9.5.Hence a substantial buckling resistance exists in this situation, with the track at a low risk of buckling.

Alternatively, considering an initial misalignment of 50mm acting over a 5m span, after resurfacing the Critical Buckling Load was expected to be reduced by 7.5% and return a factor of safety against buckling of 1.1.Hence a marginal buckling resistance exists in this situation, with the track at a high risk of buckling.

5.3 Field Testing Issues

This section discusses the technical difficulties encountered during execution of the field testing.

5.3.1 Insufficient Rail Lift

During execution of the Sleeper 4 within Zone 1 (the fourth before resurfacing test), one rail was found to be insufficiently jacked above the highest part of the sleeper. After approximately 10mm movement, the test sleeper contacted the insufficiently raised rail, which immediately caused an artificial "spike" in the measured lateral sleeper resistance as shown below.
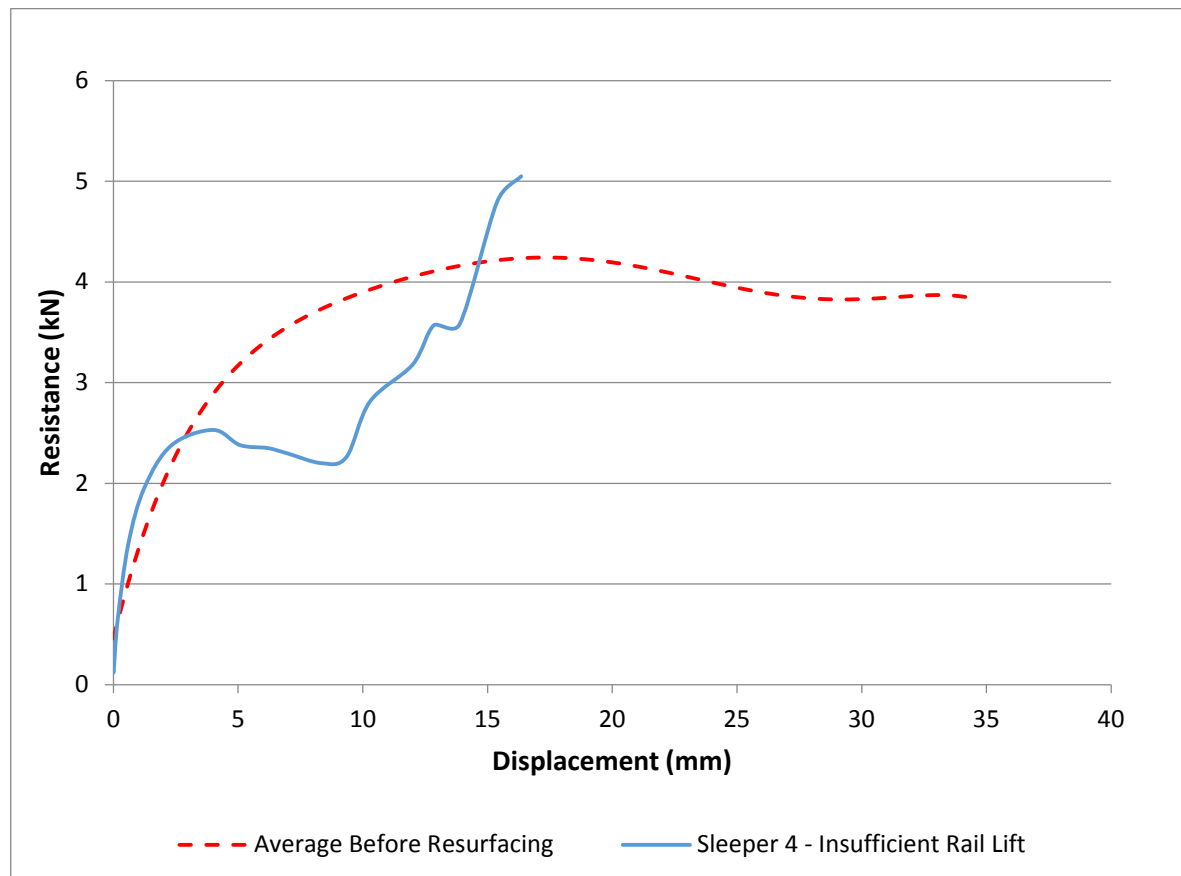
Figure 5-1: SSPT Curve for "Before Resurfacing" Sleeper 4 - Insufficient Rail Lift

As this test prematurely ended and was not representative of normal behaviour, the results of this test were omitted from the final data set.

5.3.2 Insufficient Fastener Removal

In preparation of a field test, an insufficient number of sleepers were unfastened either side of the test sleeper. When both rails were jacked to lift the rail clear of the test sleeper, the sleepers still fastened to the rails were lifted in the ballast bed. This disturbed the ballast between these sleepers, which would affect their lateral sleeper resistance. Hence these sleepers were identified during at the time of the ballast disturbance, and were not selected as candidate test sleepers.

5.4 SSPT Device Discussion

This section discusses the practicality and usefulness of the SSPT device developed.

5.4.1 Portability

Aside from functionality, a key requirement for the Single Sleeper Push Test Device was that it needed to be portable. With a length of approximately 1100mm, the manufactured SSPT device was able to be transported to site in the boot of a typical sedan motor vehicle. The mass of the device was measured to be approximately 15kg, so it enabled the equipment to be carried by one person. This was found to be particularly advantageous because vehicles could not always be relied to fully reach the test site, and the equipment would be required to be manually handled and transported from the vehicle to the test site, as well as between sleepers during tests.

5.4.2 Adjustment for Rail Sizes

The device was initially designed to suit 50kg/m and 60kg/m rail. However, during planning of the field testing, it was found that the track to be used was constructed from 41kg/m rail. Hence the device was modified prior to field testing with an adjustable bracket which enabled the hydraulic cylinder to be mounted higher or lower to account for the varying rail head position due to different rail sizes. This modification therefore increased the useful scope of the device to accommodate all rail sizes used on the QR Network.

5.4.3 Setup Time

Gill (2007) investigated a SSPT device used primarily for the testing of full profile concrete sleepers on QR's Network. A requirement for the use of this device was the need to excavate ballast away from the sleeper end, to the bottom of the test sleeper. This was so the frame of the device could be fitted to the track without interference with the ballast, and so the hydraulic cylinder was able to push off the end surface of the sleeper. This process was found to be labour and time intensive, which limited the number of tests which could be performed on track.

Additionally, the removal of ballast caused a disturbance of ballast around the test sleeper, which could potentially impact on the validity of the results. Furthermore, the ballast returned to the end of the sleeper at the completion of testing was extremely loose and not consolidated before returning the track to operate trains. This results in ballast which is highly disturbed at the end of the sleeper, lowering the lateral sleeper resistance and the critical buckling load of the track.

Hence, for the SSPT device developed as part of this study, these past SSPT device lessons were considered and used as inputs in the design process. A focus on the minimisation of time, labour and track disturbance were driving factors for the design intent.

As a result of these design drivers, it was validated during field testing that the newly developed SSPT device was capable of delivering a completed test approximately every 20 minutes using a three person team. Considering this was the first time the device had been used in the field, with further experience using the equipment the time interval between testing could be reduced significantly.

Due to the manner in which the device attached to the low profile concrete sleeper and pushed off the reaction rail, no excavation of the ballast shoulder was required. This was highly beneficial as it eliminated any pre disturbance of the ballast bed prior to the testing, meaning the lateral sleeper resistance results would be not affected by unintentional disturbance of the ballast. Furthermore, the process resulted in less disturbance of the track as the sleeper was required to be pushed approximately 25mm for sufficient data to be gained. Once the test was completed, the test sleeper was simply crow-barred 25mm back into place.

An area where the device design could be improved relates to the rail fixtures. The attachment method consisted of clamping the reaction frame to the fastener shoulder, using nuts which wound down on a threaded rod. As the length of the threaded rod was significantly longer than it was functionally required to be, the number of rotations of the nuts required was time consuming. By improving this aspect of the rail fixture design, there is an opportunity for further reductions of the setup time.

6. Conclusion

This study investigated the effect of resurfacing on the lateral resistance of narrow gauge low profile concrete sleepers, and the consequent effect on the track's critical buckling load. The investigation found that resurfacing did reduce lateral sleeper resistance and the track's critical buckling load. However, critical buckling load was also found to be highly dependent on the span and amplitude of the initial misalignment.

Resurfacing was measured to reduce lateral sleeper resistance through two separate approaches. Firstly, a theoretical method was used to calculate an 8.8% reduction in lateral sleeper resistance after resurfacing. This approach required several assumptions to be made, including the value of ballast bulk density before and after resurfacing, simplification of the sleeper geometry, and assumption that the sleeper/ballast coefficients offered by RTRI (2012) were valid for QR's track conditions.

The second approach to determine the effect of resurfacing on lateral sleeper resistance was through field testing, where a series of Single Sleeper Push Tests (SSPTs) were performed on the QR network. As there was no "off the shelf" SSPT device available to suit narrow gauge low profile concrete sleepers, a device was designed, manufactured and tested which was suited the local conditions. The SSPT device enabled the lateral resistance of the sleeper to be measured as a function of sleeper displacement. The results of field testing found that resurfacing reduced lateral sleeper resistance by 24% based on "peak" resistance, and 14% based on "limiting' resistance. Generally there was fair agreement between the two methods; however field testing returned higher values of lateral sleeper resistance than predicted by the theoretical approach.

The lateral resistance results were then applied to Bartlett's Equation to determine the effect of resurfacing on the critical buckling load of track constructed from 50kg/m rail. The initial misalignment span and amplitude parameters were modelled as variables due to their unpredictable nature in the field. The resultant charts developed showed that after resurfacing, the track's critical buckling load was reduced by 7.5% to 23%, and the track's factor of safety against buckling ranged from 14.6 to 0.9, depending on the span and amplitude of the initial misalignment. Increased amplitude and decreased span were found to be detrimental misalignment characteristics with regard to critical buckling load and factor of safety against buckling. The charts developed provided a means of predicting the likelihood of track buckling for a given misalignment, considering both before and after resurfacing track conditions. This was achieved by comparison of the determined critical buckling load against the calculated compressive rail force generated by heating the rails. 65 degrees Celsius was the assumed maximum temperature of rails on the network.

The information and modelling presented in this study may provide guidance for the management of resurfacing works in warm weather, and also a means for prioritisation and management of residual misalignments identified after resurfacing, for the prevention of track buckling.

6.1 Areas of Further Study

Many areas of further study exist, as outlined below:

6.1.1 More Field Testing to Strengthen Current Knowledge

More field tests performed on sleepers "before" and "after" resurfacing, with varying ballast shoulder depths, on "Grade A" ballast, would increase the depth of data and strengthen the knowledge gained from this study. This will provide increased confidence in the values determined for "peak" and "limiting" lateral resistance for both track conditions. Additionally, an increased amount of testing will result in training opportunities for the staff of Queensland Rail to become familiar with performing the SSPT.

6.1.2 Investigation of Resurfacing Machine Settings

More field tests to measure the effect of resurfacing machine settings on lateral sleeper resistance could be explored. Such settings include amount of track lift, compaction pressure of the ballast, number of squeeze cycles per workhead insertion, and number or insertions per sleeper. Study of this area may identify optimum machine settings for resurfacing.

6.1.3 Measurement of Lateral Sleeper Recovery Techniques

More field tests to determine the effectiveness of lateral sleeper resistance restorative techniques could be investigated. There are currently two main techniques used: cumulative traffic loading and Dynamic Track Stabilisation. Comparison of the recovery techniques would be useful information relating to how the track would be managed post resurfacing in warm weather conditions.

6.1.4 Adaption of the SSPT Device to Suit other Concrete Sleeper Designs

Further development of the SSPT device to permit testing of other concrete sleeper designs would increase the versatility of the equipment. Preliminary analysis indicated this could be achieved by modifying the ends of the SSPT device to become adaptable to other rail fastener designs.

6.1.5 Determination of Suitable Coefficients for Theoretical Equation

Values for the coefficients of the theoretical approach offered by RTRI (2012) suited the Queensland Rail sleeper and ballast conditions could be determined through further study.

References

Bartlett, DL (1960), *The Stability of Long Welded Rails*, Civil Engineering and Public Works Review, Vol. 55, No. 649, 1033-1035, NO. 650, 1170-1171, No. 651, 1299-1303, No. 653, 1591-1593

Dingqing, L, Hyslip, J, Sussmann, T, Chrismer, S 2002, *Railway Geotechnics*, Taylor & Francis Ltd, London, United Kingdom

Doyle, NF 1980, *Railway Track Design – A Review of Current Practice*, Australian Government Publishing Service, Canberra, Australia

Esveld, C 1989, *Modern Railway Track*; MRT-Productions, West Germany

Gill, B 2007, *Developing the Single Sleeper Push Test used to Determine Lateral Track Resistance*, Bachelor of Engineering Dissertation, Griffith University, Queensland Australia

Heeler, CL 1979, *British Railway Track: Design, Construction, Maintenance*, The Permanent Way Institution, Nottingham, UK

Hibbeler, RC 2005, *Mechanics of Materials*, Pearson Prentice Hall, New Jersey, USA

Howie, A 2005, *Track Buckle Report*, 2004/2005, Network Access, Queensland Rail

Kish A, Sussman T, Trosino M 2003, *Investigation of the influence of track maintenance on the lateral resistance of concrete tie track*, Transportation research board, Annual meeting, Washington DC

Kish, A 2013, *Improving Ballasted Track Lateral Resistance – the US Experience*, Karndrew Inc. Consulting Services, Railway Track Science and Engineering.

Kish, A 2011, *On the Fundamentals of Lateral Track Resistance*, Karndrew Inc. Consulting Services, [viewed 28th September 2015], <https://www.arema.org/files/library/2011_Conference_Proceedings/On_the_Fundamentals_of_Track_Lateral_Resistance.pdf>

Kish, A, Clark, D & Thompson, W 1995, *Recent Investigations on the Lateral Stability of Wood and Concrete Tie Tracks*, AREA Bulletin 752, Volume 96, October 1995

Ole, Z 2008, *Track Stability and Buckling – Rail Stress Management*, Bachelor of Engineering Dissertation, University of Southern Queensland, Toowoomba Queensland

Plasser & Theurer, Report AA-16 - *The Technology of Dynamic Track Stabilisation – General Description, Working Principle, Operating Instruction*

QR 2005, *Civil Engineering Track Standards (CETS)*, Standard MD-10-575

QR 1998, *Dynamic Track Stabiliser Evaluation – Civil Engineering Report*, Civil Engineering Division

Queensland Rail, 2012, *Track Knowledge - Resurfacing*, Technical Guide

Railways of Australia (ROA) 1988, *Track Buckling – Technology development and application,* Technical Report

Railway Technical Research Institute (RTRI), 2012, *Design standards for railway structures and commentary*, Track Structure, pp. 431

Samavedam, D 2001, *Track Resistance Measurements on the Union Pacific*, Union Pacific Test Report

Sari, G 1981, *The Influence of the Dynamic Track Stabiliser on Track Geometry*, Technical Report, Transport International June 1981.

Shenton, M.J., Powell, M.C. (1973) *The Resistance offered by the Ballast to Lateral Movement of Sleepers*, Summary CS 2.3 Tests, OR6 D117 (unpublished draft).

Sluz, A 1985, *TSC/Volpe Project Memorandum 1985*

Sluz, A 2000, *Evaluation of Dynamic Track Stabilization*, Volpe Project Technical Memorandum

Sussmann, T, Kish, A & Trosino, M 2003, *Investigation of the Influence of Track Maintenance on the Lateral Resistance of Concrete Tie Track*, Transportation Research Board Conference, January 2003

Thompson W C 1991*, Union Pacific's Approach to Preserving Lateral Track Stability*, Transportation Research Board, Washington DC.

US Department of Transportation 2013, *Track Buckling Prevention: Theory, Safety Concepts and Applications, Office of Research and Development*, Washington D.C. 20590

Van den Bosch, R & Lichtberger, B 2006, *Continuous non-destructive testing of lateral resistance of the track*, AEA Rail Technology and Plasser & Theurer, [viewed 28th September 2015], <http://www.uic.org/cdrom/2006/wcrr2006/pdf/341.pdf>

Zakeri, JA 2012, *Lateral Resistance of Railway Track, Reliability and Safety in Railway*, Dr. Xavier Perpinya (Ed.), InTech, [viewed 28th September 2015] <http://www.intechopen.com/books/reliabilityand-safety-in-railway/lateral-resistance-of-railway-track>

Appendix A – Project Specification

ENG4111/4112 Research Project

Project Specification

For: Ashley Poulton

Title: The Effect of Railway Track Resurfacing Methods on Lateral Track Resistance

(Note – initially titled: "The Effect of Dynamic Track Stabilisation on Lateral Track Resistance for the Queensland Rail Suburban Network" – I am seeking to simplify title.)

Major: Civil Engineering

Supervisor: Dr Habib Alehossein

Enrolment: ENG4111 – EXT S1, 2016
               ENG4112 – EXT S2, 2016

Project Aim: To investigate the effect of railway track resurfacing methods have on the lateral track resistance of narrow gauge low profile concrete sleepers.

Programme: Issue A - 16th March 2016

1. Investigate track resurfacing methods: tamping, ballast profiling, and dynamic track stabilisation.
2. Investigate lateral track resistance (LTR) including relationship with track resurfacing.
3. Investigate existing techniques to measure LTR for various sleeper types.
4. Design a system for the measurement of LTR of low profile concrete (LPC) sleepers.
5. Oversee manufacture of a LTR measurement device for LPC sleepers.
6. Demonstrate the effectiveness of the LTR measurement device under simulated conditions.
7. Demonstrate the effectiveness of the LTR measurement device under field conditions.
8. Field testing to measure the baseline LTR of LPC sleepers in a consolidated ballast bed.
9. Field testing to assess the LTR of LPC sleepers after tamping and ballast profiling.
10. Analysis of the effect tamping and ballast profiling has on LTR vs baseline LTR measurement.
11. Make recommendations regarding the impact tamping and ballast profiling has on LTR.
12. Make recommendations for improvement of the LTR measurement device and testing methods.

And if time and resources permit:

13. Field testing to assess the LTR of LPC sleepers after dynamic track stabilisation (DTS).
14. Analysis of the effect DTS has on LTR vs baseline, tamped & ballast profiled LTR measurements.
15. Make recommendations and limitations on use of the DTS for routine track resurfacing.

Appendix B – Before Resurfacing SSPT Raw Data

Sleeper 1			Sleeper 2			Sleeper 3	
Load (kN)	Deflection (mm)		Load (kN)	Deflection (mm)		Load (kN)	Deflection (mm)
0	1.06		0	0.14		0	0
0.02	1.06		0.01	0.14		0.59	0.74
0.33	1.59		0.01	0.14		1.19	1.43
0.94	2.19		0.01	0.15		1.93	1.97
1.01	2.34		0.01	0.15		2.86	2.63
1.13	2.39		0.13	0.59		4.72	2.77
1.2	2.42		0.66	0.94		5.75	2.82
1.24	2.48		1.74	1.34		6.76	2.88
1.32	2.52		3.41	1.54		7.71	3.07
1.35	2.53		4.32	1.66		8.6	3.22
1.45	2.65		5.91	2.1		9.72	3.33
1.58	2.7		6.89	2.42		11.6	3.21
1.88	3.08		7.63	2.73		12.47	3.44
2.69	3.29		9.16	3.1		13.48	3.35
3.43	3.75		9.94	3.24		14.42	3.46
4.13	4.15		11.46	3.62		15.49	3.29
4.6	4.33		12.24	3.66		16.48	3.61
4.93	4.38		13.91	3.92		18.31	3.5
4.99	4.43		14.79	3.94		19.13	3.72
5.02	4.41		16.35	3.95		20.17	3.42
5.03	4.4		17.26	3.83		20.93	3.59
5.09	4.47		19.06	3.84		20.96	3.56
5.24	4.51		19.71	3.88		21.77	3.73
5.29	4.55		20.96	3.91		22.5	3.78
5.41	4.64		21.79	3.75		23.27	3.66
5.62	4.89		22.45	4.06		24.33	3.66
6.14	4.91		23.64	3.75		25.71	3.85
6.49	4.95		24.24	3.76		26.9	3.87
6.94	4.98		24.53	3.81		27.46	3.89
7.46	5.15		25.26	3.73		28.2	3.94
8.3	5.18		25.78	3.65		29.23	3.79
8.44	5.21		26.78	3.59			
8.6	5.24		28.06	3.6			
8.67	5.22		29.93	3.54			
8.76	5.16		31.22	3.73			
8.81	5.25		33.17	3.67			
8.99	5.24		34.09	3.64			
9.34	5.23		34.1	3.63			
9.81	5.3		34.1	3.64			
11.26	5.5		34.1	3.65			
13.04	5.52						
14.79	5.11						
16.26	5.09						
16.99	5.32						
18.19	5.05						
19.28	5.04						
20.41	4.71						
21.34	4.79						
22.56	4.89						
23.69	4.81						

Sleeper 4 – Failed due to Insufficient Rail Lift

Sleeper 1						Sleeper 4	
Load (kN)	Deflection (mm)					Load (kN)	Deflection (mm)
24.27	4.81						
25.59	4.27					0	0.13
26.82	4.05					0	0.13
27.44	4.13					0.01	0.12
28.66	3.89					0.17	0.64
29.78	3.93					0.6	1.4
30.79	3.95					1.25	1.96
31.43	3.89					2.34	2.38
32.35	3.91					4	2.53
33.18	4.02					5.07	2.38
33.88	4.1					6.18	2.35
34.44	4.08					6.94	2.3
34.76	4.03					8.34	2.2
34.91	4.04					9.34	2.26
35.04	4.02					10.28	2.81
35.19	3.89					12	3.18
35.28	3.86					12.85	3.57
35.37	3.87					13.88	3.58
35.44	3.92					15.39	4.8
35.46	3.88					16.35	5.05
35.47	3.84						

Appendix C – After Resurfacing SSPT Raw Data

Sleeper 1			Sleeper 2			Sleeper 3	
Load (kN)	Deflection (mm)		Load (kN)	Deflection (mm)		Load (kN)	Deflection (mm)
0	0.62		0	0.19		0	0.05
0	0.62		0.03	0.24		0	0.06
0	0.63		0.03	0.26		0.09	0.01
0.01	0.62		0.04	0.25		0.09	0.01
0.01	0.62		0.5	2.2		0.58	1.81
0.53	1.1		1.89	2.63		1.59	2.37
0.86	1.72		2.27	2.86		2.8	2.91
1.88	2.74		2.83	3.06		3.89	3.07
2.77	3.15		4.75	3.09		4.19	3.14
3.28	3.23		5.75	3.19		5.04	3.11
4.09	3.19		7.72	3.14		6.18	3.09
5.15	3.3		9.7	3.13		7.22	3.17
5.6	3.36		10.74	3.28		8.62	3.1
6.89	3.39		12.84	2.86		9.79	3.32
7.92	3.41		14.79	2.82		10.52	3.44
8.41	3.47						
9.35	3.33						
10.32	3.39						
10.83	3.34						
11.66	3.46						
11.99	3.4						
12.22	3.48						
12.36	3.42						
12.41	3.44						
12.48	3.49						

Sleeper 4			Sleeper 5	
Load (kN)	Deflection (mm)		Load (kN)	Deflection (mm)
0	0.09		0	0.5
0.01	0.06		0.01	0.47
0.01	0.06		0.01	0.47
0.01	0.06		0.01	0.47
0.01	0.06		0.01	0.49
0.01	0.06		0.01	0.48
0.01	0.06		0.1	1.42
0.31	1.09		0.91	2.84
1.51	2.13		1.81	3.36
2.22	2.56		2.83	3.46
2.85	2.79		2.87	3.31
4.33	2.92		2.88	3.27
6.38	3.13		2.89	3.22
7.94	3.47		3.89	3.37
9.32	3.33		3.94	3.49
10.52	3.78		5.68	3.69
12.15	3.88		7.02	3.65
			9.22	3.72

Appendix D – SSPT Device General Arrangement Drawing

SINGLE SLEEPER push TEST DEVICE

GENERAL ARRANGEMENT DRAWING

5147-0105

5147-0103

5147-0102

BOLT_HEX_HD_M10_X_35

5147-0100

5147-0104

5147-0101

BOLT_HEX_HD_M10_X_120

WASHER-FLAT-10-HDND

NUT_HEX_M10

100

142.5

1045
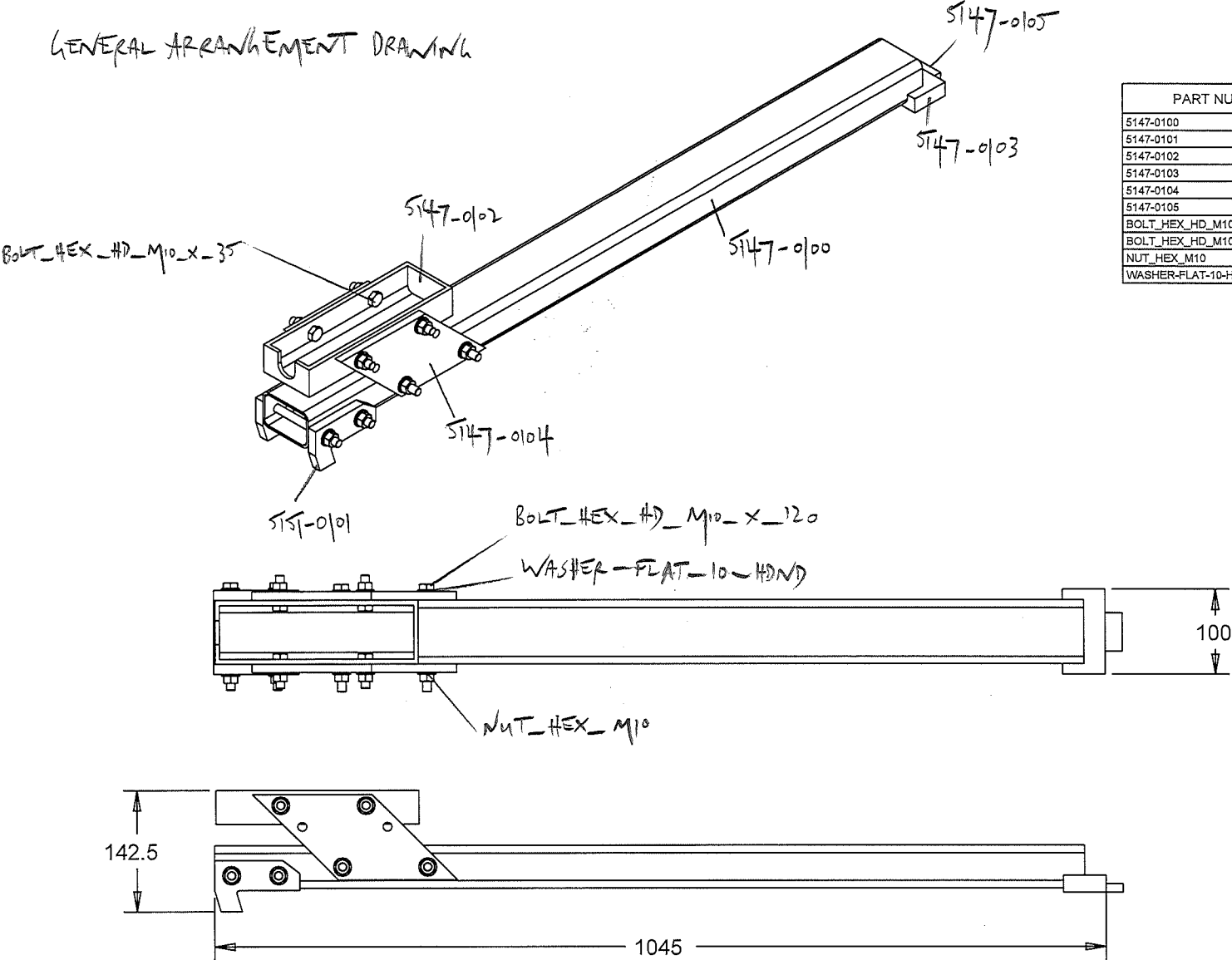
PART NUMBER	DESCRIPTION	QTY
5147-0100	STRUT	1
5147-0101	GRIPPER	2
5147-0102	CYLINDER HOLDER	1
5147-0103	BUTT BAR	1
5147-0104	ADJUSTMENT BRACKET	2
5147-0105	SPACER BAR	1
BOLT_HEX_HD_M10_X_35	BOLT-HEX HD M10 X 1.5 X 35	4
BOLT_HEX_HD_M10_X_120	BOLT-HEX HD M10 X 1.5 X 35	4
NUT_HEX_M10	NUT-HEX M10 X 1.50	8
WASHER-FLAT-10-HDND	WASHER-FLAT 10 I.D. HARDENED	12
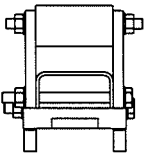
Appendix E – Maximum Compressive Rail Force for 41kg/m and 60kg/m Rail

$$P_{MAX\ COMPRESSIVE} = 2AE\alpha(T_{MAX} - T_0) \quad Equation\ 2.8$$

For 41kg/m Rail:

Parameter	Description	Value
A	Cross sectional area of 41kg/m rail	5192 mm^2
E	The Modulus of Elasticity for steel	200×10^9Pa
α	Coefficient of Thermal Expansion for steel rail	11.7×10^{-6} m/mk
T_{MAX}	The maximum expected rail temperature	65°C
T_0	The rail neutral temperature	37°C

Therefore, the maximum compressive load was calculated as follows:

$$P_{MAX\ COMPRESSIVE} = 2 \times 5192 \times 200 \times 10^9 \times 11.7 \times 10^{-6} \times (65 - 37)$$
$$P_{MAX\ COMPRESSIVE} = 680\text{kN}$$

For 60kg/m Rail:

Parameter	Description	Value
A	Cross sectional area of 60kg/m rail	7725 mm^2
E	The Modulus of Elasticity for steel	200×10^9Pa
α	Coefficient of Thermal Expansion for steel rail	11.7×10^{-6} m/mk
T_{MAX}	The maximum expected rail temperature	65°C
T_0	The rail neutral temperature	37°C

Therefore, the maximum compressive load was calculated as follows:

$$P_{MAX\ COMPRESSIVE} = 2 \times 7725 \times 200 \times 10^9 \times 11.7 \times 10^{-6} \times (65 - 37)$$
$$P_{MAX\ COMPRESSIVE} = 1012\text{kN}$$

Appendix F – Critical Buckling Load Curves for 41kg/m Rail

Chart 41kg 1A: Critical Buckling Load versus Initial Misalignment Amplitude
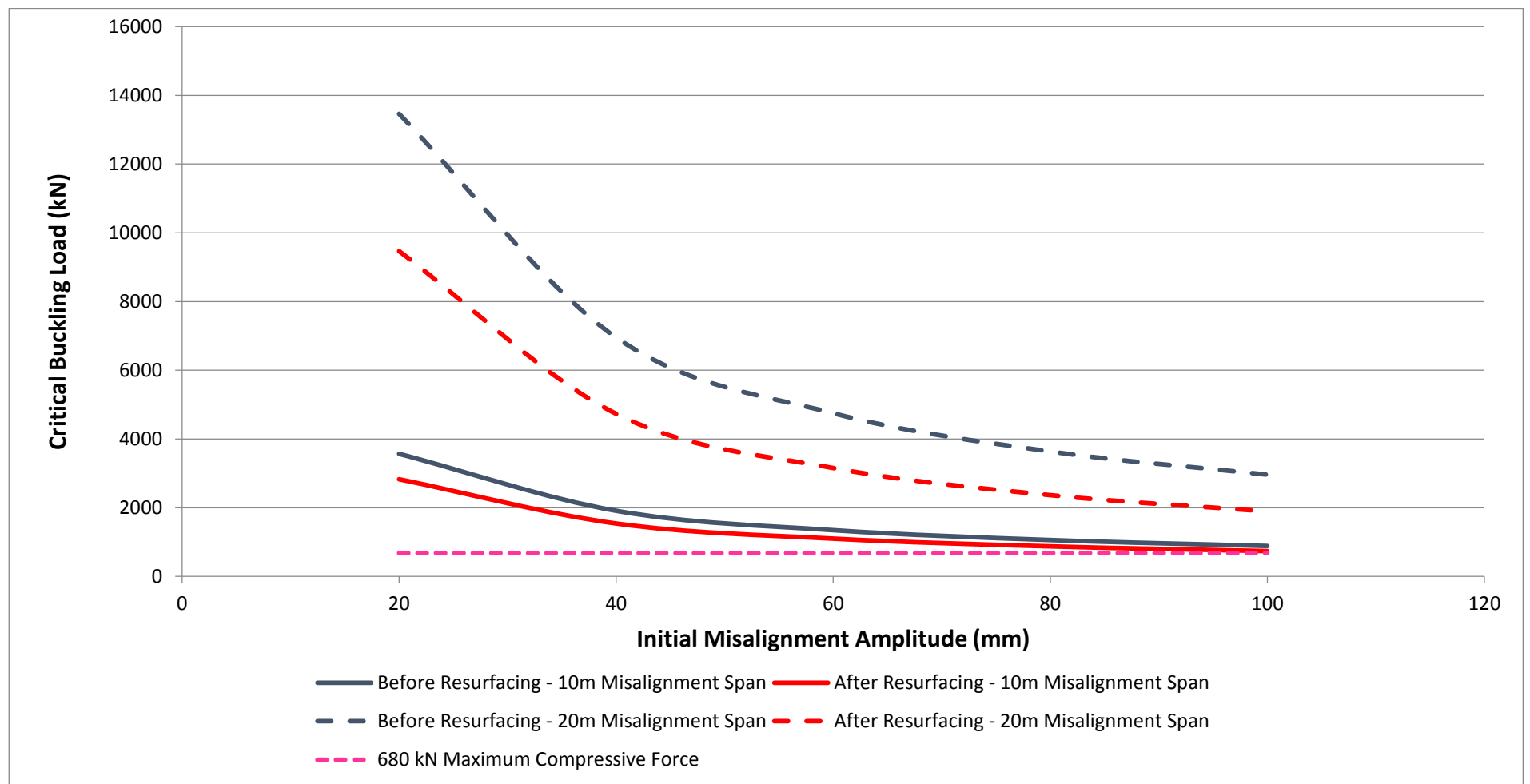
Chart 41kg 1B: % Reduction in Critical Buckling Load, and Buckling Factor of Safety versus Initial Misalignment Amplitude
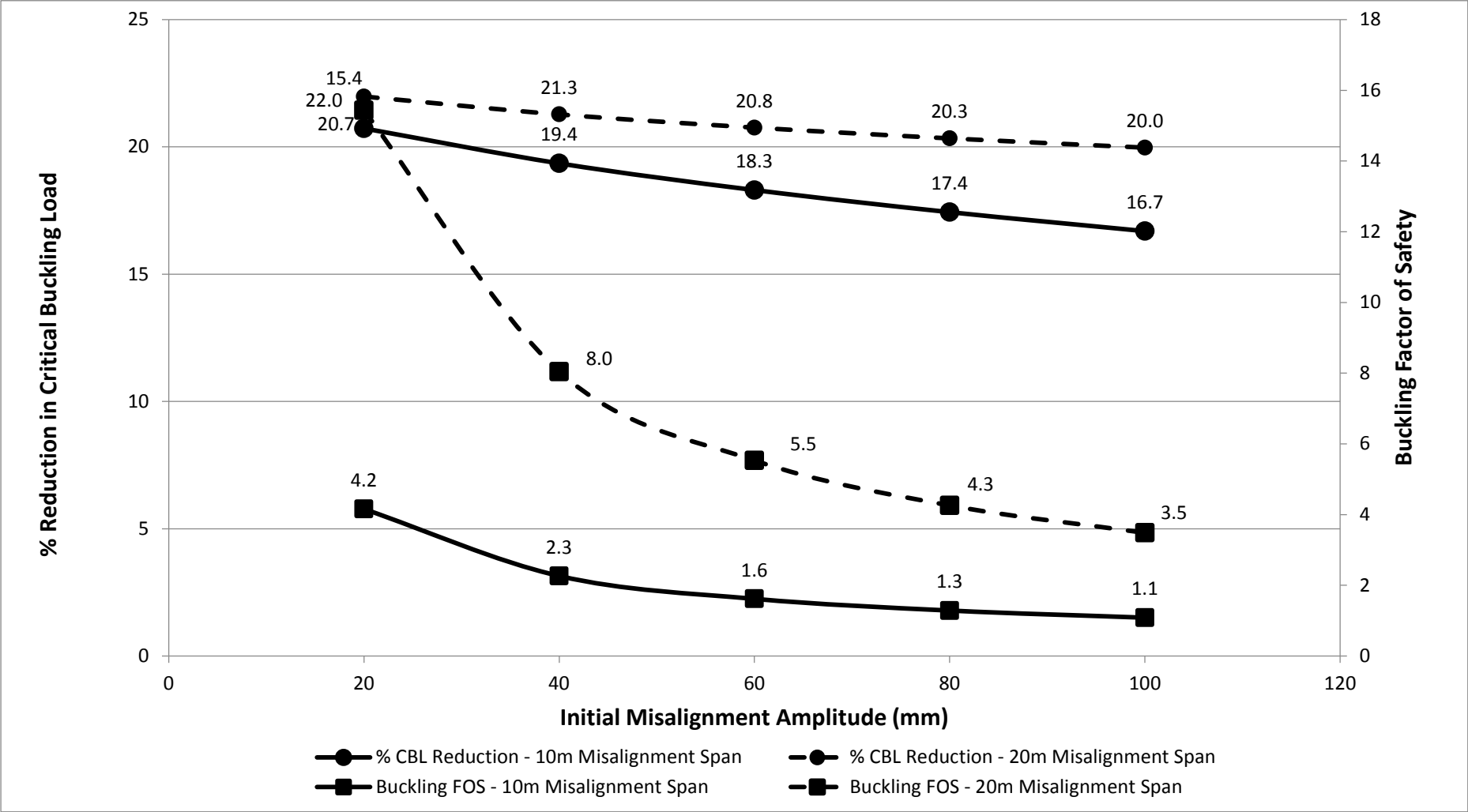
Chart 41kg 2A: Critical Buckling Load versus Initial Misalignment Span
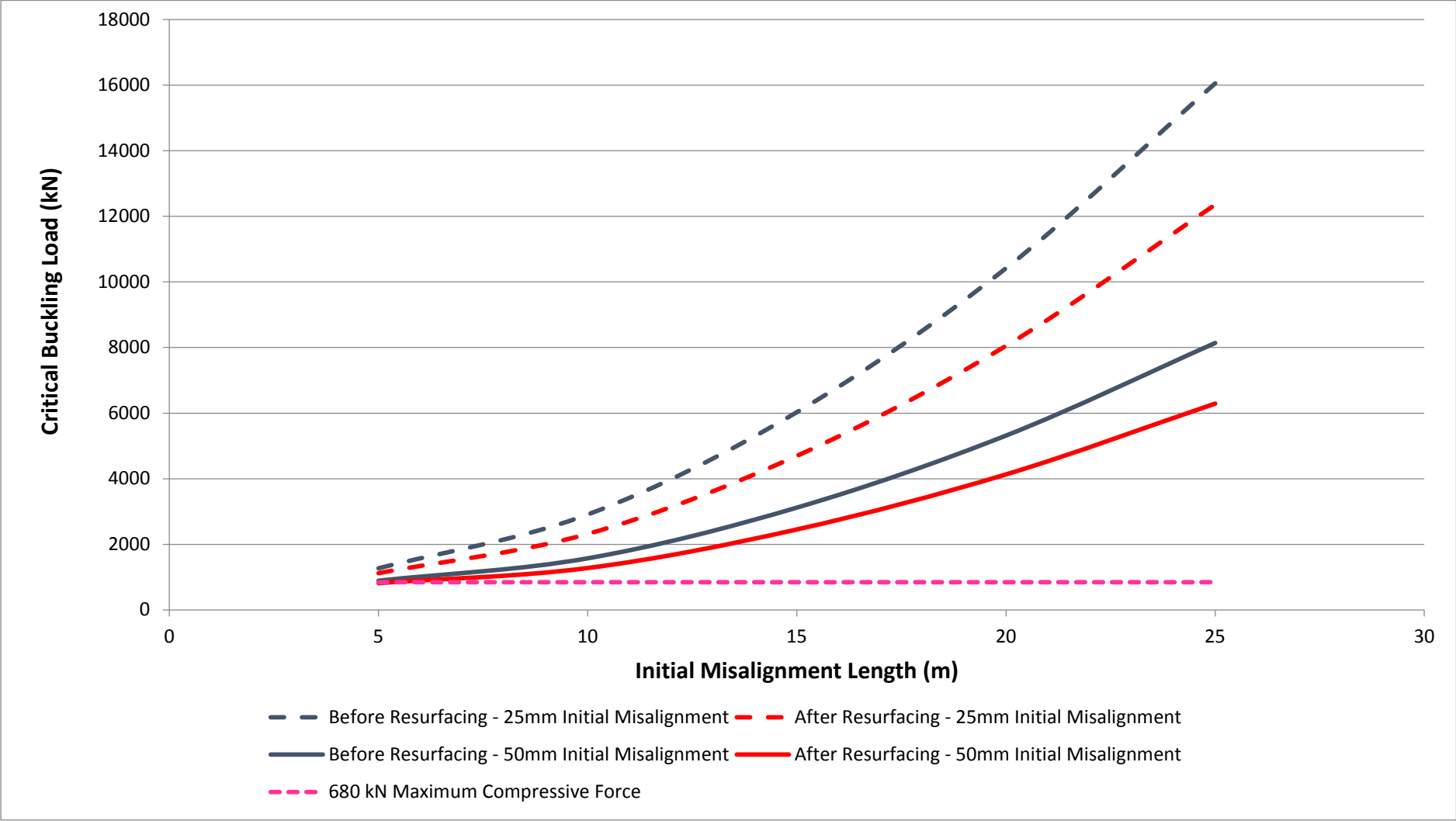
Chart 41kg 2B: % Reduction in Critical Buckling Load, and Buckling Factor of Safety versus Initial Misalignment Span
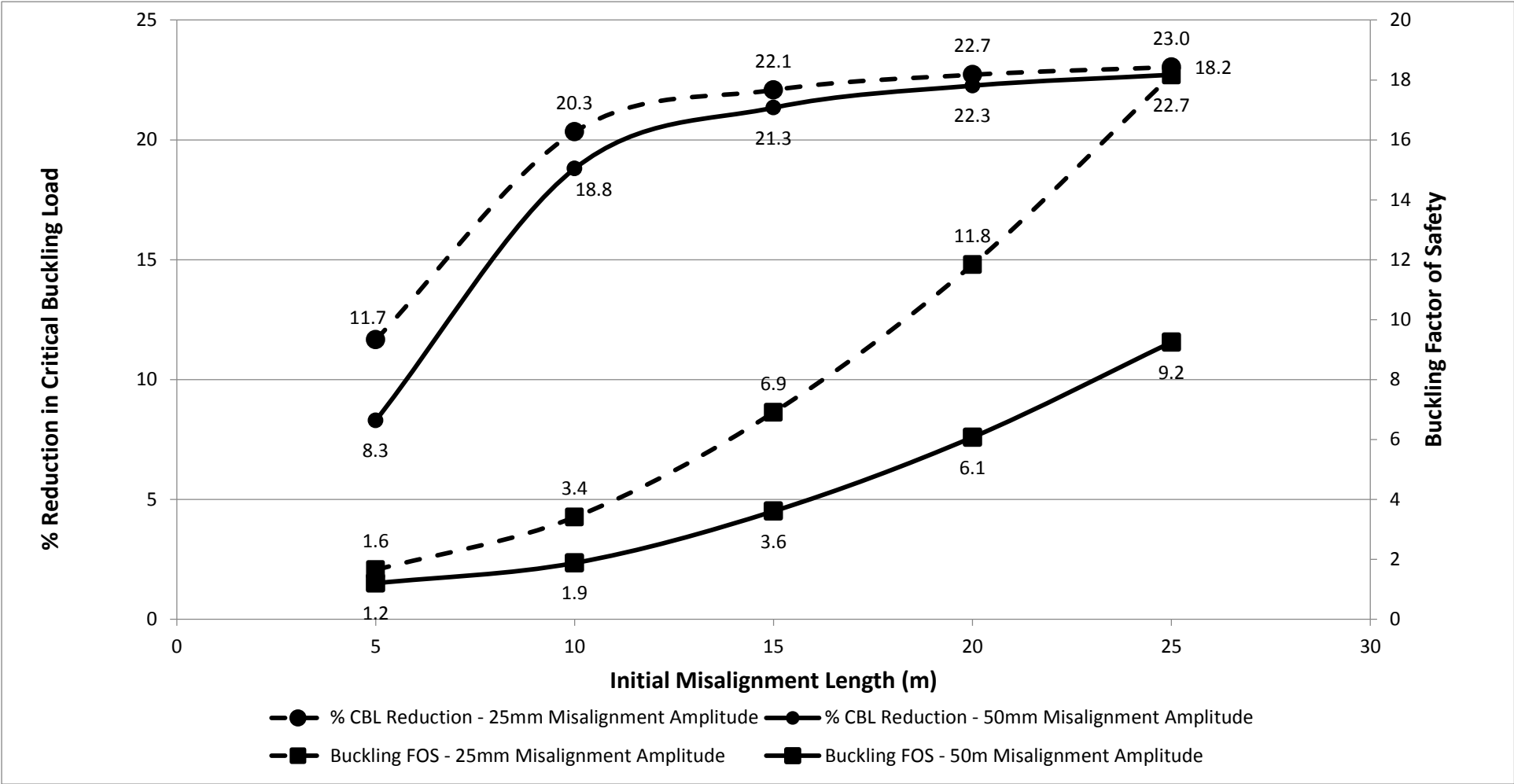
Appendix G – Critical Buckling Load Curves for 60kg/m Rail

Chart 60kg 1A: Critical Buckling Load versus Initial Misalignment Amplitude
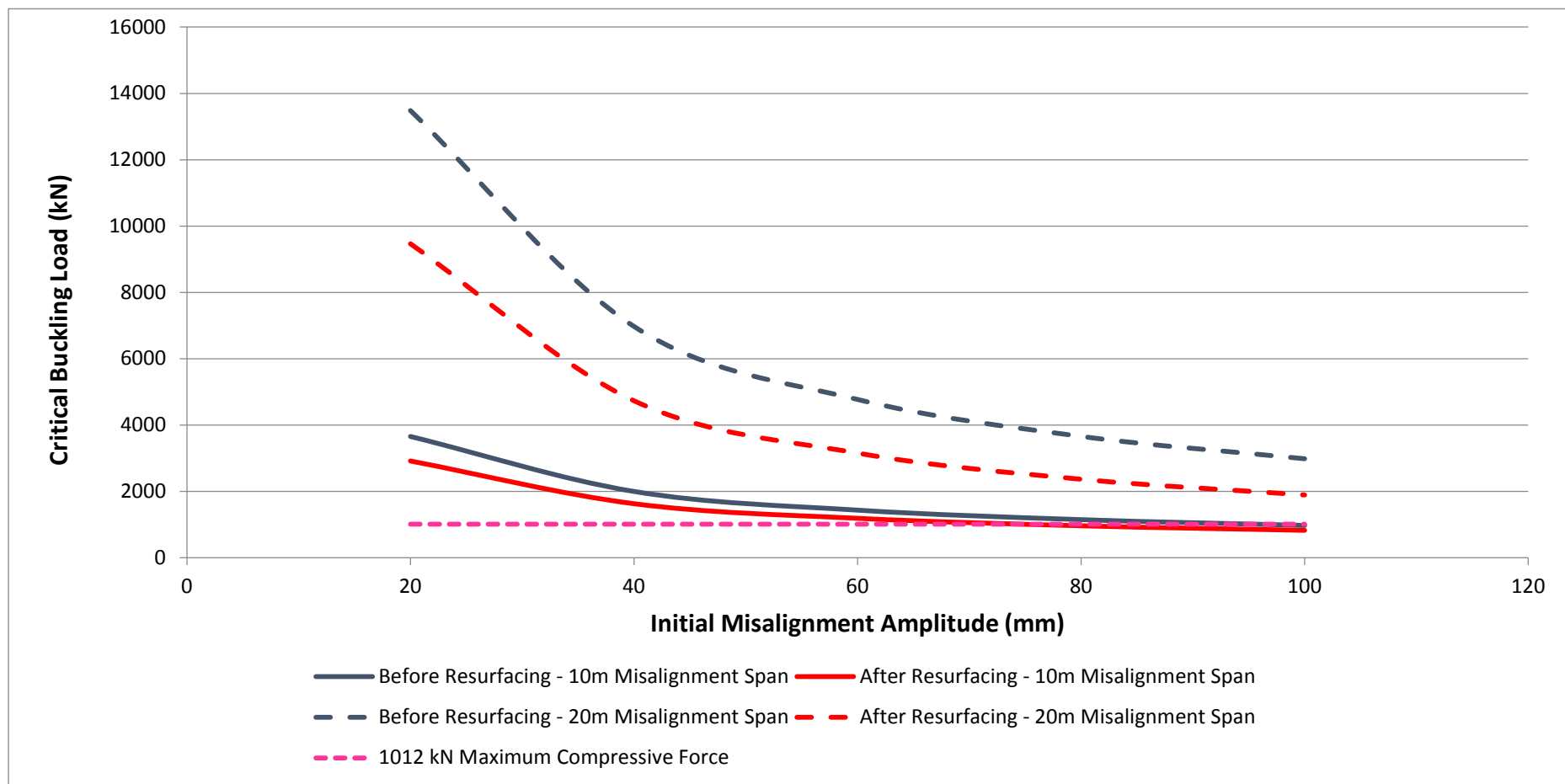
Chart 60kg 1B: % Reduction in Critical Buckling Load, and Buckling Factor of Safety versus Initial Misalignment Amplitude
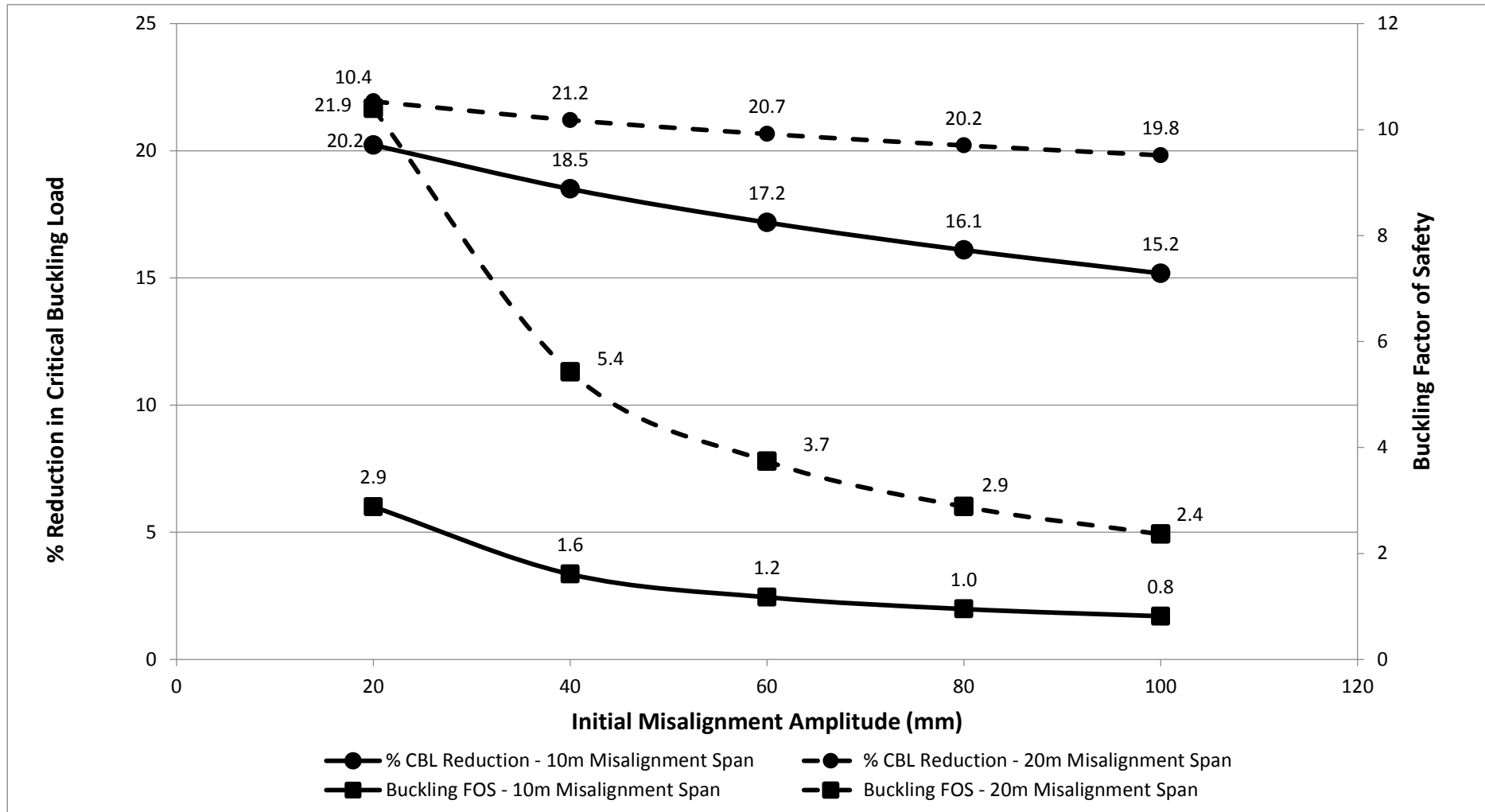
Chart 60kg 2A: Critical Buckling Load versus Initial Misalignment Span
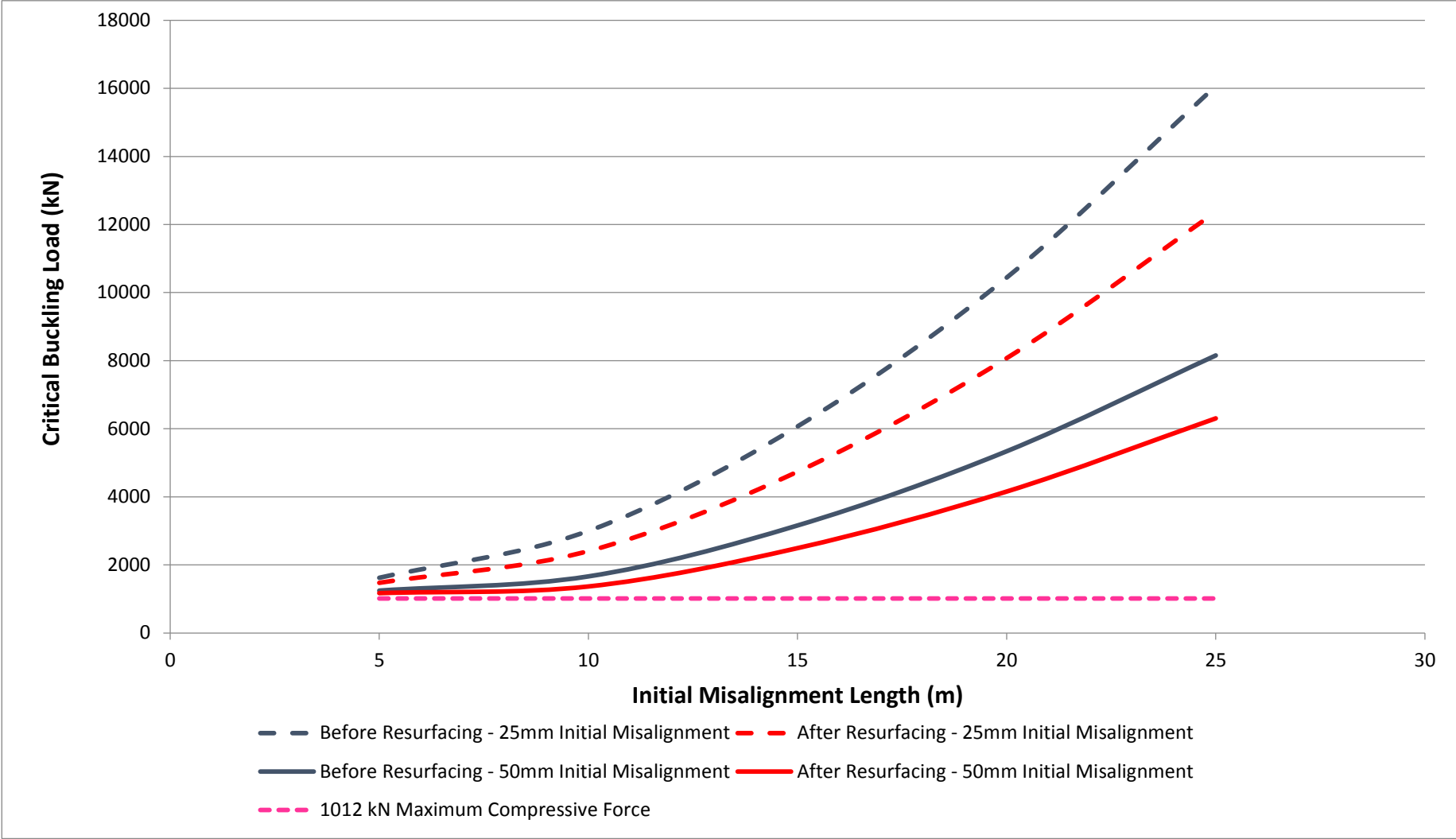
Chart 60kg 2B: % Reduction in Critical Buckling Load, and Buckling Factor of Safety versus Initial Misalignment Span
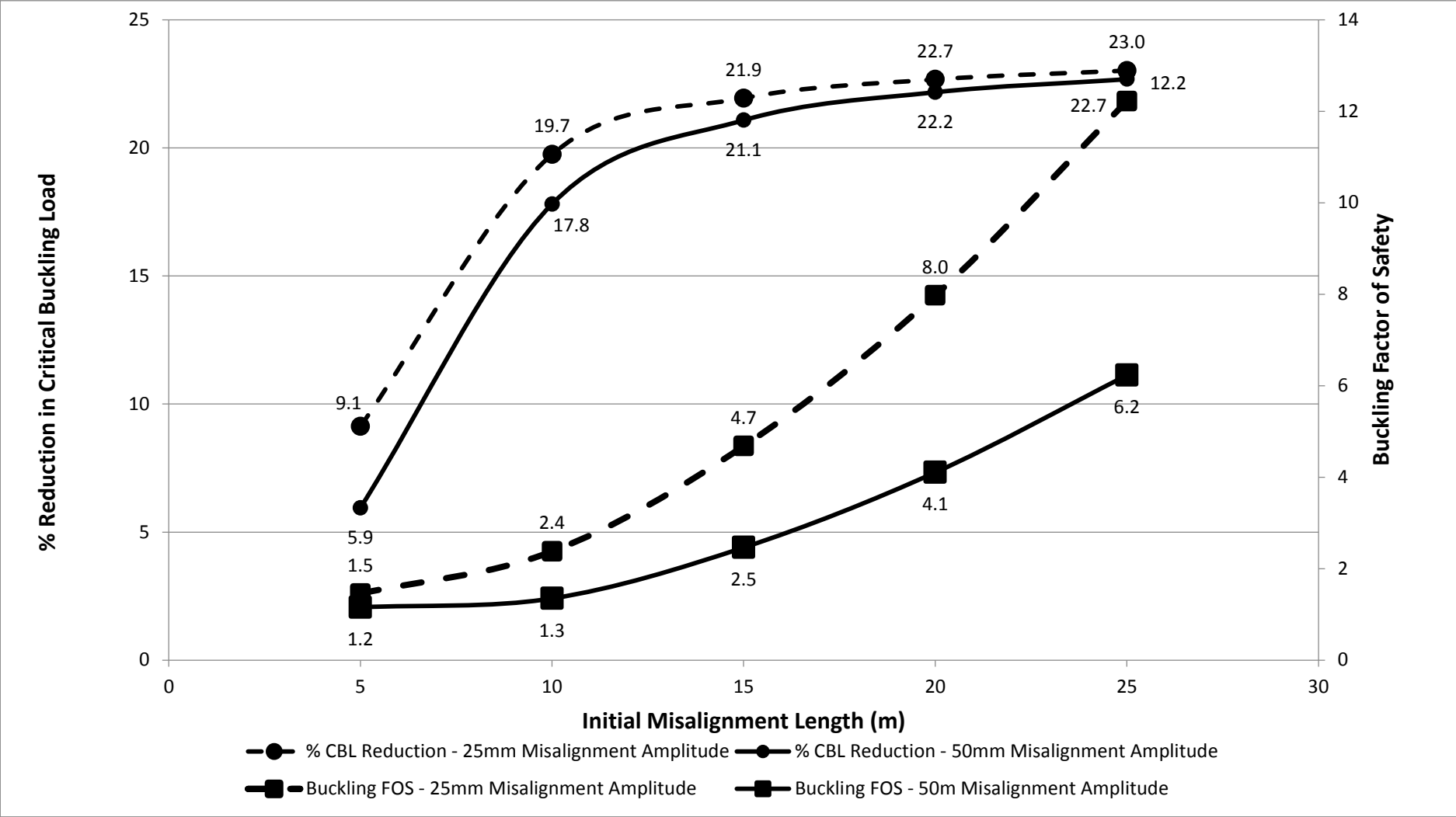
Appendix H – Rail Data Sheets

41 KG RAIL
RT 23
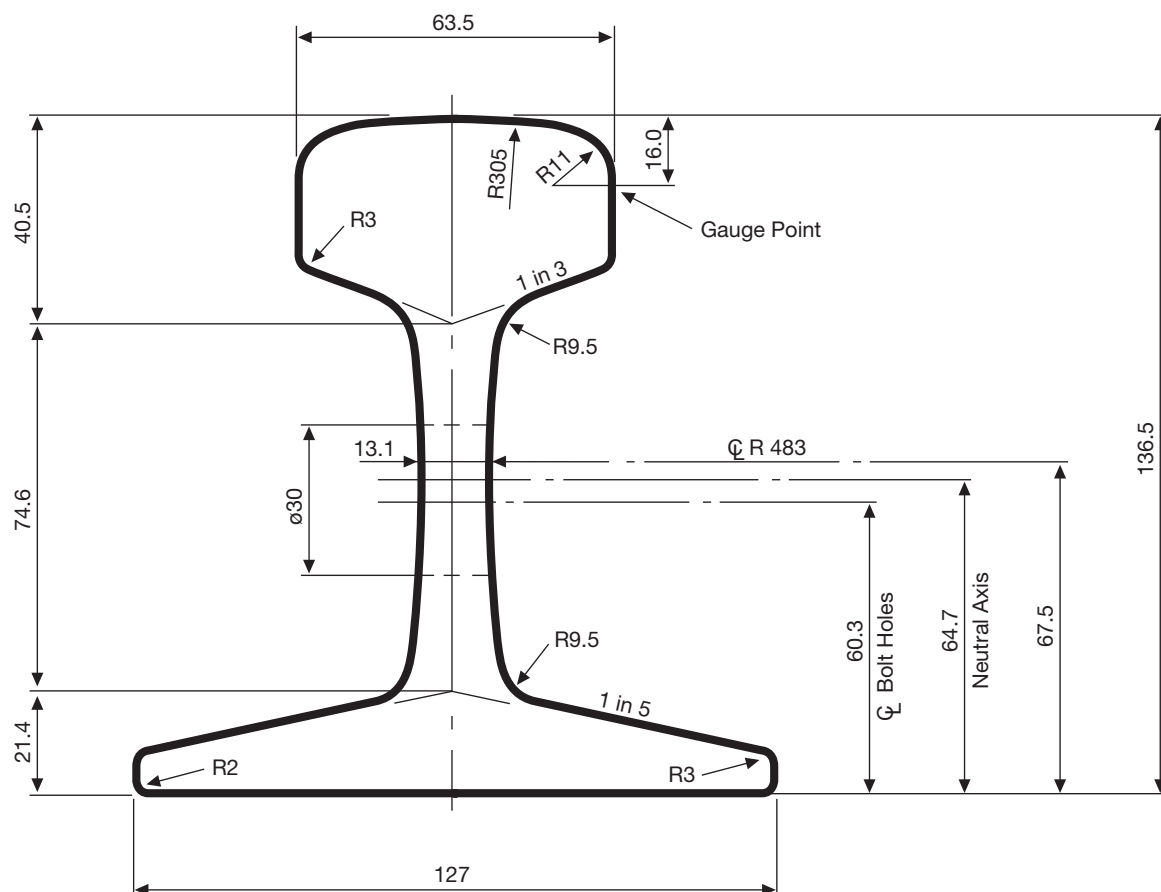
MECHANICAL PROPERTIES			
Area of Head	2162 mm²	**Horizontal Axis**	
Area of Web	1122 mm²	Second Moment of Area	13.27 x 10⁶ mm⁴
Area of Foot	1908 mm²	Section Modulus Head	184.4 x 10³ mm³
Total Area	5192 mm²	Section Modulus Foot	204.5 x 10³ mm³
Standard Lengths	**12.19 m & 13.72 m**	**Vertical Axis**	
Calculated Mass	**40.8 kg/m**	Second Moment of Area	2.67 x 10⁶ mm⁴

TYPICAL MECHANICAL PROPERTIES (Minimum)			
0.2% Proof Stress MPa	**Tensile Strength MPa**	**% Elongation Gauge length = 5.65 √S₀**	**Surface Hardness H.B.**
400	700	8	230

CHEMICAL COMPOSITION (%) Ladle Analysis				
Carbon	**Silicon**	**Manganese**	**Phosphorus**	**Sulphur**
0.53 - 0.69	0.15 - 0.58	0.60 - 0.95	0.025 max	0.025 max

50 KG RAIL

RT 23

MECHANICAL PROPERTIES			
Area of Head	2710 mm²	**Horizontal Axis**	
Area of Web	1578 mm²	Second Moment of Area	20.1 x 10⁶ mm⁴
Area of Foot	2163 mm²	Section Modulus Head	253.5 x 10³ mm³
Total Area	6451 mm²	Section Modulus Foot	269.1 x 10³ mm³
Standard Lengths	**12.19 m & 13.72 m**	**Vertical Axis**	
Calculated Mass	**50.6 kg/m**	Second Moment of Area	3.26 x 10⁶ mm⁴

TYPICAL MECHANICAL PROPERTIES (Minimum)			
0.2% Proof Stress MPa	**Tensile Strength MPa**	**% Elongation Gauge length = 5.65 √S₀**	**Surface Hardness H.B.**
420	880	8	260

CHEMICAL COMPOSITION (%) Ladle Analysis				
Carbon	**Silicon**	**Manganese**	**Phosphorus**	**Sulphur**
0.65 - 0.82	0.15 - 0.58	0.70 - 1.25	0.025 max	0.025 max

60 KG RAIL

RT 23

MECHANICAL PROPERTIES			
Area of Head	2999 mm²	**Horizontal Axis**	
Area of Web	1974 mm²	Second Moment of Area	29.3 x 10⁶ mm⁴
Area of Foot	2752 mm²	Section Modulus Head	322.4 x 10³ mm³
Total Area	7725 mm²	Section Modulus Foot	369.3 x 10³ mm³
Standard Lengths	**12.19 m & 13.72 m**	**Vertical Axis**	
Calculated Mass	**60.6 kg/m**	Second Moment of Area	4.90 x 10⁶ mm⁴

TYPICAL MECHANICAL PROPERTIES (Minimum)			
0.2% Proof Stress MPa	**Tensile Strength MPa**	**% Elongation Gauge length = 5.65 √S₀**	**Surface Hardness H.B.**
420	880	8	260

CHEMICAL COMPOSITION (%) Ladle Analysis				
Carbon	**Silicon**	**Manganese**	**Phosphorus**	**Sulphur**
0.65 - 0.82	0.15 - 0.58	0.70 - 1.25	0.025 max	0.025 max

Appendix I – Enerpac Hydraulic Cylinder Details

RC-Series, Single-Acting Cylinders

ENERPAC®
POWERFUL SOLUTIONS. GLOBAL FORCE.

▼ From left to right: **RC-506, RC-50, RC-2510, RC-154, RC-10010, RC-55, RC-1010**

The Industry Standard General Purpose Cylinder

- **The exclusive Golden Ring design absorbs eccentric loading without galling cylinder parts**
- **Collar threads, plunger threads and base mounting holes enable easy fixturing (on most models)**
- **Designed for use in all positions**
- **High strength alloy steel for durability**
- **Nickel plating available on most models (contact Enerpac for details)**
- **Heavy duty return springs**
- **Baked enamel finish for increased corrosion resistance**
- **CR-400 coupler and dust cap included on all models**
- **Plunger wiper reduces contamination, extending cylinder life.**

Saddles

All RC cylinders are equipped with hardened removable grooved saddles. For tilt and flat saddles, see the RC-Series accessory page.

Page: 10

Base Plates

To ensure the stability of cylinders for lifting applications, base plates are available for 10, 25 and 50 ton RC cylinders.

Page: 10

Specialty Attachments

For solving all kinds of application problems, specialty attachments are available for 5, 10 and 25 ton RC cylinders.

Page: 167

▼ *Stage lifting set up in Greece, where assembled pipes, 25 meters in length, were stage lifted with six RC-2514 cylinders.*

▼ *RC cylinder mounting attachments greatly extend the application possibilities (available for 5, 10,15 and 25 ton cylinders).*

Single-Acting, General Purpose Cylinders

Golden Ring Design

The exclusive Golden Ring Design is a unique bearing design which absorbs eccentric load stresses to protect your cylinder against abrasion, over-extending or plunger blow-outs and jamming or top-end mushrooming. As a result, Golden Ring cylinders provide long, trouble-free operation.

RC
Series

Capacity:
5 - 95 ton

Stroke:
16 - 362 mm

Maximum Operating Pressure:
700 bar

▼ QUICK SELECTION CHART

For complete technical information see next page.

Cylinder Capacity ton (kN)	Stroke (mm)	Model Number	Cylinder Effective Area (cm²)	Oil Capacity (cm³)	Collapsed Height (mm)	(kg)
5 (45)	16	**RC-50****	6,5	10	41	1,0
	25	**RC-51**	6,5	16	110	1,0
	76	**RC-53**	6,5	50	165	1,5
	127	**RC-55***	6,5	83	215	1,9
	177	**RC-57**	6,5	115	273	2,4
	232	**RC-59**	6,5	151	323	2,8
10 (101)	26	**RC-101**	14,5	38	89	1,8
	54	**RC-102***	14,5	78	121	2,3
	105	**RC-104**	14,5	152	171	3,3
	156	**RC-106***	14,5	226	247	4,4
	203	**RC-108**	14,5	294	298	5,4
	257	**RC-1010***	14,5	373	349	6,4
	304	**RC-1012**	14,5	441	400	6,8
	356	**RC-1014**	14,5	516	450	8,2
15 (142)	25	**RC-151**	20,3	51	124	3,3
	51	**RC-152**	20,3	104	149	4,1
	101	**RC-154***	20,3	205	200	5,0
	152	**RC-156***	20,3	308	271	6,8
	203	**RC-158**	20,3	411	322	8,2
	254	**RC-1510**	20,3	516	373	9,5
	305	**RC-1512**	20,3	619	423	10,9
	356	**RC-1514**	20,3	723	474	11,8
25 (232)	26	**RC-251**	33,2	86	139	5,9
	50	**RC-252***	33,2	166	165	6,4
	102	**RC-254***	33,2	339	215	8,2
	158	**RC-256***	33,2	525	273	10,0
	210	**RC-258**	33,2	697	323	12,2
	261	**RC-2510**	33,2	867	374	14,1
	311	**RC-2512**	33,2	1033	425	16,3
	362	**RC-2514***	33,2	1202	476	17,7
30 (295)	209	**RC-308**	42,1	880	387	18,1
50 (498)	51	**RC-502**	71,2	362	176	15,0
	101	**RC-504**	71,2	719	227	19,1
	159	**RC-506***	71,2	1131	282	23,1
	337	**RC-5013**	71,2	2399	460	37,6
75 (718)	156	**RC-756**	102,6	1601	285	29,5
	333	**RC-7513**	102,6	3417	492	59,0
95 (933)	168	**RC-1006**	133,3	2239	357	59,0
	260	**RC-10010**	133,3	3466	449	72,6

* Available as set, see note on this page.
** RC-50 cylinder has a non removable grooved saddle and no collar thread.

Think Safety
80%

Manufacturer's rating of load and stroke are maximum safe limits. Good practice encourages using only 80% of these ratings.

Page: **240**

Lightweight Aluminium Cylinders

If you need a higher cylinder capacity-to-weight-ratio the **RAC-Series** are the perfect choice.
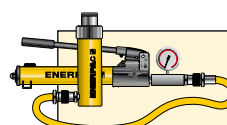
Page: **13**

Gauges

Minimize the risk of overloading and ensure long, dependable service from your equipment. Refer to the System Components Section for a full range of gauges.
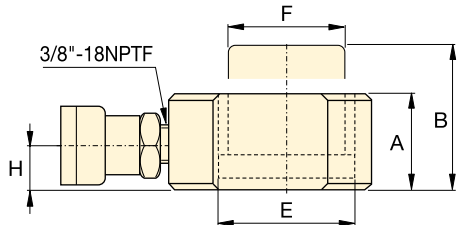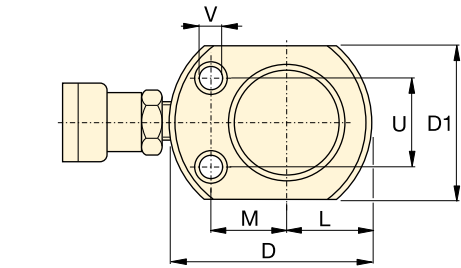
Page: **118**

Cylinder-Pump Sets

All cylinders marked with an * are available as **sets** (cylinder, gauge, couplers, hose and pump) for your ordering convenience.
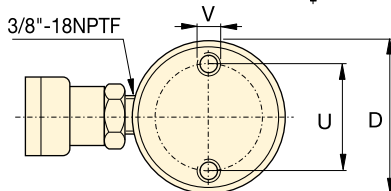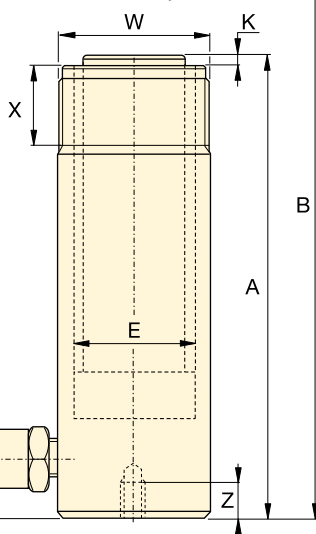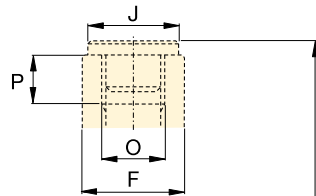
Page: **62**

ENERPAC 7

RC-Series, Single-Acting Cylinders
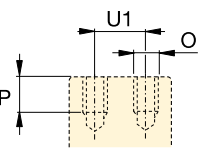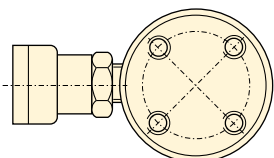
Speed Chart
See the Enerpac Cylinder Speed Chart in our 'Yellow Pages' to determine your approximate cylinder speed.

Page: 249

RC-50

RC-101 only
(U1 = 19 mm)

3/8"-18NPTF

RC-51 - RC-5013

3/8"-18NPTF

RC-1006, RC-10010

◀ For full features see previous page.

Cylinder Capacity ton (kN)	Stroke (mm)	Model Number	Cylinder Effective Area (cm²)	Oil Capacity (cm³)	Collapsed Height A (mm)	Extended Height B (mm)	Outside Dia. D (mm)
5 (45)	16	RC-50**	6,5	10	41	57	58***
	25	RC-51	6,5	16	110	135	38
	76	RC-53	6,5	50	165	241	38
	127	RC-55*	6,5	83	215	342	38
	177	RC-57	6,5	115	273	450	38
	232	RC-59	6,5	151	323	555	38
10 (101)	26	RC-101	14,5	38	89	115	57
	54	RC-102*	14,5	78	121	175	57
	105	RC-104	14,5	152	171	276	57
	156	RC-106*	14,5	226	247	403	57
	203	RC-108	14,5	294	298	501	57
	257	RC-1010*	14,5	373	349	606	57
	304	RC-1012	14,5	441	400	704	57
	356	RC-1014	14,5	516	450	806	57
15 (142)	25	RC-151	20,3	51	124	149	69
	51	RC-152	20,3	104	149	200	69
	101	RC-154*	20,3	205	200	301	69
	152	RC-156*	20,3	308	271	423	69
	203	RC-158	20,3	411	322	525	69
	254	RC-1510	20,3	516	373	627	69
	305	RC-1512	20,3	619	423	728	69
	356	RC-1514	20,3	723	474	830	69
25 (232)	26	RC-251	33,2	86	139	165	85
	50	RC-252*	33,2	166	165	215	85
	102	RC-254*	33,2	339	215	317	85
	158	RC-256*	33,2	525	273	431	85
	210	RC-258	33,2	697	323	533	85
	261	RC-2510	33,2	867	374	635	85
	311	RC-2512	33,2	1033	425	736	85
	362	RC-2514*	33,2	1202	476	838	85
30 (295)	209	RC-308	42,1	880	387	596	101
50 (498)	51	RC-502	71,2	362	176	227	127
	101	RC-504	71,2	719	227	328	127
	159	RC-506*	71,2	1131	282	441	127
	337	RC-5013	71,2	2399	460	797	127
75 (718)	156	RC-756	102,6	1601	285	441	146
	333	RC-7513	102,6	3417	492	825	146
95 (933)	168	RC-1006	133,3	2239	357	525	177
	260	RC-10010	133,3	3466	449	709	177

* Available as set, see note on this page.
** RC-50 cylinder has a non removable grooved saddle and no collar thread.
*** D1 = 41 mm, L = 20 mm, M = 25 mm.

Single-Acting, General Purpose Cylinders
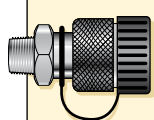
Couplers Included!
CR-400 couplers included on all models. Fits all HC-Series hoses.

Capacity:
5 - 95 ton

Stroke:
16 - 362 mm

Maximum Operating Pressure:
700 bar

RC
Series

Cylinder Bore Dia. E (mm)	Plunger Dia. F (mm)	Base to Adv. Port H (mm)	Saddle Dia. J (mm)	Saddle Protr. from Plgr. K (mm)	Plunger Internal Thread O	Plunger Thread Length P (mm)	Base Mounting Holes			Collar Thread W	Collar Thread Length X (mm)	(kg)	Model Number
							Bolt Circle U (mm)	Thread V	Thd. Depth Z (mm)				
28,7	25,4	19	**	**	**	**	28	5,6 mm	—	—	—	1,0	RC-50**
28,7	25,4	19	25	6	$^3/_4$" - 16	14	25	$^1/_4$"- 20UN	14	$1^1/_2$" - 16	28	1,0	RC-51
28,7	25,4	19	25	6	$^3/_4$" - 16	14	25	$^1/_4$"- 20UN	14	$1^1/_2$" - 16	28	1,5	RC-53
28,7	25,4	19	25	6	$^3/_4$" - 16	14	25	$^1/_4$"- 20UN	14	$1^1/_2$" - 16	28	1,9	RC-55*
28,7	25,4	19	25	6	$^3/_4$" - 16	16	25	$^1/_4$"- 20UN	14	$1^1/_2$" - 16	28	2,4	RC-57
28,7	25,4	19	25	6	$^3/_4$" - 16	16	25	$^1/_4$"- 20UN	14	$1^1/_2$" - 16	28	2,8	RC-59
42,9	38,1	19	–	–	#10 - 24UN	6	39	$^5/_{16}$"- 18UN	12	$2^1/_4$" - 14	26	1,8	RC-101
42,9	38,1	19	35	6	1" - 8	19	39	$^5/_{16}$"- 18UN	12	$2^1/_4$" - 14	26	2,3	RC-102*
42,9	38,1	19	35	6	1" - 8	19	39	$^5/_{16}$"- 18UN	12	$2^1/_4$" - 14	26	3,3	RC-104
42,9	38,1	19	35	6	1" - 8	19	39	$^5/_{16}$"- 18UN	12	$2^1/_4$" - 14	26	4,4	RC-106*
42,9	38,1	19	35	6	1" - 8	19	39	$^5/_{16}$"- 18UN	12	$2^1/_4$" - 14	26	5,4	RC-108
42,9	38,1	19	35	6	1" - 8	19	39	$^5/_{16}$"- 18UN	12	$2^1/_4$" - 14	26	6,4	RC-1010*
42,9	38,1	19	35	6	1" - 8	19	39	$^5/_{16}$"- 18UN	12	$2^1/_4$" - 14	26	6,8	RC-1012
42,9	38,1	19	35	6	1" - 8	19	39	$^5/_{16}$"- 18UN	12	$2^1/_4$" - 14	26	8,2	RC-1014
50,8	41,4	19	38	9	1" - 8	25	48	$^3/_8$"- 16UN	12	$2^3/_4$" - 16	30	3,3	RC-151
50,8	41,4	19	38	9	1" - 8	25	48	$^3/_8$"- 16UN	12	$2^3/_4$" - 16	30	4,1	RC-152
50,8	41,4	19	38	9	1" - 8	25	48	$^3/_8$"- 16UN	12	$2^3/_4$" - 16	30	5,0	RC-154*
50,8	41,4	25	38	9	1" - 8	25	48	$^3/_8$"- 16UN	12	$2^3/_4$" - 16	30	6,8	RC-156*
50,8	41,4	25	38	9	1" - 8	25	48	$^3/_8$"- 16UN	12	$2^3/_4$" - 16	30	8,2	RC-158
50,8	41,4	25	38	9	1" - 8	25	48	$^3/_8$"- 16UN	12	$2^3/_4$" - 16	30	9,5	RC-1510
50,8	41,4	25	38	9	1" - 8	25	48	$^3/_8$"- 16UN	12	$2^3/_4$" - 16	30	10,9	RC-1512
50,8	41,4	25	38	9	1" - 8	25	48	$^3/_8$"- 16UN	12	$2^3/_4$" - 16	30	11,8	RC-1514
65,0	57,2	25	50	10	$1^1/_2$" - 16	19	58	$^1/_2$"- 13UN	19	$3^5/_{16}$" - 12	49	5,9	RC-251
65,0	57,2	25	50	10	$1^1/_2$" - 16	25	58	$^1/_2$"- 13UN	19	$3^5/_{16}$" - 12	49	6,4	RC-252*
65,0	57,2	25	50	10	$1^1/_2$" - 16	25	58	$^1/_2$"- 13UN	19	$3^5/_{16}$" - 12	49	8,2	RC-254*
65,0	57,2	25	50	10	$1^1/_2$" - 16	25	58	$^1/_2$"- 13UN	19	$3^5/_{16}$" - 12	49	10,0	RC-256*
65,0	57,2	25	50	10	$1^1/_2$" - 16	25	58	$^1/_2$"- 13UN	19	$3^5/_{16}$" - 12	49	12,2	RC-258
65,0	57,2	25	50	10	$1^1/_2$" - 16	25	58	$^1/_2$"- 13UN	19	$3^5/_{16}$" - 12	49	14,1	RC-2510
65,0	57,2	25	50	10	$1^1/_2$" - 16	25	58	$^1/_2$"- 13UN	19	$3^5/_{16}$" - 12	49	16,3	RC-2512
65,0	57,2	25	50	10	$1^1/_2$" - 16	25	58	$^1/_2$"- 13UN	19	$3^5/_{16}$" - 12	49	17,7	RC-2514*
73,2	57,2	57	50	10	$1^1/_2$" - 16	25	—	—	—	$3^5/_{16}$" - 12	49	18,1	RC-308
95,2	79,5	33	71	2	—	—	95	$^1/_2$"- 13UN	19	5" - 12	55	15,0	RC-502
95,2	79,5	33	71	2	—	—	95	$^1/_2$"- 13UN	19	5" - 12	55	19,1	RC-504
95,2	79,5	35	71	2	—	—	95	$^1/_2$"- 13UN	19	5" - 12	55	23,1	RC-506*
95,2	79,5	35	71	2	—	—	95	$^1/_2$"- 13UN	19	5" - 12	55	37,6	RC-5013
114,3	95,2	30	71	5	—	—	—	—	—	$5^3/_4$" - 12	44	29,5	RC-756
114,3	95,2	30	71	5	—	—	—	—	—	$5^3/_4$" - 12	44	59,0	RC-7513
130,3	104,9	41	71	2	—	—	140	$^3/_4$"- 10UN	25	$6^7/_8$"- 12	44	59,0	RC-1006
130,3	104,9	41	71	2	—	—	140	$^3/_4$"- 10UN	25	$6^7/_8$"- 12	44	72,6	RC-10010

Appendix J –Hydraulic Oil Safety Data Sheet

ENERPAC

Material Safety Data Sheet

ENERPAC HYDRAULIC OIL

Issue Date   November 2013

1. IDENTIFICATION OF THE MATERIAL AND SUPPLIER

Product Name	Enerpac Hydraulic Oil
Product Code	HF105L, HF102L & HF104L
Company Name	Actuant Australia Pty Ltd (ABN 14 008 462 271)
Address	Block V, Unit 3, Regents Park Estate, 391 Park Road, Regents Park, NSW 2143, Australia
Emergency Tel.	+61 (0)2 9743 8988
Tel.	+61 (0)2 9743 8988
Fax.	+61 (0)2 9743 8640
Email	info@enerpac.com.au
Recommended Use	Supplied as a mineral hydraulic oil for use in suitable applications only.
Other Information	Visit our website: www.enerpac.com.au
	Enquiries Freecall (in Australia): 1 800 225 084
	Enquiries Freecall (in New Zealand): 0 800 363 772

2. HAZARDS IDENTIFICATION

Hazard Classification	Not classified as hazardous
	AUSTRALIA
	Not classified as hazardous according to the criteria of the NOHSC.
	Not classified as dangerous goods according to the ADG Code.
	NEW ZEALAND
	Not classified as hazardous according to the Hazardous Substance (Minimum Degree of Hazard) regulations 2001.
	Not classified as Dangerous Goods for transport according to the New Zealand Standard NZS 5433:2012 Transport of Dangerous Goods on Land.

3. COMPOSITION/INFORMATION ON INGREDIENTS

Ingredients	Name	CAS	Proportion	Hazard Symbol	Risk Phrase
	Mineral oil		>60%		
	Other ingredients determined not to be hazardous		To 100%		

4. FIRST AID MEASURES

Inhalation	Remove victim from exposure - avoid becoming a casualty. Allow patient to assume most comfortable position and keep warm. Keep at rest until fully recovered. If symptoms develop seek medical attention.
Ingestion	DO NOT induce vomiting. Seek medical attention.
Skin	Wash with plenty of soap and water. If symptoms develop seek medical attention.

Eye	Immediately irrigate with copious quantity of water for at least 15 minutes. Eyelids to be held open. If symptoms persist seek medical attention.
Advice to Doctor	Treat symptomatically.

5. FIRE FIGHTING MEASURES

Suitable Extinguishing Media.	Use CO2, dry chemical or foam.
Hazards from Combustion Products.	Combustion products may include oxides of carbon, nitrogen and sulphur as well as unidentified organic and inorganic compounds.
Precautions in connection with Fire.	Fire fighters to wear self-contained breathing apparatus if risk of exposure to products of combustion.
Unsuitable Extinguishing Media.	Straight streams of water.

6. ACCIDENTAL RELEASE MEASURES

Spills & Disposal	Contain - prevent contamination of drains and waterways. Use absorbent (soil or sand, sawdust, inert material, vermiculite). Collect and seal in properly labelled drums for disposal. Dispose of waste as per Local, State and Federal Land Waste Management Authorities.
Environmental Precautions	Do not discharge into the drains/surface waters/groundwater. Do not discharge into the subsoil/soil.

7. HANDLING AND STORAGE

Precautions for Safe Handling	Put on appropriate personal protective equipment (see Section 8). Workers should wash hands and face before eating, drinking and smoking. Take precautionary measures against static discharges. Keep containers tightly closed when not in use. Empty containers retain product residue. Do not reuse container.
Conditions for Safe Storage	Store in a cool, dry, well-ventilated area away from sources of ignition, strong oxidizing agents and foodstuffs.

8. EXPOSURE CONTROLS/PERSONAL PROTECTION

National Exposure Standards	No value assigned for this specific material by the National Occupational Health and Safety Commission (Safe Work Australia). National Exposure Standards: Oil mist TWA 5mg/m3, STEL 10mg/m3
Engineering Controls	Maintain concentration below recommended exposure limit. Special ventilation is not normally required due to the low volatility of the product at normal temperatures. However, in the operation of certain equipment or at elevated temperatures, mists or vapour may be generated and exhaust ventilation should be provided to maintain airborne concentration levels below the exposure standard or where no exposure standard is allocated, as low as is reasonably practicable.
Respiratory Protection	Respirator not normally required. Airborne concentrations should be kept to lowest levels possible. If vapour, mist or dust is generated and the occupational exposure limit of the product is exceeded, use appropriate AS/NZS 1715/1716 approved half-face filter respirator suitable for organic vapours or air supplied respirator after determining the airborne concentration of the contaminant. Air supplied respirators should always be worn when airborne concentration of the contaminant or oxygen content of the air is unknown.
Eye Protection	Safety glasses, goggles or face shield as appropriate.
Hand Protection	Impervious gloves, e.g. nitrile rubber gloves.
Footwear	Enclosed footwear.

Body Protection   Overalls or similar protective apparel.

9. PHYSICAL AND CHEMICAL PROPERTIES

Appearance	Clear blue liquid
Boiling Point	>300°C/typical
Solubility in Water	Soluble
Specific Gravity	0.85 @ 15°C/typical
Viscosity	Viscosity @ 40°C = 30 cSt/typical
	Viscosity @ 100°C = 5.4 cSt/typical
Flash Point	>200°C/typical
Flammability	Combustible liquid C2 according to Australian Standard AS 1940.
Flammable Limits - Lower	Approximately 0.9%
Flammable Limits - Upper	Approximately 7.0%

10. STABILITY AND REACTIVITY

Conditions to Avoid	Heat and other sources of ignition.
Incompatible Materials	Strong oxidising agents.

11. TOXICOLOGICAL INFORMATION

Inhalation	No harmful effects at appropriate handling and determined usage.
Ingestion	No adverse effects expected if swallowed in small doses.
	Ingestion of large quantities may cause gastro-intestinal effects.
Skin	No harmful effects at appropriate handling and determined usage.
Eye	May cause slight eye irritation.
Chronic Effects	Prolonged or repeated exposure may result in irritation, with the possibility of dermatitis
Other Information	Used oils may contain harmful impurities that have accumulated during use. The concentration of such impurities will depend on use and they may present risks to health and environment on disposal. All used oils should be handled with caution and skin contact avoided as far as possible.

12. ECOLOGICAL INFORMATION

Environ. Protection	Dispose of waste according to federal, EPA, state and local regulations.

13. DISPOSAL CONSIDERATIONS

Disposal. Considerations	Dispose of waste according to federal, EPA, state and local regulations.

14. TRANSPORT INFORMATION

Transport Information	Not classified as a Dangerous Good according to the Australian Code for the Transport of Dangerous Goods by Road and Rail.
UN Number (Air Transport, ICAO)	Not regulated for air transport according to IATA Dangerous Goods Regulations (54th Ed. 2013).
IMDG UN No	Not regulated for sea transport according to IMDG Code (2010 Ed.).

15. REGULATORY INFORMATION

Poison Schedule	Not Scheduled.

ENERPAC

16. OTHER INFORMATION

|	
Contact Person/Point	Engineering Manager +61 (0)2 9743 8988
	This information was prepared in good faith from the best information available at the time of issue. It is based on the present level of research and to this extent we believe it is accurate. However, no guarantee of accuracy is made or implied and since conditions of use are beyond our control, all information relevant to usage is offered without warranty. The manufacturer will not be held responsible for any unauthorized use of this information or for any modified or altered versions. If you are an employer it is your duty to tell your employees, and any others that may be affected, of any hazards described in this sheet and of any precautions that should be taken. Material Safety Data Sheets are updated frequently. Please ensure you have a current copy.
Literature References	* NOHSC:2011 National Code of Practice for the Preparation of Material Safety Data Sheets
	* NOHSC:1008 Approved Criteria for Classifying Hazardous Substances
	* NOHSC:10005 List of Designated Hazardous Substances
	* NOHSC:1005 Control of Workplace Hazardous Substances, National Model Regulations
	* NOHSC:2007 Control of Workplace Hazardous Substances, National Code of Practice
	* NOHSC:1003 Exposure Standards for Atmospheric Contaminants in the Occupational Environment, National Exposure Standards
	* NOHSC:3008 Exposure Standards for Atmospheric Contaminants in the Occupational Environment, Guidance Note
	* NOHSC:1015 Storage and Handling of Workplace Dangerous Goods, National Standard
	* NOHSC:2017 Storage and Handling of Workplace Dangerous Goods, National Code of Practice
	* SUSMP, Standard for the Uniform Scheduling of Medicines and Poisons
	* ADG, Australian Dangerous Goods Code
	* MSDS of component materials
Last Changes	Issue Date: 28/11/2013
	Supersedes Issue Date: December 2008.
	Reason(s) for issue: Five year review.
	Safety data sheets are updated frequently. Please ensure that you have a current copy.

….End of MSDS….

Appendix K – Calculation - First Moment of Areas

RTRI (2012) offer a theoretical approach to calculate lateral sleeper resistance, which requires the determination of the first moment of the end and side areas of the sleeper about the top edge (Ge and Gs). The calculation used to determine Gs and Ge for the narrow gauge low profile concrete sleepers at the centre of this dissertation is shown below.
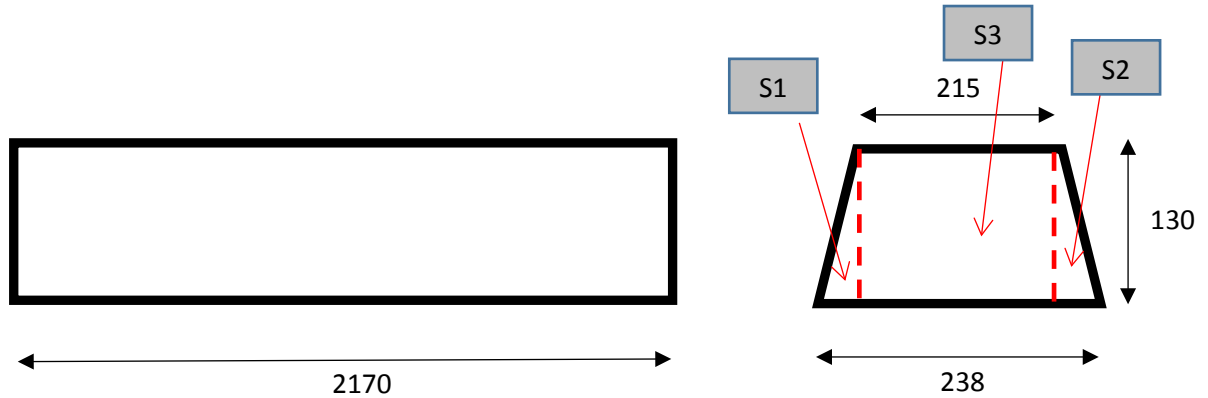
Step 1: Determine Ge, First Moment of Sleeper End Area

Shape	Shape Area (mm^2)	Shape Centroid (mm) (From Top Edge)	Area x Centroid (mm^3)
S1	$\dfrac{238 - 215}{2} \times 130 = 1495$	$\dfrac{2}{3} \times 130 = 86.7$	129.62×10^3
S2	$215 \times 130 = 27950$	$\dfrac{130}{2} = 65$	1816.75×10^3
S3	$\dfrac{238 - 215}{2} \times 130 = 1495$	$\dfrac{2}{3} \times 130 = 86.7$	129.62×10^3
	$\Sigma = 30940$		$\mathbf{Ge = \Sigma = 2.076 \times 10^3}$

Step 2: Determine Centroid of Sleeper

$$\mathrm{Y - Bar} = \frac{\mathrm{Ge}}{\Sigma\,\mathrm{Area}} = \frac{2076 \times 10^3}{30940} = \mathbf{67.1mm}$$

Step 3: Determine Gs, First Moment of Sleeper Side Area

$$\mathrm{Gs = Side\ Area} \times \mathrm{Y - Bar} = (2170 \times 130) \times 67.1 = \mathbf{18.93 \times 10^6\ mm^3}$$